KAISER–HILL
COMPANY

Air Transport and Deposition of Actinides for the Actinide Migration Evaluation at the Rocky Flats Environmental Technology Site

Environmental Media Management
Rocky Flats Environmental Technology Site

December 2001

SEP 2002

ADMIN RECORD

SW-A-004548

1/133

Air Transport and Deposition of Actinides for the Actinide Migration Evaluation at the Rocky Flats Environmental Technology Site

FY01 Report

Prepared for:

Kaiser-Hill Company, LLC
Rocky Flats Environmental Technology Site
10808 Highway 93, Unit B
Golden, CO 80403-8200

Prepared by:

URS Corporation
8181 E. Tufts Avenue
Denver, Colorado 80237

December 2001

EXEMPT FROM CLASSIFICATION
CEX-105-01

2

EXECUTIVE SUMMARY

The Rocky Flats Environmental Technology Site (RFETS or Site) has been a source of airborne actinides throughout its history. Over time, small amounts of plutonium, americium, and other actinides have been deposited on or mixed with surface soils at the Site. Wind or mechanical disturbance of the contaminated soil can result in actinide-laden soil particles becoming airborne. These resuspended particles, along with particles emitted from building stacks and vents, are transported some distance downwind before being deposited on the ground or in water. As a result, airborne migration is one of several transport pathways that redistribute actinides in the environment in the vicinity of the Site.

Prior to 1989, the Site fabricated nuclear weapons components from plutonium, uranium, beryllium, and stainless steel. Weapons production operations were curtailed at the Site in 1989 and, in February 1992, the Site's weapons production mission was discontinued.

The Site is now undergoing deactivation, decommissioning, and cleanup, and is moving toward final closure. Closure of the Site entails removal of nuclear material and waste products. Buildings will be removed and areas of contamination cleaned up. The Site is expected to be dedicated to open space or wildlife refuge use following closure.

Scope of Work

During fiscal year 1999 (FY99), a Site-specific emission estimating method was developed to calculate fugitive particulate matter and actinide emissions due to resuspension of contaminated soil particles by wind. An equation was derived relating hourly particulate matter and actinide emissions to wind speed, underlying surface-soil contamination levels, and the presence or absence of snow cover. A Site-specific implementation of the U.S. Environmental Protection Agency's (EPA's) Industrial Source Complex Short Term dispersion and deposition model was developed. In FY00, several refinements were made to the modeling approach and the resulting emission estimating method and Site-specific model implementation were used to simulate emissions and dispersion from several types of activities that could result in airborne particulate matter and actinide emissions.

During FY01, the emission estimating method for wind erosion was revised based on wind tunnel data collected at the Site in April and June 2000. The baseline scenario developed in FY99 and FY00 has been remodeled using the revised emission approach. In addition, wind tunnel data collected in conjunction with a prescribed test burn at the Site in April 2000 and a small wildfire that occurred in the east Buffer Zone in July 2000 have been used in revised modeling of several post-fire wind erosion scenarios.

3

The revised emission estimating method more accurately reflects the current vegetation state of Site surfaces, limitations in erodible particulate matter mass, and dilution of actinide concentrations by particulate matter originating outside the contaminated areas. Comparisons of model results to measured actinide concentrations showed significant improvement relative to previous years. Modeled plutonium and americium emissions from undisturbed areas at the Site, when added to regional background concentrations, now provide a good fit to measured data at all sampler locations analyzed.

Modeling Results

Modeled wind erosion emissions representing current Site conditions showed maximum concentrations and deposition of actinides to the east of the primary source areas on Site, reflecting the prevailing direction of higher speed winds at the Site. Post-closure wind erosion impacts are expected to exhibit similar patterns but the impacts will increase slightly because removal of buildings and pavement will increase the soil surface areas available for wind erosion. Although only small amounts of actinides will be left in Site surface soils, particles and actinides will be resuspended from a significantly larger source area, with resulting increases in airborne concentrations. However, maximum post-closure concentrations of plutonium and americium were predicted to be an order of magnitude less than the annual EPA air dose limit of 10 millirem; at the fenceline, impacts would be two to three orders of magnitude below the EPA limit.

Sensitivity analyses revealed several interesting interactions. The analyses indicated that dilution of contaminated surface soil with "clean" particulate matter is probably a very important effect in limiting total actinide emissions. The rate at which erosion potential is renewed by small-scale soil disturbances such as freeze/thaw, rainsplash, animal activity, etc. is also important in determining actinide emissions due to wind erosion. While most of the particulate matter that is available for wind erosion from undisturbed areas is probably derived from deposition of airborne particulate matter, the majority of the actinide content of airborne emissions is derived through soil disturbances.

Wind erosion following a fire in the 903 Pad area was predicted to cause a 5- to 13-fold increase in annual actinide concentrations when compared to unburned conditions. Particulate matter concentrations were predicted to increase by smaller amounts. The increases in particulate matter and actinide concentrations would vary with the location of the fire and with the time of the year that the fire occurred. A fall fire would cause greater concentration increases than a spring fire because vegetation would recover more slowly over the winter months than during the spring and summer.

The analyses indicated that emissions from a burned surface would be significantly limited by the rate at which erodible material is renewed. This observation parallels previous erosion studies that have shown that emissions decrease from a surface over

4

time unless the surface is disturbed. The erodible material is exhausted and no additional emissions occur until the erodible material can be resupplied.

This effect is important in limiting emissions following a fire. For example, the simulations indicated that fall post-fire particulate matter emissions, assuming unlimited erodible material, would have been double what was predicted by these simulations. Similarly, spring post-fire particulate matter emissions would have increased by 1.5 times the predicted amount. These emission increases would generally have translated into comparable increases in particulate matter and actinide concentrations.

The post-fire simulations also revealed additional interactions that may influence actinide concentrations. Changes in assumed particle size distribution affected not only the predicted deposition and concentration patterns downwind from the source areas but also altered the amount of particulate matter and actinide available for erosion. Increased emissions from the burned areas were assumed to increase particulate matter concentrations over them, creating a feedback loop that further enhanced particulate matter emissions but that may have decreased predicted actinide emissions through dilution. For the spring fire scenario, predicted emissions were limited because the summer period, during which the ground was assumed to be relatively bare and erosion potential highest, experienced lower wind speeds than fall and winter, by which time substantial vegetative recovery was expected. These types of interactions indicate that airborne actinide concentrations following a fire event cannot be accurately predicted by taking into account the potential increase in erosion potential alone.

TABLE OF CONTENTS

1.0 INTRODUCTION 1-1
- 1.1 Background 1-1
- 1.2 Overview of FY99 and FY00 Air Pathway Investigations 1-5
  - 1.2.1 FY99 Air Pathway Scope and Results 1-5
  - 1.2.2 FY00 Air Pathway Work Scope and Results 1-5
- 1.3 Overview of FY00 Wind Tunnel Investigations 1-6
- 1.4 FY01 Scope of Work and Report Contents 1-7

2.0 REVISED RESUSPENSION EMISSION ESTIMATION 2-1
- 2.1 Overview of FY99 and FY00 Wind Erosion Emission Estimates 2-1
- 2.2 FY00 Wind Tunnel Data Collection 2-2
  - 2.2.1 Wind Tunnel Field Trials 2-2
  - 2.2.2 DustTRAK Monitoring 2-6
  - 2.2.3 Test Analysis 2-7
  - 2.2.4 Test Results 2-8
  - 2.2.5 Use of the Wind Tunnel Data in Emission Estimates 2-8
- 2.3 FY01 Revised Particulate Matter Emissions 2-10
  - 2.3.1 Revised Emission Equation 2-10
  - 2.3.2 Application of the Revised Equation 2-10
  - 2.3.3 Effect of Snow Cover and Precipitation 2-12
  - 2.3.4 Initial Erosion Potential 2-13
  - 2.3.5 Deposition Inputs 2-14
  - 2.3.6 Small-Scale Disturbances 2-15
- 2.4 Revised Actinide Emissions 2-16
  - 2.4.1 Deposition Inputs 2-16
  - 2.4.2 Small-Scale Disturbances 2-18
  - 2.4.3 Calculation of Actinide Emissions 2-18

3.0 REVISED WIND EROSION MODELING 3-1
- 3.1 Modeling Methods 3-1
- 3.2 Modeling Wind Erosion for Existing Site Source Areas 3-2
  - 3.2.1 Initial Modeling Results 3-2
  - 3.2.2 Background Actinide Concentrations 3-6
  - 3.2.3 Comparisons With 1996 Data 3-8
  - 3.2.4 Sensitivity Analyses 3-9
- 3.3 Revisions to Emission Estimation Methods 3-11
- 3.4 Revised Pre-Closure Wind Erosion Results 3-13

4.0 POST-CLOSURE WIND EROSION 4-1
- 4.1 Scenario Description and Emission Estimation 4-1
- 4.2 Modeling Methods 4-2
- 4.3 Modeling Results 4-2

6

TABLE OF CONTENTS (CONTINUED)

5.0 POST-FIRE WIND EROSION 5-1
5.1 Post-Fire Emission Estimates 5-1
5.1.1 Scenario Description 5-1
5.1.2 Emission Source Locations 5-2
5.1.3 Emission Estimation 5-2
5.2 Modeling Methods 5-13
5.3 Modeling Results 5-14
5.3.1 Spring Fire Results 5-15
5.3.2 Fall Fire Results 5-16
5.4 Conclusions 5-16

6.0 FY01 AIR PATHWAY DISCUSSION AND CONCLUSIONS 6-1
6.1 Air Pathway Findings 6-1
6.2 Discussion of Revised Wind Erosion Modeling Methods 6-2

7.0 REFERENCES CITED

APPENDIX A: Effects of Prescribed Grass Fire on Wind Erosion Rates from Surface Soil at Rocky Flats, CO

APPENDIX B: Wind Erosion Tracking Program

7

LIST OF FIGURES

Figure 1-1 Area Map of the Rocky Flats Environmental Technology Site and Surrounding Communities 1-3

Figure 1-2 Rocky Flats Environmental Technology Site Location Map 1-4

Figure 2-1. Existing Pu-239/240 Source Areas 2-3

Figure 2-2. Existing Am-241 Source Areas 2-4

Figure 2-3. MRI Portable Wind Tunnel 2-5

Figure 2-4. Example PM_{10} Concentration History From Wind Tunnel 2-6

Figure 2-5 Wind Tunnel Test Results 2-9

Figure 2-6. Monthly Average TSP Concentrations at the Site in 1996 2-14

Figure 2-7. RAAMP Sampler Locations 2-17

Figure 3-1. Initial Modeling Results for Pu-239/240 (Including S-107) 3-4

Figure 3-2. Initial Modeling Results for Am-241 (Including S-107) 3-4

Figure 3-3. Initial Modeling Results for Pu-239/240 (Excluding S-107) 3-5

Figure 3-4. Initial Modeling Results for Am-241 (Excluding S-107) 3-5

Figure 3-5. Comparison of 1996 Pu-239/240 Concentrations at S-107 3-8

Figure 3-6. Results of Sensitivity Analyses (S-107) 3-9

Figure 3-7. Revised Modeling of Wind Erosion Emissions of Pu-239/240 3-12

Figure 3-8. Pu-239/240 Error Ratios for FY00 and FY01 Revised Simulations 3-12

Figure 3-9. Predicted Pre-Closure Annual Average Pu-239/240 Concentrations 3-15

Figure 3-10. Predicted Pre-Closure Annual Pu-239/240 Deposition 3-16

Figure 3-11. Predicted Pre-Closure Annual Average Am-241 Concentrations 3-17

Figure 3-12. Predicted Pre-Closure Annual Am-241 Deposition 3-18

Figure 4-1 Post-Closure Pu-239/240 Source Areas 4-3

8

Figure 4-2 Post-Closure Am-241 Source Areas 4-4

Figure 4-3 Predicted Post-Closure Annual Average Pu-239/240 Concentrations 4-6

Figure 4-4 Predicted Post-Closure Annual Pu-239/240 Deposition 4-7

Figure 4-5 Predicted Post-Closure Annual Average Am-241 Concentrations 4-8

Figure 4-6 Predicted Post-Closure Annual Am-241 Deposition 4-9

Figure 5-1. Source Areas for Post-Fire Scenarios 5-3

Figure 5-2. Normalized Wind Tunnel Results 5-4

Figure 5-3 Erosion Potential Multipliers for Post-Fire Scenarios 5-7

Figure 5-4. Calculated Monthly Variation in Post-Fire TSP Concentrations 5-10

Figure 5-5 Pre-Closure Base Case:
Predicted Annual Average Particulate Matter Concentrations 5-18

Figure 5-6 Pre-Closure Spring Fire:
Predicted Annual Average Particulate Matter Concentrations 5-19

Figure 5-7 Pre-Closure Fall Fire:
Predicted Annual Average Particulate Matter Concentrations 5-20

Figure 5-8 Post-Closure Base Case:
Predicted Annual Average Particulate Matter Concentrations 5-21

Figure 5-9 Post-Closure Spring Fire:
Predicted Annual Average Particulate Matter Concentrations 5-22

Figure 5-10 Post-Closure Fall Fire:
Predicted Annual Average Particulate Matter Concentrations 5-23

Figure 5-11 Pre-Closure Base Case:
Predicted Annual Average Pu-239/240 Concentrations 5-24

Figure 5-12 Pre-Closure Spring Fire:
Predicted Annual Average Pu-239/240 Concentrations 5-25

Figure 5-13 Pre-Closure Fall Fire:
Predicted Annual Average Pu-239/240 Concentrations 5-26

Figure 5-14 Pre-Closure Base Case:
Predicted Annual Average Am-241 Concentrations 5-27

9

Figure 5-15 Pre-Closure Spring Fire:
Predicted Annual Average Am-241 Concentrations 5-28

Figure 5-16 Pre-Closure Fall Fire:
Predicted Annual Average Am-241 Concentrations 5-29

Figure 5-17 Post-Closure Base Case:
Predicted Annual Average Pu-239/240 Concentrations 5-30

Figure 5-18 Post-Closure Spring Fire:
Predicted Annual Average Pu-239/240 Concentrations 5-31

Figure 5-19 Post-Closure Fall Fire:
Predicted Annual Average Pu-239/240 Concentrations 5-32

Figure 5-20 Post-Closure Base Case:
Predicted Annual Average Am-241 Concentrations 5-33

Figure 5-21 Post-Closure Spring Fire:
Predicted Annual Average Am-241 Concentrations 5-34

Figure 5-22 Post-Closure Fall Fire:
Predicted Annual Average Am-241 Concentrations 5-35

10

LIST OF TABLES

Table 3-1. Results Summary—Pre-Closure Wind Erosion Scenario 3-14

Table 4-1. Surface Soil Action Levels for Post-Closure 4-1

Table 4-2. Results Summary—Post-Closure Wind Erosion Scenario 4-2

Table 5-1. Monthly Erosion Potential Multipliers for Hypothetical Spring and Fall Fires 5-7

Table 5-2. Revised Particulate Matter Deposition Velocities for Post-Fire Scenarios 5-11

Table 5-3. Revised Activity Deposition Velocities for Post-Fire Scenarios 5-12

Table 5-4. Particle Size Data Used for Fire Recovery Dispersion Modeling 5-14

Table 5-5. Particulate Matter Results Summary—Post-Fire Recovery Scenarios 5-14

Table 5-6. Activity Results Summary—Post-Fire Recovery Scenarios 5-15

11

ABBREVIATIONS AND ACRONYMS

Am	Americium
APCD	Air Pollution Control Division
CDPHE	Colorado Department of Public Health and Environment
CFR	Code of Federal Regulations
Ci/m^3	Curies per cubic meter
Ci/yr	Curies per year
cm	Centimeter(s)
cm/s	Centimeters per second
COMRAD	Community Radiation Program
DOE	U.S. Department of Energy
EDE	Effective dose equivalent
EPA	U.S. Environmental Protection Agency
ERAMS	Environmental Radiation Ambient Monitoring System
FY	Fiscal year
g/cm^3	Grams per cubic centimeter
g/m^3	Grams per cubic meter
g/m^2	Grams per square meter
g/m^2/15-minutes	Grams per square meter per 15-minutes
$g/m^2/s$	Grams per square meter per second
H_2O_2	Hydrogen peroxide
ISCST3	Industrial Source Complex Model Short-Term
Kaiser-Hill	Kaiser-Hill Company, LLC
km	Kilometer(s)
km^2	Square kilometer(s)
m	Meter(s)
m^2	Square meter(s)
m^3/s	Cubic meters per second
mph	Mile(s) per hour
mrem	Millirem
mrem/yr	Millirem per year
MRI	Midwest Research Institute
m/s	Meter(s) per second
OU3	Operable Unit 3
pCi/g	Picocuries per gram
pCi/m^2	Picocuries per square meter
$pCi/m^2/s$	Picocuries per square meter per second
pCi/m^2/15-minutes	Picocuries per square meter per 15-minutes
$pCi/m^2/yr$	Picocuries per square meter per year
Pu	Plutonium
RAAMP	Radioactive Ambient Air Monitoring Program
RFCA	Rocky Flats Cleanup Agreement
RFETS	Rocky Flats Environmental Technology Site
RFFO	Rocky Flats Field Office

12

ABBREVIATIONS AND ACRONYMS (CONTINUED)

s^{-1}	Inverse Seconds
s, sec	Second(s)
Site	Rocky Flats Environmental Technology Site
TP	Total particulate
TSP	Total suspended particulate
U	Uranium
μg	Microgram(s)
μm	Micrometer(s)

13

1.0 INTRODUCTION

The Rocky Flats Environmental Technology Site (RFETS or Site) has been a source of airborne actinides throughout its history. Over time, small amounts of plutonium (Pu), americium (Am), and other actinides have been deposited on or mixed with surface soils at the Site. Wind or mechanical disturbance of the contaminated soil can result in actinide-laden soil particles becoming airborne. These resuspended particles, along with particles emitted from building stacks and vents, are transported some distance downwind before being deposited on the ground or in water by a variety of mechanisms that remove particles from the air, such as rainout or dry deposition. As a result, airborne migration is one of several transport pathways that redistribute actinides in the environment in the vicinity of the Site (other primary pathways include soil erosion, and surface and groundwater movement).

During fiscal year 1999 (FY99), a Site-specific emission estimating method was developed to calculate fugitive particulate matter and actinide emissions due to resuspension of contaminated soil particles by wind. The estimating method was based on wind speed, size of the contaminated areas, and surface soil concentrations of actinides within each contaminated area. A Site-specific implementation of the U.S. Environmental Protection Agency's (EPA's) Industrial Source Complex Short Term (ISCST3) dispersion and deposition model was developed and one year of meteorological data was processed for use with this model. Preliminary modeling suggested several improvements that could be made to the emission and modeling methods based on a comparison of modeled impacts to measured airborne actinide levels at the Site.

In FY00, several refinements were made to the modeling approach. The resulting emission estimating method and Site-specific model implementation were used to simulate emissions and dispersion from several types of activities that could result in airborne particulate matter and actinide emissions.

During FY01, the emission estimating method for resuspension was revised based on wind tunnel data collected at the Site in April and June 2000. The baseline scenario developed in FY99 and FY00 has been remodeled using the revised emission approach. In addition, data collected in conjunction with a prescribed test burn at the Site in April 2000 and with a small wildfire that occurred in the east Buffer Zone in July 2000 have been used in revised modeling of several post-fire wind erosion scenarios. This report summarizes the revised emission approach and modeling analyses.

1.1 Background

The Rocky Flats Environmental Technology Site is operated by Kaiser-Hill Company, L.L.C. (Kaiser-Hill), with oversight by the Rocky Flats Field Office (RFFO) of the U.S. Department of Energy (DOE). The Site occupies an area of 26.5 square kilometers (km^2)

114

in northern Jefferson County, Colorado, about 25.7 kilometers (km) northwest of Denver. Over 2.8 million people live within 80 km of the Site. Adjacent land use is a mixture of agriculture, open space, industry, and residential housing. Surrounding communities include the city of Golden to the south of the Site; the cities of Arvada, Broomfield, and Westminster to the east; and the city of Boulder to the north. Figure 1-1 shows the Site location.

Prior to 1989, the Site fabricated nuclear weapons components from plutonium, uranium (U), beryllium, and stainless steel. Production activities included metal fabrication and assembly, chemical recovery and purification of transuranic radionuclides, and related quality control functions. Plutonium weapons operations were curtailed at the Site in 1989 due to safety concerns and, in February 1992, the Site's weapons production mission was discontinued. Figure 1-2 shows the overall Site layout; former production areas are clustered in a central Industrial Area, which is surrounded by support facilities and a Buffer Zone of vacant land.

The Site is now undergoing deactivation, decommissioning, and cleanup, and is moving toward final closure. Closure of the Site entails removal of nuclear material and waste products, which are being shipped to off-Site repositories and disposal facilities. Buildings will be removed and areas of contamination cleaned up. Clean fill dirt will be brought in from off Site to cap remaining building foundations and structures. The Site is expected to be dedicated to open space or wildlife refuge use following closure.

Between 1989 and 1995, resuspension of actinide-containing soils and transport through the air pathway occurred primarily due to natural processes, such as wind erosion. Remediation of contaminated soils and waste disposal areas at the Site and building decommissioning activities began in 1995. Such activities disturb contaminated soils or contamination on building or equipment surfaces, and result in additional airborne particulates. Future resuspension of actinide-containing material will occur due to both natural and anthropogenic activities.

The most significant soil contamination areas contributing to airborne actinides at the Site are the 903 Pad and the adjacent "lip" area. During the 1950s and 1960s, the 903 Pad was contaminated with plutonium-laden cutting oil that leaked from metal drums into the soil beneath the drums. Removal of the drums in the late 1960s and associated cleanup activities resulted in dispersion of contaminated soil to the east and south of the 903 Pad. The storage pad was covered with asphalt in 1969 and is not currently a source of resuspendable actinides. However, the initial spread of the contaminated soil prior to the installation of the asphalt pad resulted in a plume of actinides in the surface soils extending to the east and southeast from the 903 Pad itself.

Other spills and releases have resulted in smaller areas at the Site where the surface soils are contaminated with different actinides (such as uranium isotopes). In addition,

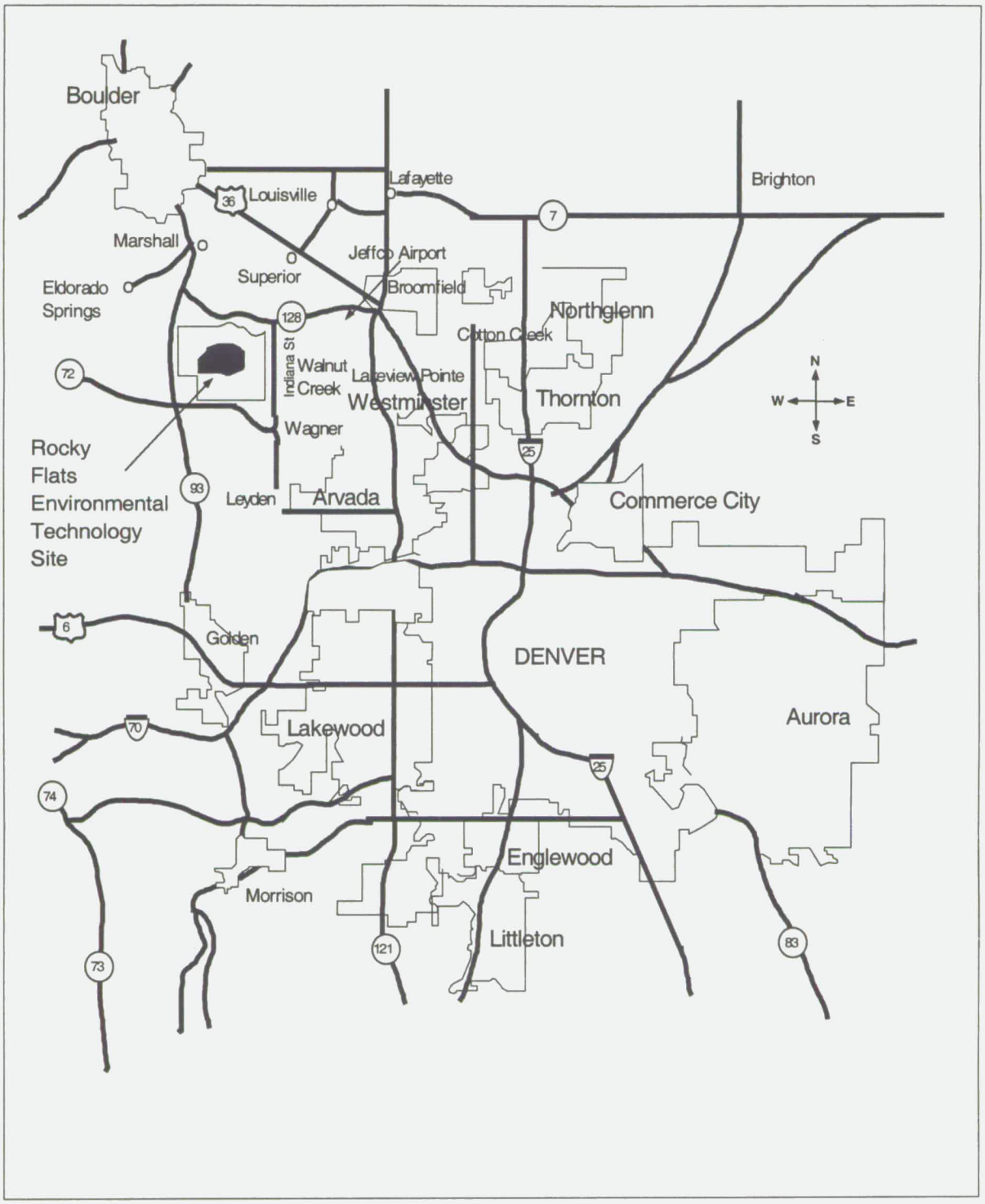

Figure 1-1. Area Map of the Rocky Flats Environmental Technology Site and Surrounding Communities

116

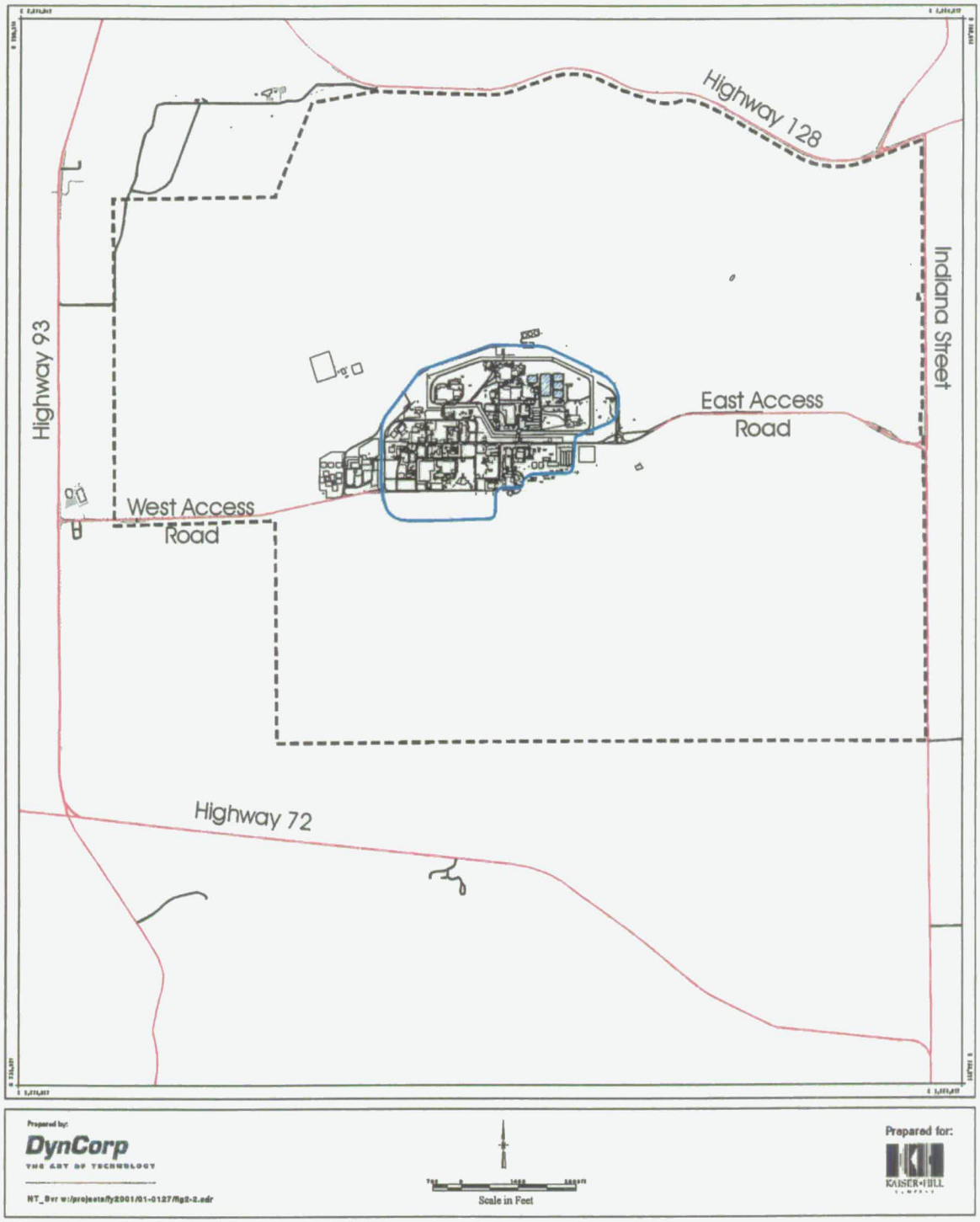

Figure 1-2. Rocky Flats Environmental Technology Site Location Map

17

naturally occurring uranium deposits may also result in areas of elevated surface soil uranium concentrations. Actinide concentrations in surface deposits at the Site have been sampled and mapped, and the resulting data form the basis of the actinide emission estimates developed as part of the work reported here.

1.2 Overview of FY99 and FY00 Air Pathway Investigations

The FY01 air pathway work represents a continuation and refinement of portions of the work performed during FY99 and FY00. As a result, the scope and results of the FY99 and FY00 work that relate to the FY01 analyses are briefly reviewed here.

1.2.1 FY99 Air Pathway Scope and Results

Actinide resuspension due to wind erosion is episodic in nature and influenced primarily by meteorological variables (wind speed and rainfall); particle and soil properties (moisture level, and particle size and density); and surface characteristics (density and type of vegetative growth, and snow cover). Given the density of vegetation growing on the contaminated soil areas at the Site, an important source of contaminated soil resuspension is likely to be the dust-laden vegetation and litter, with direct resuspension from soil surfaces occurring primarily during high wind events or after disturbances.

Past wind tunnel experiments at the Site relate wind erosion rates to ambient wind speed. Limited data collected from undisturbed areas just to the east of the Site in 1993 suggested that dust resuspension varies with wind speed raised to the third power.

An equation was derived relating hourly particulate and actinide emissions to wind speed, underlying surface-soil contamination levels, and the presence or absence of snow cover, based on the 1993 wind tunnel data. This equation was used to calculate hourly emissions due to wind erosion for five actinides for a full year. The calculated emissions were used as input to dispersion and deposition simulations.

An annual scenario was modeled representing the "chronic" resuspension of actinides by wind erosion. Airborne actinide concentrations due to these ongoing emissions were estimated at a variety of locations on and around the Site and were compared with air sampling data for Pu-239/240. Model-predicted concentrations were found to be higher, by one to two orders of magnitude, than the measured concentrations.

1.2.2 FY00 Air Pathway Work Scope and Results

The focus of the FY00 work was to use the model and emission estimating technique developed in FY99 to look at the impact of specific activities on airborne actinide concentration/dose and actinide deposition. As Site closure proceeds, remediation projects and building decommissioning will result in airborne actinide emissions as

contaminated soils or materials are disturbed. One goal of the FY00 modeling was to estimate reasonable upper bounds on the amount of airborne actinides that could result from these types of activities.

Other situations that could result in elevated actinide levels in air include wildfires, post-fire wind erosion, and high wind events. The FY00 work also estimated emissions and dispersion from these types of activities, again with the goal of generating reasonable upper bound values. Airborne actinide levels and deposition rates that would result from wind erosion of undisturbed areas following Site closure were also estimated.

Refinements suggested by the FY99 work were incorporated into the modeling of wind erosion. The baseline scenario developed in FY99 (wind erosion of contaminated soils under current Site conditions) was remodeled using these refinements in FY00. A comparison of modeled estimates to measured actinide concentrations showed that the revised model underestimated measured actinide concentrations at samplers in the nondominant downwind directions, while overestimating concentrations to the east and southeast of the source areas (dominant downwind directions). The model performance at the locations where concentrations appeared to be underpredicted was generally within the accuracy of the measurements themselves. Model overpredictions in the direction of the stronger winds at the Site were thought to be at least partly due to inaccuracies in the emission estimating method. Even so, the model overpredictions were reduced from the FY99 modeling.

1.3 Overview of FY00 Wind Tunnel Investigations

During FY99 and FY00, the Site evaluated a program of annual prescribed burns to reduce the buildup of flammable litter, restore native grasses, and control noxious weeds in portions of the Site. Several prescribed burns were planned for the Spring of 2000 and Kaiser-Hill developed a wind tunnel investigation in conjunction with those burns. The purpose of the wind tunnel study was to measure resuspension of soil and ash immediately following a fire and at intervals after a fire to determine how the resuspension rates varied from those measured over unburned, undisturbed areas of the Site. The post-fire sequence of wind tunnel tests was designed to investigate the time period over which wind erosion rates would recover to pre-fire conditions.

Because of delays due to public communication issues and the timing of spring precipitation and wind events, the Site was unable to conduct a full-scale prescribed burn in 2000. However, a 50-acre test burn was conducted in early April. Wind tunnel tests were conducted over the burned area and paired tests were conducted in an adjacent, unburned area immediately following the test burn. Additional tests were conducted over the burned area in early May and late June. The June series also gathered additional data on resuspension from an adjacent, unburned plot for comparison.

Midwest Research Institute (MRI) performed the wind tunnel tests, using the same wind tunnel configuration that was used in a 1993 investigation at the Site (EG&G, 1994). The data from the 1993 MRI study formed the basis for the chronic wind erosion emission equation developed in the FY99 air pathway work (Radian, 1999). Consequently, the FY00 wind tunnel measurements provided additional data with which to refine the emission estimating technique, as well as providing new information regarding post-fire recovery.

Additional wind tunnel investigations were implemented because of a small grass fire that occurred at the Site in July 2000. Lightening ignited a grass fire in an area with low levels of actinide contamination (approximately 2 picocuries per gram soil [pCi/g]) in the east Buffer Zone. The additional wind tunnel study gathered data on particle and actinide activity in different size fractions of resuspended material and in the underlying soil.

1.4 FY01 Scope of Work and Report Contents

The FY01 work was designed to incorporate new wind tunnel data into the previously developed emission estimating technique, as well as to make use of the post-fire data gathered during the 2000 wind tunnel investigation to predict post-fire impacts. Sections 2.0 and 3.0 of this report describe revisions to the emission estimating and modeling techniques used to determine wind erosion impacts at the Site. Model results were again compared to measured actinide levels around the Site to verify the improvements. The revised emission and modeling methods were used to remodel wind erosion impacts under current (pre-closure) and future (post-closure) conditions (see Sections 3.0 and 4.0). Section 5.0 describes results for several post-fire scenarios. Section 6.0 presents the findings and conclusions of the FY01 air pathway studies.

2.0 REVISED WIND EROSION EMISSION ESTIMATION

This section describes refinements made in FY01 to wind erosion emission estimates at the Site. Previous comparisons of model predictions to measured airborne actinide concentrations indicated that the model used in FY00 overpredicted impacts in the dominant downwind directions and underpredicted impacts in the nondominant downwind directions. A primary goal of the FY01 work was to improve the wind erosion emission estimates to better predict actinide impacts due to chronic dust resuspension.

2.1 Overview of FY99 and FY00 Wind Erosion Emission Estimates

A significant amount of research in particle and actinide resuspension has occurred over the years (see Radian, 1999). This research emphasizes the need to customize any approach to the particular location of interest. Site-specific meteorological, soil, and surface characteristics must be taken into account to produce a reliable emission estimating approach for a given area.

Past wind tunnel experiments at the Site relate wind erosion rates to ambient wind speed. In FY99, a method was developed to estimate actinide emissions from vegetated surfaces based on wind tunnel data taken in Operable Unit 3 (OU3) in June 1993 (EG&G, 1994) (OU3 is located just east of Indiana Street). Although the number of data points in the data set was extremely limited, the 1993 OU3 wind tunnel data were considered the most representative of conditions on Site at the time. Wind speed was plotted against the measured flux of resuspended dust. Applying a power fit to the data produced the following expression:

$$E = 2 \times 10^{-9} (U^{3.014}) \qquad (1)$$

where:

E is the total particulate matter emission rate in grams per square meter per second ($g/m^2/s$); and
U is the 10-meter (m) wind speed in meters per second (m/s).

Estimated emission rates were set equal to zero if snow cover was present, based on 1996 meteorological data. Meteorological data for 1996 were used in the FY99 and FY00 studies for both emission estimation and modeling.

Estimates of particle resuspension rate ($g/m^2/s$) provided the basis for predicting emissions of actinides. The distribution of actinides in Site surface soils has been determined in units of pCi/g from historical soil sampling activities. Soil isopleth maps showing the distribution of actinide activity in surface soils were electronically digitized and reduced to a series of points. The points defined polygons approximating each

contour's shape for emission estimating and modeling purposes. Particulate matter (resuspension) emissions from each isopleth area were combined with this information to yield actinide emissions in picocuries per square meter per second [pCi/m^2/s] for each actinide source area. The size and location of the existing Pu-239/240 and Am-241 source areas used for emission estimation and modeling are shown in Figures 2-1 and 2-2.

2.2 FY00 Wind Tunnel Data Collection

Wind tunnel tests conducted at the Site in April, May, and June 2000 primarily focused on emissions from burned areas of grassland. However, for comparison, wind erosion emissions were also measured from adjacent, unburned areas in April and June. The unburned area data were used to revise the emission estimating technique described in Section 2.1.

The MRI wind tunnel and the data collection programs at the Site in 2000 are described in detail in two reports: *Effect of Controlled Burning on Soil Erodibility by Wind, Final Test Report* (MRI, 2001a) and *Effect of Wildfires on Soil Erodibility by Wind, Final Test Report* (MRI, 2001b). In addition, a paper describing the test burn wind tunnel data and how those data could be used in emission estimating and modeling was presented at the 10th annual International Emission Inventory Conference in Denver, Colorado, in May 2000. The paper is included as Appendix A to this report and presents additional details regarding the wind tunnel apparatus and measurement technique.

2.2.1 Wind Tunnel Field Trials

Wind tunnel tests were performed by MRI using a portable reference wind tunnel, described in the *Air/Superfund National Technical Guidance Study Series, Volume II, Estimates of Baseline Air Emissions at Superfund Sites* (EPA, 1989). The portable wind tunnel is shown in Figure 2-3. A TSI DustTRAK monitor was used to provide real-time concentrations of PM_{10} (particles less than or equal to 10 micrometers [μm] in aerodynamic diameter) in the tunnel effluent.

Although the portable wind tunnel does not generate the larger scales of turbulent motion found in the atmosphere, the turbulent boundary layer formed within the tunnel simulates the smaller scales of atmospheric turbulence. It is the smaller-scale turbulence that penetrates the wind flow in direct contact with the erodible surface and contributes to particle entrainment (wind erosion). The wind tunnel method relies on a straightforward mass balance technique to calculate particulate matter emission rates. Previous wind erosion studies using the MRI reference wind tunnel have led to the EPA recommended emission factors for industrial wind erosion presented in *Compilation of Air Pollutant Emission Factors (AP-42)* (EPA, 2000).

22

Figure 2-1. Existing Pu-239/240 Source Areas Based on Surficial Soil Contamination

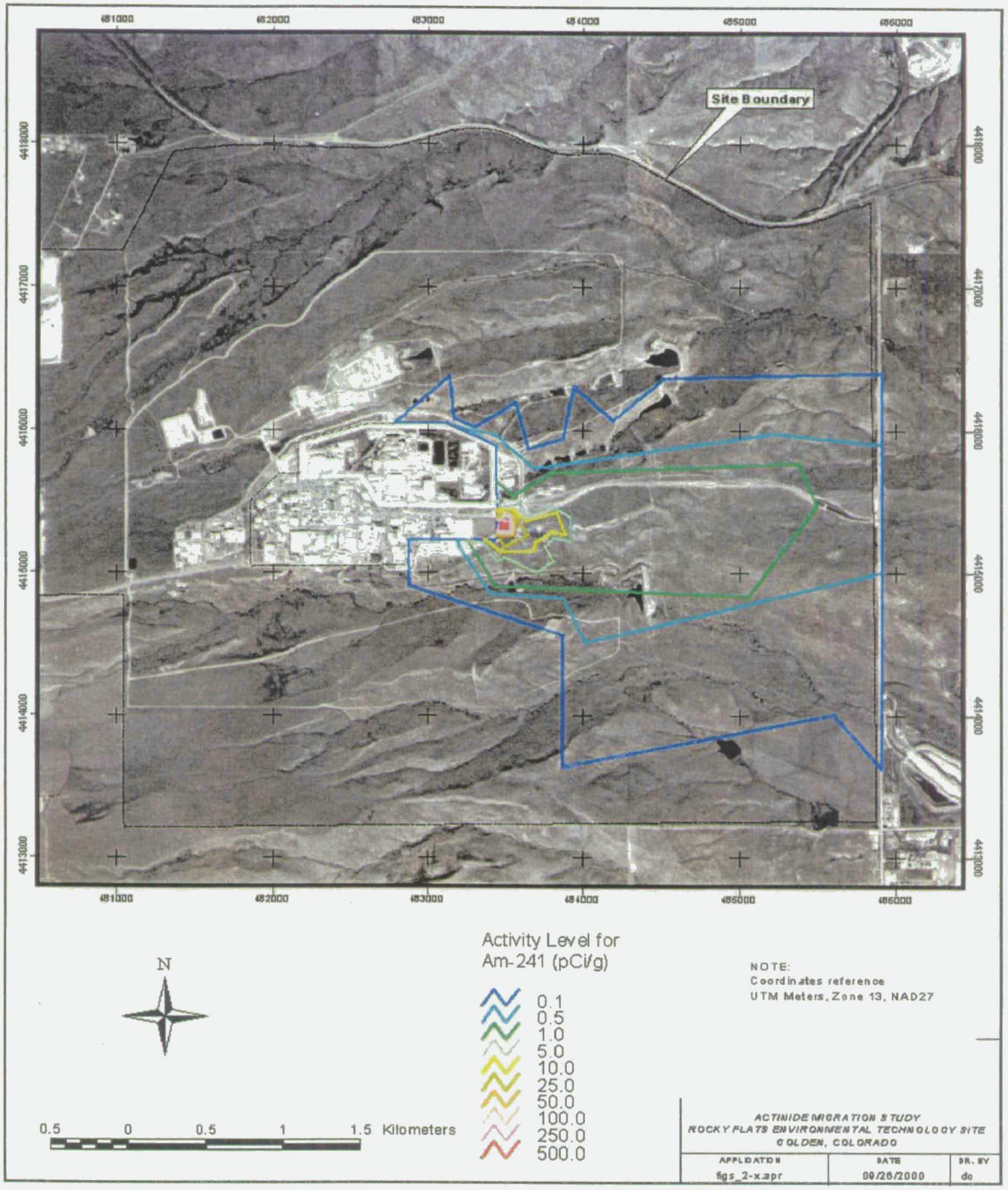

Figure 2-2. Existing Am-241 Source Areas Based on Surficial Soil Contamination

24

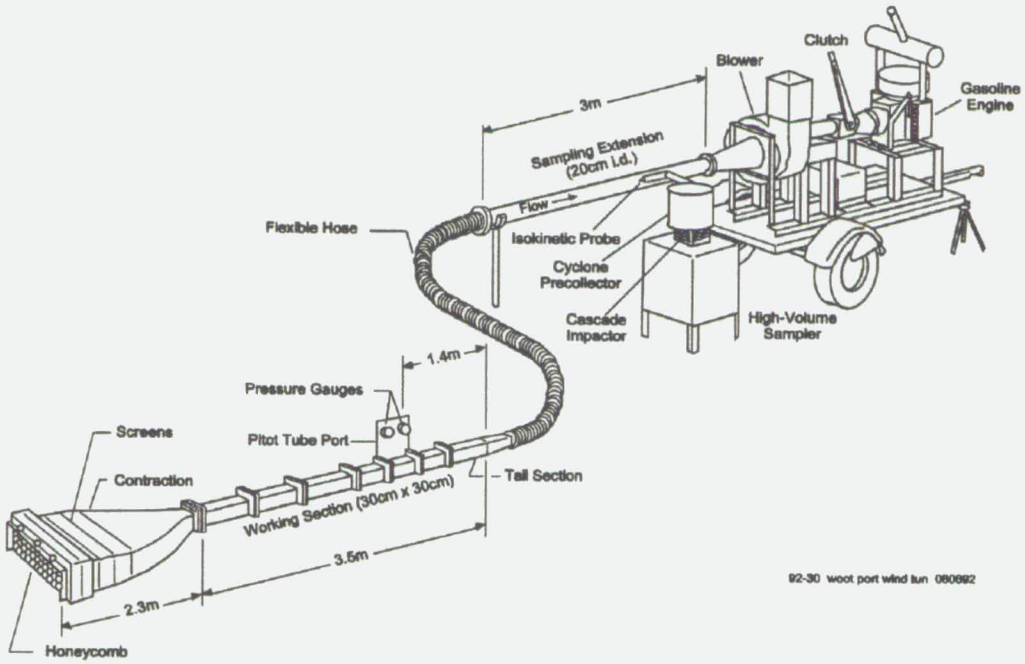

Figure 2-3. MRI Portable Wind Tunnel

For each wind tunnel run, the open-floored test section of the tunnel was placed directly over the surface to be tested. Air was drawn through the tunnel at controlled velocities, increasing at 2 m/s (5 mile per hour [mph]) increments, to a maximum velocity of about 40 mph at the tunnel centerline. This corresponded to a wind speed between 97 and 145 mph at a 10-m height; the equivalent 10-m wind speed varied with the roughness of the surfaces tested in each trial.

Typically, each time the wind speed was increased, a PM_{10} concentration spike was observed on the DustTRAK monitor. Upon each successive increase in wind speed, the peak value of the spike increased and the rate of decay decreased. The PM_{10} concentration values for each wind speed plateau were observable in the "real-time" concentration histories recorded by the DustTRAK monitor. For higher wind speed plateaus, the duration of sampling was increased to allow additional time for the spike to decay. An example of the concentration spikes that occurred during wind tunnel testing on the burned area can be seen in Figure 2-4.

The exit air stream from the wind tunnel test section was passed through a circular duct fitted with a sampling probe near the downstream end. The particulate matter sampling train consisted of the tapered sampling probe, a cyclone pre-collector, a quartz backup filter, and a high-volume motor. Sampled total airborne particulate (TP) emissions were separated into two particle size fractions by the cyclone—particles larger than PM_{10} were collected inside the cyclone, and PM_{10} was collected on the backup filter below the cyclone.

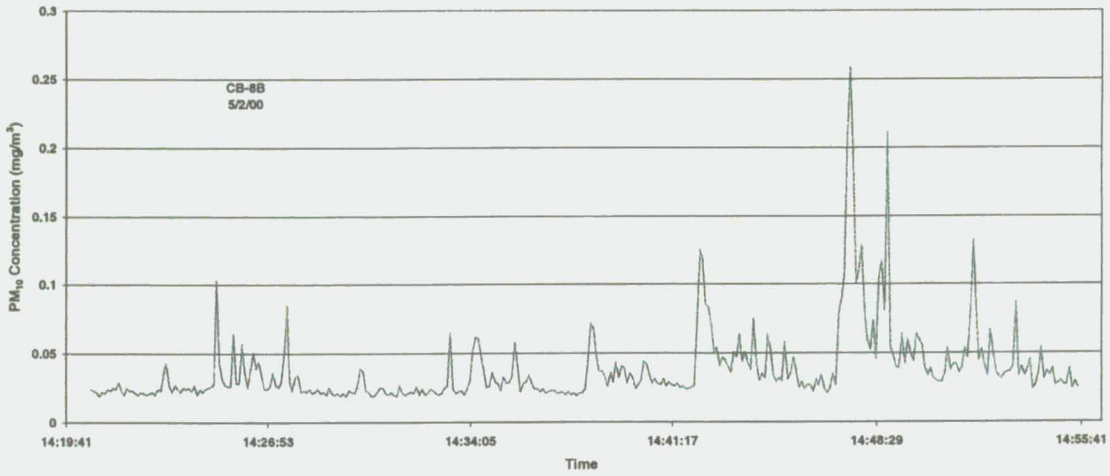

Figure 2-4. Example PM_{10} Concentration History From Wind Tunnel

A high-volume ambient air sampler was operated near the inlet of the wind tunnel to provide for measurement and subtraction of the contribution of the ambient background particulate level. The filter was vertically oriented, parallel to the tunnel inlet face.

At the completion of each test series, the sampling train was disassembled and taken to the field instrument van, where the collected samples of dust emissions (cyclone catch and backup filter) were placed in protective containers. Dust samples from the field tests were returned to an environmentally controlled laboratory for gravimetric analysis.

2.2.2 DustTRAK Monitoring

Continuous monitoring of particulate concentrations in the sampling extension provides for a greater level of detail in tracking the dynamics of the wind erosion process than use of the cyclone and backup filter alone. For this study, a portable DustTRAK Aerosol Monitor (TSI, Inc., St. Paul, Minnesota) was used to continuously sample the air between the cyclone and the backup filter to track the PM_{10} concentrations in the tunnel effluent.

The DustTRAK monitor is a portable, battery-operated instrument that gives real-time measurements and has a built-in data logger. The operating principle of the DustTRAK is based on 90° light scattering. Light scattering (deflection) is caused by the presence of particles whose sizes are comparable to the wavelength of the incident light. The theoretical detection efficiency peaks at about 0.2-0.3 μm and gradually decreases for larger particle sizes. A pump draws aerosol into the optics chamber where particles are detected. The instrument can store measurements for later trending and reporting.

26

It should be noted that the actual average PM_{10} concentration in the tunnel effluent was several times higher than the average PM_{10} concentration indicated by the DustTRAK. This reflects the fact that while the coarse mode of PM_{10} (particles larger than 2.5 μm) constitutes much of the PM_{10} sample mass, these larger particles do not scatter light very effectively. Calibration of DustTRAK results to backup filter mass corrected for this bias.

2.2.3 Test Analysis

Because wind erosion is an avalanching process, it is reasonable to assume that the loss rate from a surface is proportional to the amount of erodible material remaining:

$$\frac{dM}{dt} = -kM \qquad (2)$$

where:

M is the quantity of erodible material on the surface at any time in grams per square meter (g/m^2);
k is a proportionality constant, in inverse seconds (s^{-1}); and
t is the cumulative erosion time in seconds (s).

Integration of Equation 2 yields:

$$M = M_o e^{-kt} \qquad (3)$$

where:

M_o is the erosion potential (i.e., quantity of erodible material present on the surface before the onset of erosion), g/m^2.

For a specific surface, the erosion potential is dependent not only on the wind speed, but also on the frequency of disturbance (each time that a surface is disturbed, its erosion potential is restored).

The loss of erodible material (g/m^2) from the exposed surface area during a test (assumed equal to the erosion potential) is calculated:

$$L = \frac{CQt}{A} \qquad (4)$$

where:

C is the average particulate concentration in the tunnel exit stream (after subtraction of background concentration), g/m^3;
Q is the wind tunnel flow rate in cubic meters per second (m^3/s); and

A is the exposed test surface area (0.918 square meters [m^2] for the reference wind tunnel).

Alternatively, the erosion potential can be directly calculated from the cyclone and filter net mass (after correction for background).

The approach taken in this study was to expose each test surface to a well-defined time history of increasing wind speeds, while simultaneously monitoring the PM_{10} concentration in the tunnel effluent. Each time the wind speed was increased, a concentration spike was observed. Whenever a surface is tested at sequentially increasing wind speeds, the measured losses from the lower speeds are added to the losses at the next higher speed and so on. This reflects the hypothesis that if the lower speeds had not been tested beforehand, correspondingly greater losses would have occurred at the higher speeds.

The logging mode of the DustTRAK provided 6-second average concentration values for each of the test runs. After subtracting out a minimum value assumed to be background, these values were used to find an average concentration value from the beginning of the test run to the end of the run time for each 10-m wind speed. The average concentration, along with the tunnel volumetric flow rate, the length of time from the beginning of the test until the end of the specified wind speed plateau, and the exposed test surface area were used to determine the (cumulative) erosion potential for that wind speed. The test results for each test surface also included the cumulative particle mass loss from the surface, equivalent to the erosion potential for a maximum wind speed.

2.2.4 Test Results

PM_{10} erosion potentials for the two unburned area tests are shown in Figure 2-5 as a function of 10-m equivalent wind speed. The June tests showed lower emissions than the April tests because the growth of vegetation over time provided a greater degree of erosion protection to the soil surface, thatch, and lower portions of the vegetation. Overall, the PM_{10} erosion potential for the unburned grassland remained consistently low between early April and late June, in the range of 0.05 g/m^2 or less.

2.2.5 Use of the Wind Tunnel Data in Emission Estimates

The wind tunnel results shown in Figure 2-5 were used to revise the wind resuspension equation that was developed in FY99 (Equation 1).

Several differences between the 1993 OU3 data set and the test burn data set should be noted. First, the OU3 test equipment did not use DustTRAK monitors or their equivalent to monitor and record "real time" concentration data. As a result, the emissions could

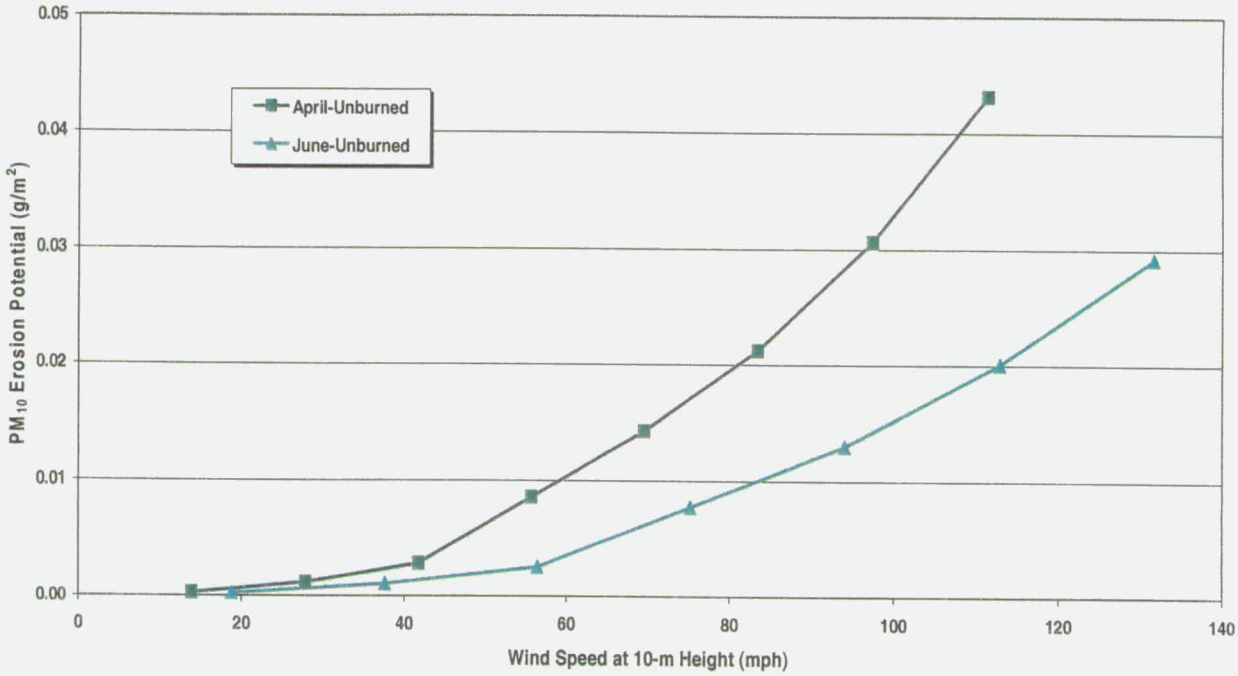

Figure 2-5. Wind Tunnel Test Results

only be expressed as a function of the **maximum** wind speed tested during each OU3 trial—intermediate values could not be obtained.

Second, the OU3 data used previously were for the total suspended particulate (TSP) size fraction, generally representing particles smaller than approximately 30 μm aerodynamic diameter. In contrast, the test burn data were recorded as TP, which includes larger particles (up to 100 μm or larger), and PM_{10}, particles smaller than 10 μm. Much like the OU3 data, emissions for the larger fractions were only available from the test burn data as a function of maximum wind speed during a given trial because the DustTRAK monitors do not record emissions of larger particles (larger particles do not scatter light effectively). For this study, emissions of TSP were desired because TSP represents the size range for which ambient monitoring data are available at and around the Site. Consequently, TSP emissions had to be developed indirectly from the data shown in Figure 2-5.

A third difference was that OU3 data were expressed as emission rates ($g/m^2/s$), whereas the test burn data are expressed as erosion potentials (g/m^2), representing the total mass of material available for resuspension at a given wind speed. As can be seen from Figure 2-4, erosion potential is rapidly depleted at a given wind speed. For this project, a key assumption was that the entire mass available for resuspension at a given wind speed (as shown in Figure 2-5) would be eroded over a 15-minute period of steady winds at that

speed; additional wind duration at the same speed would produce no further erosion until the erosion potential was renewed.

Finally, the vegetation cover differed between the OU3 wind tunnel tests and the April and June 2000 tests. Vegetation was sparser in the OU3 areas that were tested than is currently seen over much of the Site. As a result, the 2000 tests are more representative of current Site conditions. The changes in vegetation cover are related to a parameter called the roughness height, which was measured for each wind tunnel trial. For comparison, average roughness height increased from 0.61 centimeters (cm) in the OU3 tests to 1.44 cm in April and 3.22 cm in June 2000.

2.3 FY01 Revised Particulate Matter Emissions

This section describes the revised wind erosion emission methodology that was developed in FY01. Application of the revised emission method is described in Section 3.0 of this report.

2.3.1 Revised Emission Equation

The data shown in Figure 2-5 were converted to TSP erosion potentials by assuming that the average ratio of PM_{10} to TSP-size particles in the particulate matter collected by the wind tunnel was 0.39. This ratio was based on the average PM_{10}/TSP ratio observed in ambient particulate matter collected around the perimeter of the Site by the Colorado Department of Public Health and Environment (CDPHE), Air Pollution Control Division (APCD) (CDPHE, 1996). For comparison, the average ratio of PM_{10} to total particulate (TP) collected by the wind tunnel for the two unburned area trials was 0.24.
After conversion to TSP, a power function was fitted to the resulting combined April and June unburned area data ($R^2 = 0.88$). The resulting erosion potential equation, as a function of 10-m wind speed in meters per second, is:

$$EP = 3.933 \times 10^{-6} (U^{2.516}) \qquad (5)$$

where:

EP is the TSP erosion potential per 15-minute period in grams per square meter (g/m^2); and
U is the 10-m wind speed (m/s).

2.3.2 Application of the Revised Equation

The meteorological data collected at the Site is routinely processed into 15-minute averages. The 15-minute data were obtained for 1996 (the data year used for the dispersion modeling) and the above equation was applied to each 15-minute average,

30

10-m wind speed. A sequential file of **potential** emissions of particulate matter from undisturbed areas of the Site (g/m^2/15-minutes) was generated for the year.

As noted previously, however, wind erosion emissions are a function not only of wind speed but are also dependent on mechanisms such as periodic disturbances that act to renew the erosion potential of the surface. If erosion potential is not renewed following an erosive event, additional emissions will not occur. Consequently, **actual** wind erosion emissions will be a function of potential emissions, coupled with the amount of erodible particulate matter present on Site surfaces during any given time period. If potential emissions exceed the amount of erodible material, actual emissions will be limited to the mass of particles that constitute the erodible material "reservoir".

How frequently and to what extent is Site erosion potential renewed by disturbances? In most of the Site Buffer Zone, large-scale disturbances (i.e., excavations, traffic, etc.) are rare and isolated. Instead, small-scale disturbances are expected to occur fairly frequently due to freeze/thaw action, burrowing animals, movement of large animals such as deer over the surface, splashing caused by raindrops, disturbance of surface crusts by vegetation growth, and turbulence caused by dust devils and thunderstorm convective activity. These frequent small disturbances renew erosion potential to some extent, but no measurements of this phenomenon are available for the Site.

Erosion potential is also renewed by deposition of airborne particulate matter. There is always some particulate matter in the air over the Site and it is constantly being deposited on Site soil and vegetation surfaces. Deposition rates will vary with wind speed and other conditions. For example, high winds may resuspend dust that is then redeposited at the end of the erosive episode. As with small-scale generation of erosion potential, the dynamic nature of deposition has not been measured at the Site.

In the absence of specific data regarding the rate and dynamics of deposition and erosion potential generation by small-scale disturbances, the revised emission estimating procedure assumed that both phenomena occur at a relatively constant rate over the year. This allowed the amount of erodible material available for resuspension to be tracked over time as the erodible material reservoir was renewed by deposition and small-scale disturbances and depleted by resuspension. For each 15-minute period of the year-long data set, the mass of particles in the erodible material reservoir was compared with the potential particulate matter emissions defined by Equation 5. Actual particulate matter emissions were calculated as the lesser of the potential emissions or the amount of material available for resuspension at the appropriate wind speed. "Leftover", unresuspended material was carried forward to the next 15-minute period, so that during periods of low wind speeds, the "available material" reservoir was built up and during windy periods it was depleted. A computer code was written to track these dynamics, which are described in greater detail in Section 3.0 of this report.

2.3.3 Effect of Snow Cover and Precipitation

As in previous years (see Radian, 1999 and Radian, 2000), it was assumed that no wind erosion emissions would occur while there was snow cover. The presence or absence of snow cover was determined from solar reflectance (albedo) data; the information was applied in the emission tracking program so that no emissions were calculated for periods when snow cover was present. Deposition and small-scale erosion potential generation were assumed to continue during snow cover periods.

The effect of precipitation was also considered. Tests performed on soil samples from the wind tunnel test areas showed that moisture is very effective in limiting PM_{10} erosion potential. As moisture was increased from 2% to 8% in laboratory testing, the potential for release of airborne PM_{10} was seen to decrease by over an order of magnitude. Consequently, no wind erosion emissions were expected to occur from soil surfaces during precipitation events and for a short period thereafter as the soil was drying.

It should be noted that this assumption does not take into account Langer's observations (1986) that some Pu-239/240 emissions were evident from the areas around the 903 Pad even when the ground was saturated. Langer attributed this phenomenon to resuspension of dust directly from vegetation surfaces, which would dry faster than the soil surface. As a result, the treatment of precipitation effects in this simulation, as described below, may underestimate emissions immediately following precipitation events. This simplifying assumption was made because emissions during these periods are expected to be relatively small; however, it may be desirable to treat precipitation effects in a more complex manner in future enhancements to the modeling method.

For the revised emission estimating method, the extent of the period following a precipitation event during which wind erosion emissions were eliminated was based on the amount of precipitation and on soil temperature, both of which were obtained from Site 1996 meteorological data records. Higher soil temperatures were assumed to speed the restitution of erosion potential by increasing moisture evaporation rate.
Hours of zero erosion potential (ZEP_h) were calculated for each 15-minute interval in the 1996 data set using the following equations:

When the soil temperature was below 15°C (59°F):

$$ZEP_h = 50(p) \qquad (6)$$

where:

p is inches of precipitation in a 15-minute period.

38

When soil temperatures were between 15°C and 21°C (59° - 70°F):

$$ZEP_h = 50(p)(0.75) \quad (7)$$

where:

p is inches of precipitation in a 15-minute period; and
0.75 is a moisture impact reduction factor for warm soil.

When soil temperatures were between 21°C and 27°C (70° - 81°F):

$$ZEP_h = 50(p)(0.525) \quad (8)$$

where:

p is inches of precipitation in a 15-minute period; and
0.525 is a moisture impact reduction factor for warmer soil.

When soil temperatures were above 27°C (81°F):

$$ZEP_h = 50(p)(0.2625) \quad (9)$$

where:

p is inches of precipitation in a 15-minute period; and
0.2625 is a moisture impact reduction factor for warmest soil.

These factors were developed in consultation with MRI personnel and are largely based on their previous experience in measuring and studying wind erosion phenomena.

For each precipitation event, the subsequent number of hours of zero emissions was converted to a sequential number of 15-minute periods, which, in turn, were converted to flags that were used by the tracking program to determine whether emissions would occur for a given 15-minute period. As with snow cover, deposition and small-scale generation of erosion potential were assumed to continue during periods of no emissions due to precipitation effects.

2.3.4 Initial Erosion Potential

To initialize the simulation, the particulate matter erosion potential was set to 0.128 g/m^2 TSP at the beginning of the year (equivalent to 0.05 g/m^2 PM_{10} erosion potential, slightly higher than the average erosion potential measured during the April and June 2000 wind tunnel trials for the unburned areas).

2.3.5 Deposition Inputs

The renewal of erosion potential through deposition of particulate matter was estimated using APCD monitoring data. The APCD monitors PM_{10} and TSP concentrations at five locations around the Site perimeter. Monthly average TSP concentrations from four of the locations were averaged for each month in 1996 and used to estimate particulate matter deposition across the Site. Data from the fifth location (X-5, located along the northwest Site boundary on Highway 93) were excluded because they showed locally increased concentrations of particulate matter due to traffic, quarry operations, and sand and gravel extraction. Monthly TSP concentrations, which ranged from a low of 1.52 x 10^{-5} g/m^3 in December 1996 to a high value of 4.76 x 10^{-5} g/m^3 in July 1996, are plotted in Figure 2-6.

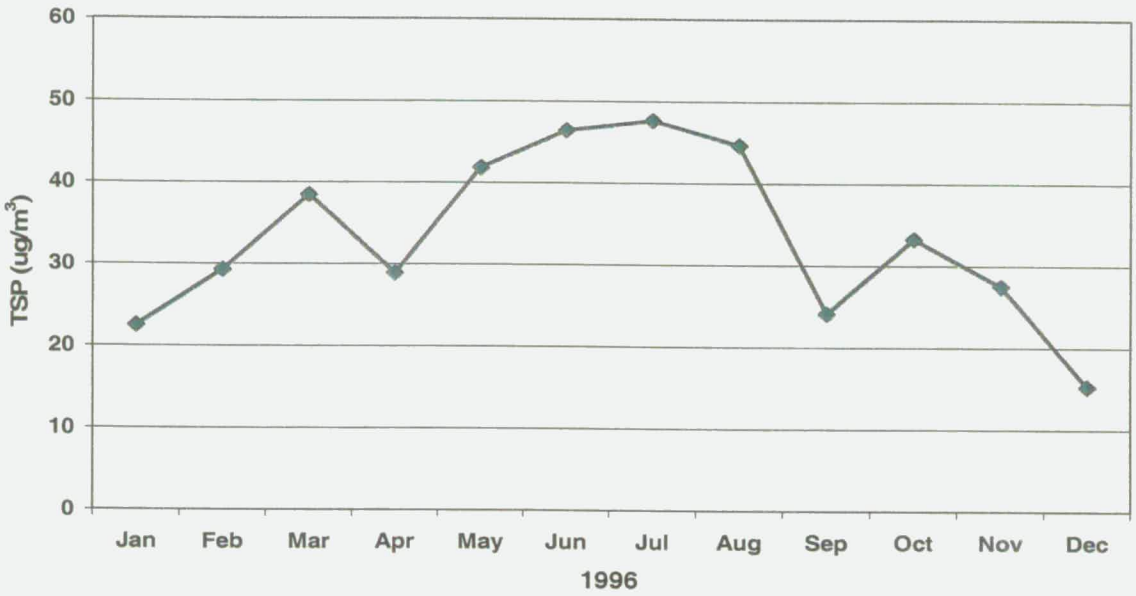

Figure 2-6. Monthly Average TSP Concentrations at the Site in 1996

Particulate matter deposition was calculated by multiplying the average monthly concentration of TSP (in g/m^3) by a deposition velocity (in m/15-minute time step) to yield deposition estimates (in g/m^2/15-minute period) for each month. Hourly deposition velocities were calculated for three particle-size ranges using an algorithm contained in the *User's Guide for the Industrial Source Complex (ISC3) Dispersion Models* (EPA, 1995) and 1996 meteorological data for the Site. The size ranges used were 1-3 μm, 3-15 μm, and 15-30 μm. Mass fractions for these size ranges were determined by Langer

(1986) for airborne particulate matter near the 903 Pad, as described in Radian, 2000, Section 2.2.1. Langer's mass fraction data were used to calculate mass-weighted average deposition velocities for each hour of the 1996 data set. Because there was little hour-to-hour variation in the calculated deposition velocities, an annual average particulate matter deposition velocity of 17.73 m/15-minutes (equivalent to 1.97 centimeters per second [cm/s]) was used in the simulation.

2.3.6 Small-Scale Disturbances

The rate of ongoing erosion potential renewal through small-scale disturbances was estimated indirectly. In 2000, a calculation was performed to determine the net loss of Pu-239/240 and Am-241 from the Site each year through the air pathway, based on the results of FY00 post-closure simulation modeling (Radian, 2000, Section 7.3). Similar calculations have been performed for current Site conditions using the FY00 emission estimating and modeling methodology. The resulting net loss was estimated as 0.000418 curies per year (Ci/yr) Pu-239/240 and 0.000062 Ci/yr Am-241. In addition, a "lower-bound" net loss estimate based on annual average wind data for the Site and annual average perimeter monitoring data suggest that the net loss is at least 0.0000199 Ci/yr Pu-239/240 and 0.0000115 Ci/yr Am-241. These monitoring-based estimates are expected to be low, perhaps by an order of magnitude or more, because they do not adequately capture the gust-driven dynamics of the wind resuspension process. Both modeling- and monitoring-based net loss estimates excluded regional background concentrations of Pu-239/240 and Am-241 from the calculations and should therefore represent the off-Site movement of **Site-generated** actinide emissions through the air pathway.

The modeling-based net loss estimates were used to calculate the rate at which erosion potential is renewed by small-scale disturbances. Basically, an assumption was made that an ongoing actinide loss from the Site through the air pathway can only be sustained by the corresponding generation of new, erodible actinide-containing material in at least equal amounts. The total annual net loss of Pu-239/240 and Am-241 from the Site was partitioned among the actinide source areas based on their size and soil activity levels (in $pCi/m^2/yr$ for each source area). The estimated loss rate from each source area was used to calculate a rate of generation of particulate matter erosion potential by factoring out the soil activity concentration levels ($pCi/m^2/yr$ divided by $pCi/g = g/m^2/yr$). These values were converted to particulate matter generation per 15-minute time step, assuming that erosion potential renewal is constant throughout the year. The resulting estimate of particulate matter erosion potential generation through small-scale disturbances was 0.00112 g/m^2/15-minute period. (This value was later decreased to 0.00067 g/m^2/15-minute period for the final modeling; see Section 3.3.)

35

2.4 Revised Actinide Emissions

As described previously, actual particulate matter emissions were calculated by comparing the potential emissions, based on 15-minute wind speeds, snow cover information, and precipitation data, to the amount of available erodible material for each 15-minute period. Actual emissions were the lesser of the potential emissions or the available erodible material.

To model actinides, the estimated actual particulate matter emissions for each 15-minute period (in g/m^2/15-minute period) were combined with information regarding the activity concentration of the available particulate matter (in pCi/g) to yield estimated actinide emissions (in pCi/m^2/15-minute period). This required tracking additional information for each actinide source area.

While both potential and actual particulate matter emissions were assumed to be uniform across undisturbed areas of the Site, actinide emissions will vary by source area. The renewal of erosion potential by small-scale disturbances will generate erodible material that will reflect the actinide concentration levels in the underlying surface soil. The renewal of erodible material by deposition, in contrast, will generate erodible material that will reflect the actinide concentration levels in the air over the Site. The calculation of source-specific erodible activity is described below.

2.4.1 Deposition Inputs

To calculate the rate of activity deposition, average airborne actinide concentrations were estimated over each of the actinide source areas. (Note that only Pu-239/240 and Am-241 were modeled for the revised simulation; therefore, air concentrations were determined for these two actinides only.) The Site operates a network of ambient radioparticulate samplers at various locations across the Site and at the Site perimeter (Radioactive Ambient Air Monitoring Program [RAAMP]). Monthly average actinide concentration data were obtained for 14 samplers around the Site perimeter and for a location just east of the 903 Pad for 1997 through 1999. These data were averaged for each location; the resulting 3-yr average Pu-239/240 and Am-241 concentrations were used to estimate air concentrations over other portions of the Site, as described below. The locations of the samplers used in this analysis are shown in Figure 2-7.

Air concentrations of Pu-239/240 and Am-241 over the Site were assumed to reach a maximum at sampler S-107. Sampler S-107 is located just east of the 903 Pad, which is thought to represent the major source of emissions of these two actinides at the Site during the 1997 through 1999 period. Actinide concentrations were assumed to decrease from S-107 to each of the perimeter samplers according to a power curve relationship. This assumption was based on the fact that the decrease in the underlying surface soil

36

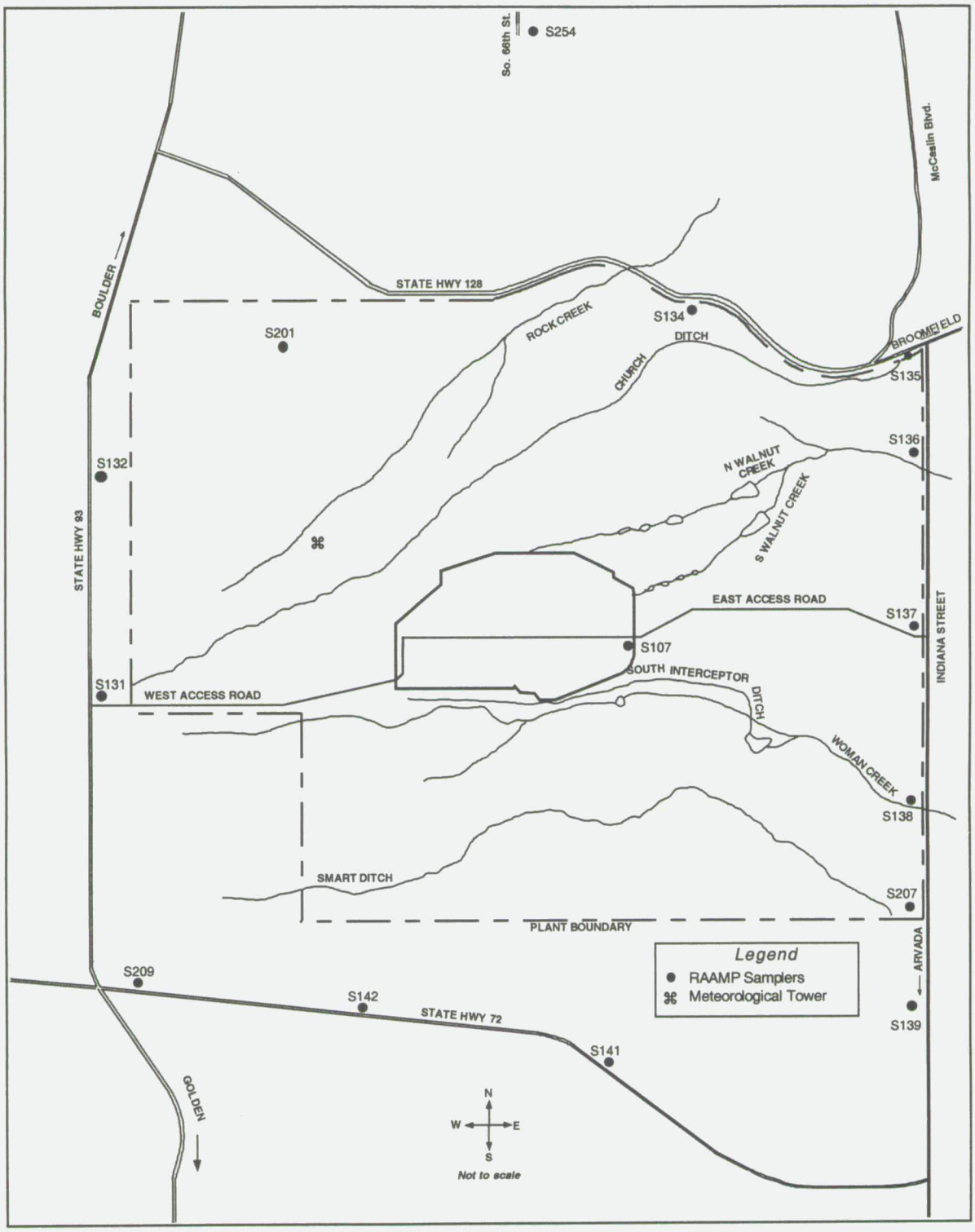

Figure 2-7. RAAMP Sampler Locations

37

concentrations outward from the 903 Pad can be represented by a power curve relationship that varies by direction (Radian, 2000).

Power curves were estimated for each pair of samplers, where a pair consisted of S-107 and a perimeter sampler, based on 3-yr average Pu-239/240 data. Each sampler-specific power relationship was then applied to the 3-yr average concentrations of Pu-239/240 and Am-241 at S-107 to estimate distances to a series of selected concentration levels along each sampler-specific "radial". The matrix of distances was used to produce annual average air concentration isopleths over the Site for Pu-239/240 and Am-241. The air concentration patterns were mapped to the actinide source areas used for emission estimation and modeling, and average concentrations of Pu-239/240 and Am-241 were determined for each actinide source area.

As with particulate matter, deposition of actinides was estimated by multiplying an average air concentration (in picocuries per cubic meter [pCi/m^3]) by a deposition velocity (in m/15-minutes) to calculate deposition of Pu-239/240 and Am-241 (in pCi/m^2/15-minute period). Hourly deposition velocities were calculated for three particle size ranges using an algorithm contained in the *User's Guide for the Industrial Source Complex (ISC3) Dispersion Models* (EPA, 1995) and 1996 meteorological data for the Site. Activity fractions were also determined by Langer (1986) for these size ranges from airborne particulate matter near the 903 Pad (Radian, 2000, Section 2.3). Langer's activity fraction data for Pu-239/240 were used to calculate activity-weighted average deposition velocities for each hour of the 1996 data set. Because there was little hour-to-hour variation in the calculated deposition velocities, an annual average actinide deposition velocity of 21.90 m/15-minutes (equivalent to 2.433 cm/s) was used in the simulation. Rates of erosion potential renewal by actinide deposition were tracked separately for each actinide source area.

2.4.2 Small-Scale Disturbances

The ongoing generation of actinide erosion potential was described in Section 2.3.6. As with deposition, the period-by-period renewal of erosion potential through this mechanism was tracked separately for each actinide source area.

2.4.3 Calculation of Actinide Emissions

For each actinide and source area, the available activity was initialized by multiplying the initial particulate matter erosion potential (0.128 g/m^2 TSP) by the pCi/g activity concentration in the soil.

For each 15-minute time period, the increase in available erodible activity was calculated due to deposition and small-scale disturbances for each actinide and source area (in picocuries per square meter [pCi/m^2]) and added to the erodible activity remaining from

38

the previous time step. The activity concentration of the available erodible material was calculated by dividing the total pCi/m^2 for each actinide and source area by the total available particulate matter (in g/m^2) for each time step. The resulting pCi/g value determined for each actinide and source area was then multiplied by the calculated actual particulate matter emissions for each time step to determine actinide emissions.

A computer code was written to track these dynamics and to produce a variable emission rate file for each source area for input to ISCST3. A program listing is given in Appendix B.

3.0 REVISED WIND EROSION MODELING

As described in Section 2.0, the method used to estimate actinide emissions due to wind erosion was extensively revised. Revised emission estimates for current (pre-closure) Site conditions were modeled and compared to measured concentrations of airborne actinides. This section presents a brief overview of the modeling methods used and describes the results of the initial modeling efforts, the results of various sensitivity analyses, and the final emission equation selected for use in additional modeling. Pre-closure wind erosion emissions were modeled over the entire Site area and the results of those analyses are also presented in this section.

3.1 Modeling Methods

Predicting the impact of various emission events at the Site requires the use of a dispersion model to simulate the transport of pollutants from emission locations to other locations of interest (termed receptors). The air pathway work performed in FY99 reviewed a variety of model formulations and concluded that the Industrial Source Complex Short-Term model (ISCST3), a Gaussian plume formulation, would be the best model for this application. ISCST3 is described in detail in the *User's Guide for the Industrial Source Complex (ISC3) Dispersion Models, Volumes I and II* (EPA, 1995) and is also described briefly in the FY99 air pathway report (Radian, 1999).

As in the FY99 and FY00 air pathway studies, ISCST3 was used to estimate the transport of airborne actinides from source areas to the Site fenceline (dispersion) and their removal from the air to soil or water surfaces (deposition). Particles are brought down to the surface through the combined processes of turbulent diffusion, wet deposition, and gravitational settling. Once near the surface, they may be removed from the atmosphere and deposited on soil or vegetation. Other forces such as electrophoresis and thermophoresis also enhance particle deposition on vegetation. These processes gradually reduce the amount of particulate matter remaining in the plume as it is transported downwind.

To perform these calculations, ISCST3 needs information about source characteristics, meteorological conditions, dispersion modeling option selections, and receptor locations. To account for deposition, particle size categories must also be defined for each source. Associated with each particle size category is a mass (or actinide activity) fraction, a particle density (in grams per cubic centimeter [g/cm^3]), and a particle diameter. The particle density and diameter affect gravitational settling, with larger and more dense particles depositing closer to their area of origin than smaller or less dense particles. Particle size category bounds were chosen based on the joint particle size/actinide activity data available for airborne particulate matter at the Site (Langer, 1986).

As previously discussed, the main source of resuspended actinides at the Site is the area surrounding the 903 Pad. The plutonium particles in the cutting oil that leaked at the 903 Pad were small (<3 μm diameter). Once in contact with the soil, however, the plutonium particles became attached to soil particles. As a result, the transport of plutonium is dependent on the soil or aggregate particle properties and not the properties of the individual plutonium particles. The same is true of americium because Am-241 occurs in association with Pu-239/240 contamination at the Site due to americium ingrowth into decaying weapons-grade plutonium (Am-241 is formed by radioactive decay of Pu-241 atoms).

The modeling methodology used for the FY01 air pathway studies was generally the same as that described in Radian, 2000 (see Section 2.3 of that report). The current version of the ISCST3 model (Version 00101) was used in the analysis. The following inputs were unchanged from the FY00 analyses:

- Model options;
- Receptor grid;
- Meteorological data;
- Spatial definition of source areas; and
- Source inputs for deposition.

3.2 Modeling Wind Erosion for Existing Site Source Areas

The revised wind erosion emissions of Pu-239/240 and Am-241 described in Section 2.4 were modeled using 1996 meteorological data. The source areas used were those shown in Figures 2-1 and 2-2. Annual average concentration estimates were predicted for the RAAMP sampler locations shown in Figure 2-7.

3.2.1 Initial Modeling Results

In FY99, a comparison was made between the modeling results for the wind erosion scenario and air quality sampling data from a limited number of ambient samplers at the Site. The comparison used data paired by location and time period. Because the meteorological data were from 1996, the sampling data used in the comparison were also limited to 1996. As described in the FY99 air pathway report (Radian, 1999), the 1996 sampling data set was very limited: samples were routinely analyzed from only three locations in 1996 and the only isotope analyzed for was Pu-239/240 until late in 1996.

The FY99 report determined that the modeling seemed to overestimate concentrations by one to two orders of magnitude. Possible reasons for the apparent overpredictions were explored and included the fact that the model, as run, did not account for plume depletion by deposition. The emission estimating method also ignored dilution of soil actinide levels by deposition of uncontaminated particulate matter. Refinements were made to the

41

modeling for FY00 to account for plume depletion but dilution of the erodible material could not be addressed. Several other minor revisions were also made to the emission estimating and modeling methods between FY99 and FY00.

The wind erosion scenario was remodeled in FY00 and a similar comparison to sampling results was made. Impacts were predicted at receptors representing 15 RAAMP sampler locations (the RAAMP sampler locations are shown in Figure 2-7). RAAMP data for Pu-239/240 and Am-241 were analyzed for 1996 through 1999, so that instead of pairing the data by time and location, as was done in FY99, the data were paired only by location. Although both Site activities and weather have varied from year to year, there is substantial consistency over this time period in the overall magnitude and patterns in the sampling data.

An interesting pattern was apparent in the FY00 modeling results. Modeled concentrations for both actinides were generally higher than measured values (although lower than the FY99 modeled values) in the dominant downwind directions. In contrast, the model appeared to underpredict measured concentrations at samplers in other directions from the 903 Pad by up to an order of magnitude.

The results of the initial FY01 modeling using the revised wind erosion emissions were again plotted against 1996 through 1999 RAAMP data. The results of the comparison are shown in Figures 3-1 through 3-4, along with the results of the FY99 and FY00 modeling for the same scenario. The first two figures, Figures 3-1 and 3-2, are plotted on a logarithmic scale and include both S-107 and the perimeter samplers. The second set of figures, Figures 3-3 and 3-4, are plotted on a non-logarithmic scale and exclude S-107, which has concentration values one to two orders of magnitude higher than the perimeter samplers. Perimeter sampler data are graphed beginning at the west gate and proceeding clockwise around the Site.

It is apparent from both sets of figures that the initial FY01 model results are a better match to the monitoring data than the FY99 or FY00 modeling results. The model overpredicted concentrations in the dominant downwind directions only slightly and the underprediction at other samplers was much reduced.

The improved fit is primarily due to two changes in the emission estimating and modeling methodology. First, actinide emissions have been reduced by the following revisions: 1) the exponent in the wind erosion equation has been reduced from 3.014 to 2.516 (as a result, potential emissions increase more slowly as wind speed rises, consistent with other studies of emission dependence on wind speed above a threshold value); 2) the effect of precipitation events and wet soil have been taken into account; and 3) emissions have been limited to the amount of erodible material available for resuspension at any given time during the year. The change in the wind erosion equation

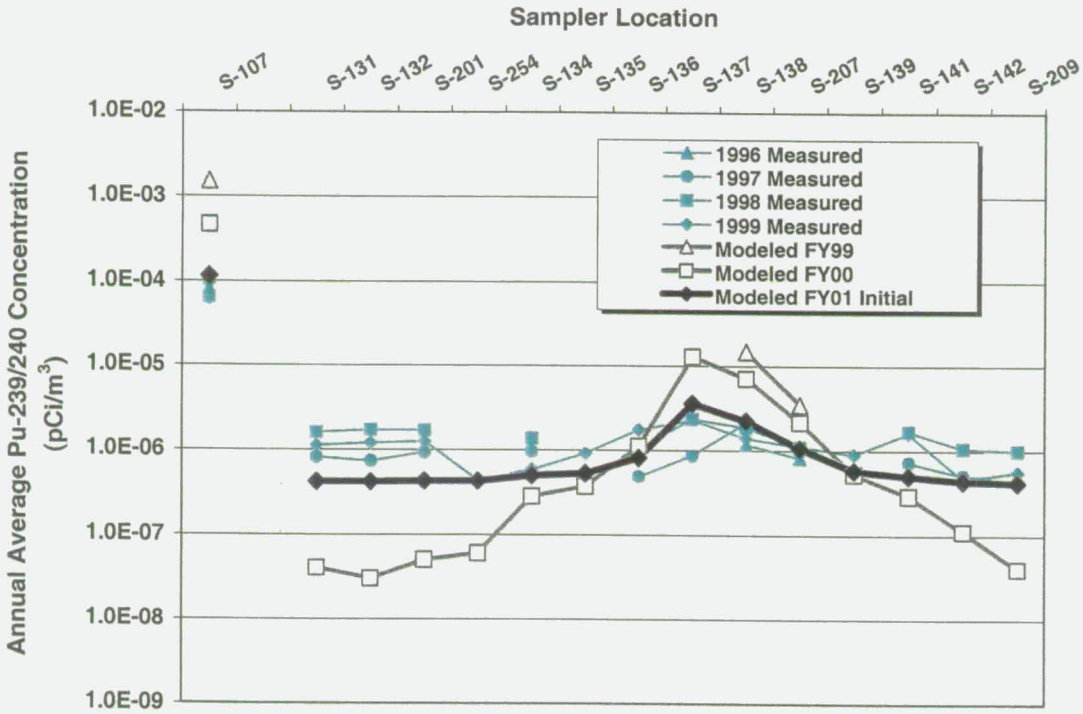

Figure 3-1. Initial Modeling Results for Pu-239/240 (Including S-107)

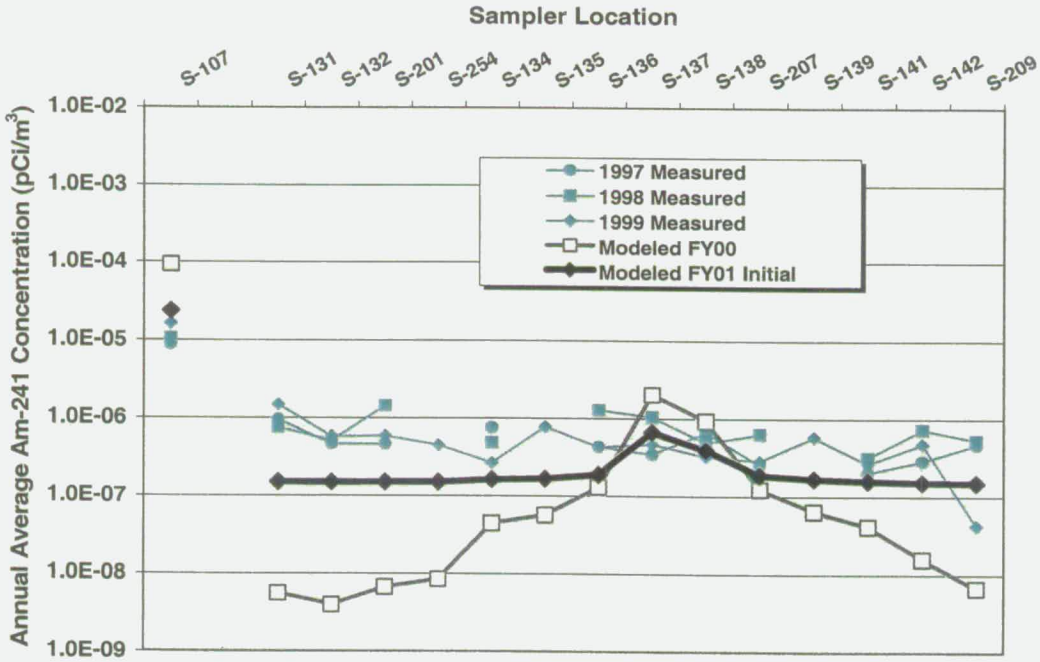

Figure 3-2. Initial Modeling Results for Am-241 (Including S-107)

43

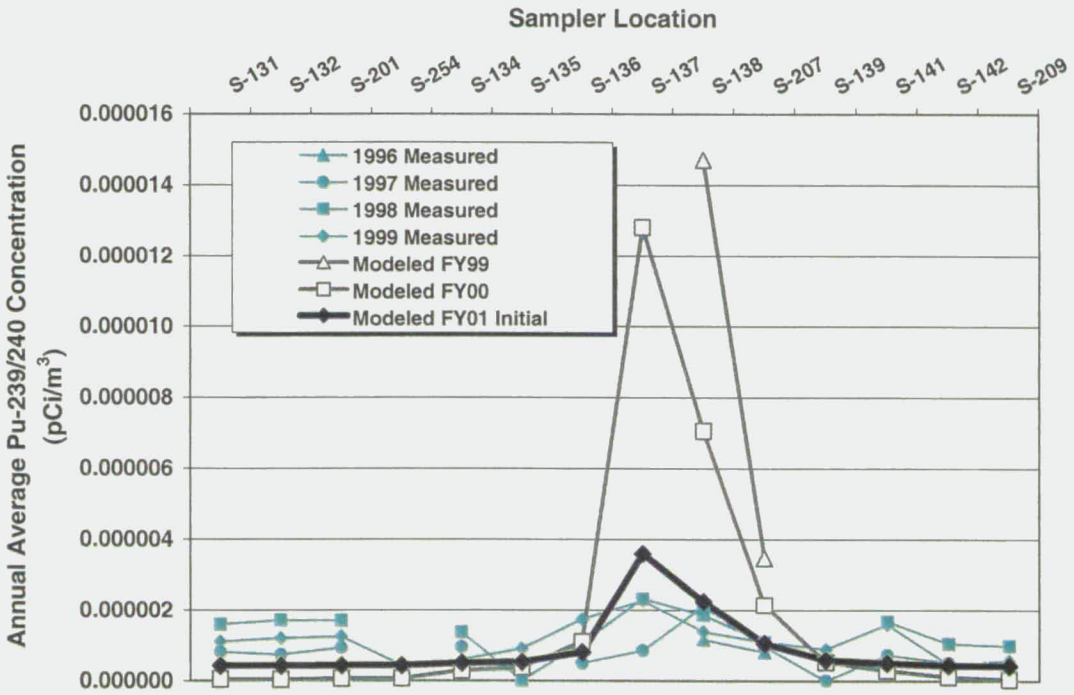

Figure 3-3. Initial Modeling Results for Pu-239/240 (Excluding S-107)

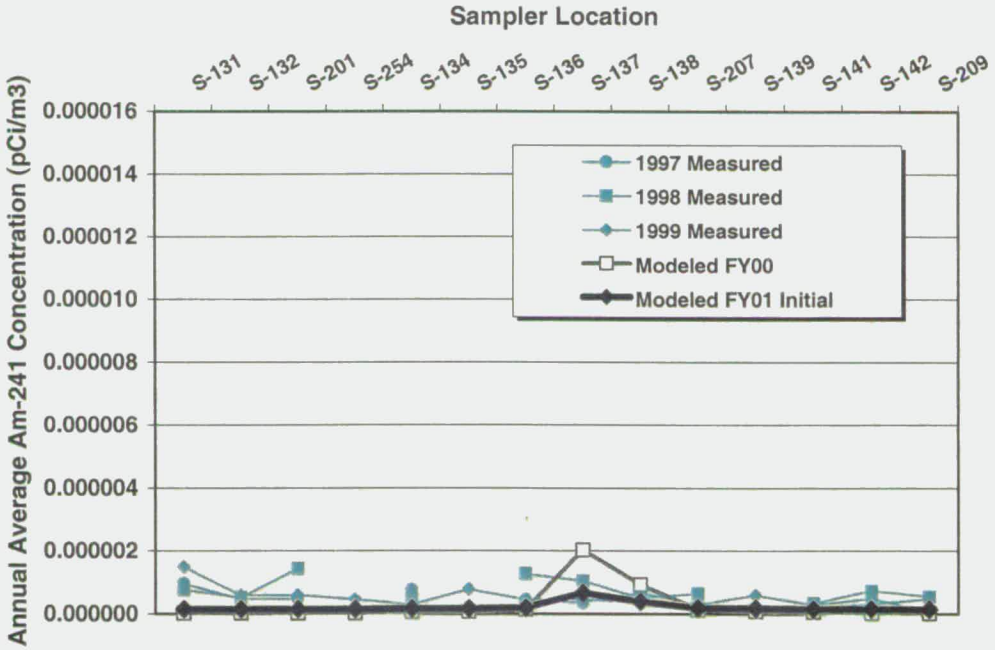

Figure 3-4. Initial Modeling Results for Am-241 (Excluding S-107)

44

(decreased exponent) probably reflects wind tunnel sampling over a more completely vegetated surface than was tested at OU3.

The second factor is the inclusion of background actinide concentrations. Model results were added to regional background concentrations of Pu-239/240 and Am-241 and the combined concentrations are plotted in Figures 3-1 through 3-4. The regional background concentrations, which are described below, do not contribute significantly to total Pu-239/240 or Am-241 concentrations at S-107 and produce only a minor increase in total Pu-239/240 concentrations at samplers along the southeastern fenceline (i.e., at samplers that are in the dominant downwind direction from the 903 Pad). However, regional background concentrations account for nearly all of the Pu-239/240 and Am-241 measured at the "upwind" samplers, as well as nearly all of the Am-241 measured at all locations other than S-107.

3.2.2 Background Actinide Concentrations

Measured airborne actinide concentrations in the vicinity of the Site include both Site contributions and background concentrations of actinides in ambient air (i.e., those naturally occurring and man-made actinides present in the global atmosphere due to fallout from weapons testing, resuspension of isotopes in soils, and other ubiquitous sources). Data from Pan and Stevenson (1996) show that fallout of Pu-239/240 from nuclear testing during the 1950s through 1970s decreased with time following the last atmospheric test in 1980. After 1984, fallout had leveled off, indicating that an equilibrium condition had been reached. Fallout levels of Pu-239/240 are now thought to be due to resuspension of material in the lower atmosphere. During and for a few years after atmospheric testing, fallout was instead controlled by the amount of stratospheric Pu-239/240 that was exchanged with the troposphere and subsequently deposited at the surface.

The following concentrations of Pu-239/240 in air were measured by the EPA Environmental Radiation Ambient Monitoring System (ERAMS) between 1984 and 1992 in locations without localized actinide sources:

- Chicago, IL. 4.0×10^{-7} pCi/m^3
- New York, NY 3.0×10^{-7} pCi/m^3
- Denver, CO 5.1×10^{-7} pCi/m^3
- Portland, OR 3.0×10^{-7} pCi/m^3

These values are in general agreement with the overall magnitude of Pu-239/240 measured in air at other locations globally during similar time periods (Pan and Stevenson, 1996).

45

Fallout of Pu-239/240 is expected to vary between locations due to latitude and climatology, primarily the annual precipitation. Consequently, it is desirable to have more localized estimates of fallout Pu-239/240 levels to apply to the Site environment.

Samplers located in communities surrounding the Site and at some distance from the Site fenceline provide another set of data points. The Community Radiation Monitoring (COMRAD) program operates five monitors to the east of the Site that collect particulate matter on filters that are analyzed for Pu-239/240 on a monthly basis. The Northglenn station is generally downwind of the Site but, as the most distant monitor, is the least likely to show significant Site influence. Airborne Pu-239/240 concentrations at that station averaged 4.1×10^{-7} pCi/m^3 for a recent 18-month period, within the range of concentrations reported for U.S. cities by Pan and Stevenson (1996).

Two other monitoring locations were examined. The Site operated an ambient air sampler in Boulder in the early 1990s that collected samples that were analyzed for Pu-239/240 on a monthly basis. The average Pu-239/240 recorded at that location between 1990 and 1994 was 3.6×10^{-7} pCi/m^3. Finally, a sampler was installed at a distance of approximately 5.8 km to the north of the Site in late 1998, making it the most distant of the Site's perimeter samplers. In 1999, the average annual airborne Pu-239/240 concentration from that sampler totaled 4.35×10^{-7} pCi/m^3.

The results of these comparisons suggest that regional background levels of Pu-239/240 in air due to fallout are somewhere between the concentrations reported by Pan and Stevenson (1996) for Denver (5.1×10^{-7} pCi/m^3) and those reported for New York and Chicago (3.0×10^{-7} pCi/m^3). For use in the modeling analyses, a background concentration of 4.1×10^{-7} pCi/m^3 Pu-239/240 (the Northglenn monitored value) was chosen. (Note that this value does not account for **all** Pu-239/240 in the air in the immediate vicinity of the Site beyond that attributable to wind erosion of Site soils. This is because other sources of Pu-239/240 emissions, including periodic emissions from Site projects and soil disturbance activities, as well as minor amounts of Pu-239/240 emitted from Site stacks and vents, will also contribute to concentrations recorded at the perimeter samplers and S-107.)

Airborne Am-241 background concentrations are more difficult to define due to the lack of studies on this topic. One approach, using the ratio of Am-241 to Pu-239/240 found in Colorado surface soils at some distance from RFETS, would estimate the background concentration of Am-241 to be in the range of 1.1×10^{-7} pCi/m^3 to 1.8×10^{-7} pCi/m^3, based on the previously presented Pu-239/240 data (Hulse et al., 1999). A background value of 1.48×10^{-7} pCi/m^3 Am-241 was used in the modeling analyses.

46

3.2.3 Comparisons With 1996 Data

In addition to the annual simulations described in Section 3.2.1, individual months and 3-month periods were modeled for the three sample locations for which ambient data were available for 1996. Ambient Pu-239/240 concentration data were collected and analyzed as 3-month composite samples for January through March, April through June, and July through September for samplers S-107, S-138, and S-207 in 1996. Beginning in October 1996, ambient Pu-239/240 concentration data were analyzed by month for these three locations.

Figure 3-5 compares predicted Pu-239/240 concentrations at S-107 with measured concentrations for each of these periods in 1996. Predicted concentrations at S-138 and S-207 showed similar patterns; however, the ambient Pu-239/240 concentrations at those locations showed greater variability than those at S-107. Because S-107 is more directly impacted by wind erosion emissions from the 903 Pad area than either S-138 or S-207 (which is what the model is simulating), S-107 provides the most appropriate comparison.

The results show that the model predictions agreed fairly well with measured Pu-239/240 concentrations between July and November, while concentrations for the rest of the year were slightly overpredicted. With the exception of December, modeled concentrations were within a factor of two of the measured values. The model-predicted concentration in December was 2.6 times the measured value.

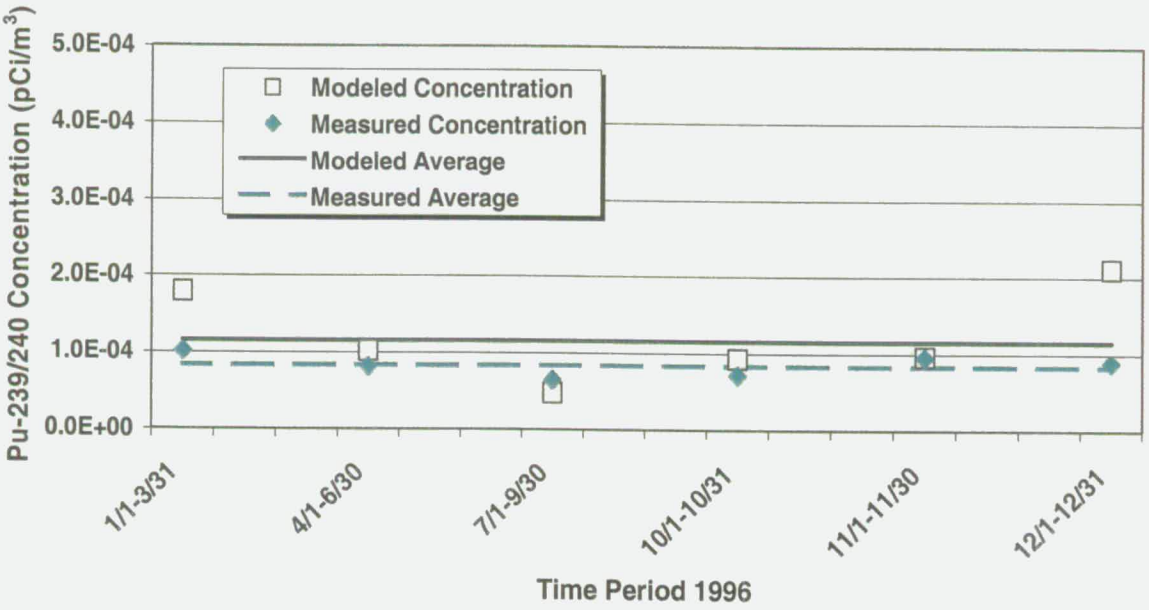

Figure 3-5. Comparison of 1996 Pu-239/240 Concentrations at S-107

47

3.2.4 Sensitivity Analyses

A series of sensitivity analyses was performed to determine which factors had the most and the least influence on the modeled concentrations. For these analyses, Pu-239/240 emissions were recalculated and the model rerun for the full year of meteorological data and all perimeter sampler locations plus S-107.

The following sensitivity tests were conducted:

- Double amount of available erodible particulate matter and Pu-239/240 at beginning of year vs. zero initial concentrations;
- Double vs. halve particulate matter deposition rates;
- Double vs. halve Pu-239/240 deposition rates;
- Double vs. halve both particulate matter and Pu-239/240 deposition rates;
- Double vs. halve erodible material renewal rate due to small-scale disturbances;
- Change emission equation exponent from 2.516 to 2.316 vs. change exponent to 2.716; and
- Revise emission equation assuming PM_{10}/TSP ratio of 0.50 vs. assuming a ratio of 0.24.

Figure 3-6 shows the results of the sensitivity analyses at sampler S-107. Results at other downwind samplers, such as S-137, S-138, and S-207, showed similar patterns. At the upwind samplers, total estimated concentrations of Pu-239/240 continued to be dominated by regional background concentrations.

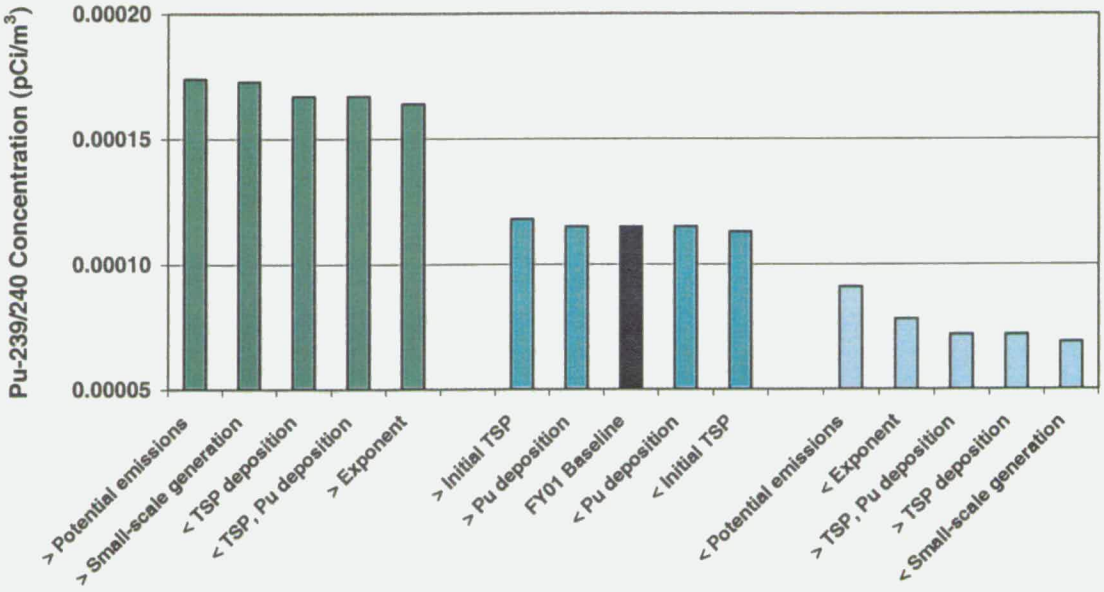

Figure 3-6. Results of Sensitivity Analyses (S-107)

48

The results of the sensitivity analyses show that the amount of available erodible material assumed to be present at the beginning of the year-long simulation and changes in Pu-239/240 deposition rates made little difference in the results. In contrast, changes in particulate matter deposition rates or the rate at which erosion potential is renewed by small-scale disturbances were both important. Increases or decreases in potential particulate matter emissions also significantly influenced annual Pu-239/240 concentrations.

Changes in the rate of deposition of Pu-239/240 made little difference in the final results because deposition adds much less activity to the erodible material than the assumed rate at which erosion potential is renewed through small-scale soil disturbances. The amount of Pu-239/240 in the air over the Site is several orders of magnitude less (on a pCi/g basis) than that present in Site surface soils near the 903 Pad. Erosion potential renewal through small-scale soil disturbances was correspondingly more important in determining airborne actinide concentrations at S-107.

Particulate matter deposition rate was inversely correlated with annual Pu-239/240 concentrations. As a simplifying assumption, the total activity derived from deposition and from soil disturbances was assumed to be thoroughly and homogenously mixed into the erodible particulate matter mass at each time step. As a result, increasing particulate matter deposition diluted the resulting Pu-239/240 emissions and lowered predicted concentrations. Decreasing particulate matter deposition had the opposite effect.

Changes in potential particulate matter emissions also significantly influenced predicted Pu-239/240 concentrations. For the scenario modeled, actual particulate matter emissions were predicted to nearly equal potential particulate matter emissions, indicating that there was sufficient material available for erosion during most or all time steps. As a result, changes in potential particulate matter emissions, either up or down, changed calculated actual particulate matter emissions, thereby affecting the final predicted Pu-239/240 concentrations at S-107.

To provide additional information about emissions, the tracking program summed each of the following items over the year-long simulation:

1) Total potential particulate matter emissions (g/m^2);
2) Total particulate matter deposited (g/m^2);
3) Total erodible particulate matter generated by small-scale soil disturbances (g/m^2); and
4) Total actual particulate matter emissions (g/m^2).

For the baseline scenario (with inputs as described in Section 2.3), potential emissions totaled 12.6 g/m^2 over the year. Small-scale disturbances added approximately 9.8 g/m^2 and particulate matter deposition added about 20.7 g/m^2 over the year, giving an annual

total of 30.6 g/m^2 erodible material. As a result, potential emissions were the limiting factor in determining actual particulate matter emissions in this simulation. However, the sensitivity analyses indicated that when the total annual erodible material dropped to between 20 and 25 g/m^2 (by decreasing either deposition or small-scale disturbances), the actual emissions also decreased, indicating that the erodible material would become limiting under those circumstances.

3.3 Revisions to Emission Estimation Methods

Based on the above comparisons, a decision was made to revise the emission estimating methods as described in Sections 2.3 and 2.4 prior to final modeling. The revisions are described in this section.

In general, the FY01 comparisons showed an improved fit to the RAAMP data compared with FY99 and FY00 modeling analyses. The continued slight underprediction of Pu-239/240 and Am-241 concentrations at upwind samplers is thought to be due to the influence of other Site sources that were not included in the modeling analyses. Emissions from Site projects and soil disturbance activities, as well as Site stacks and vents, contribute a small amount of Pu-239/240 and Am-241 to the local atmosphere. These emissions were not modeled, nor were they reflected, to any great extent, in the background concentrations used in this study. In addition, samplers located near roads and other local dust sources may show elevated concentrations of background Pu-239/240 and Am-241 due to mechanical resuspension of surface dust by traffic. This is probably especially effective for Am-241, which has a higher ratio relative to Pu-239/240 in fallout-derived background material than in Site emissions (for the background values used in this study, Am-241 activity was assumed to be 36% of Pu-239/240 activity, compared to approximately 15% for Am-241 ingrowth into Site weapons-grade plutonium).

The results of the initial revised modeling, discussed in Section 3.2, showed continued slight overpredictions at S-107 and at dominant downwind perimeter samplers. To improve the overall fit to the data, the final simulation decreased the rate of generation of erodible material through small-scale disturbances to 60% of the initial value. Although changes in several parameters would have had similar effects, as shown in Figure 3-6, this variable was chosen because it was considered the most uncertain.

Figure 3-7 shows the results of the revised modeling of Pu-239/240 with small-scale generation of erodible material reduced to 60% of the original value. This method and the input values used formed the basis for revised modeling of post-closure wind erosion and several post-fire scenarios, which are described in Sections 4.0 and 5.0 of this report.

Figure 3-8 shows the improvement of model predictions from FY00 to the final emission method chosen. The graph plots the ratio of the absolute error at each sampler (absolute

50

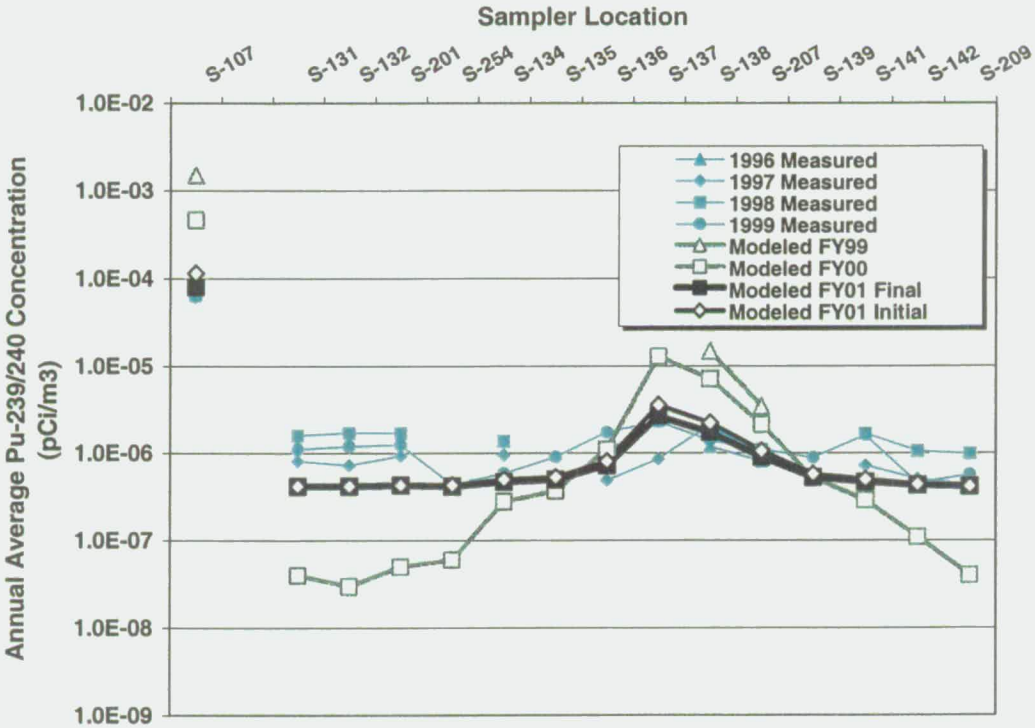

Figure 3-7. Revised Modeling of Wind Erosion Emissions of Pu-239/240

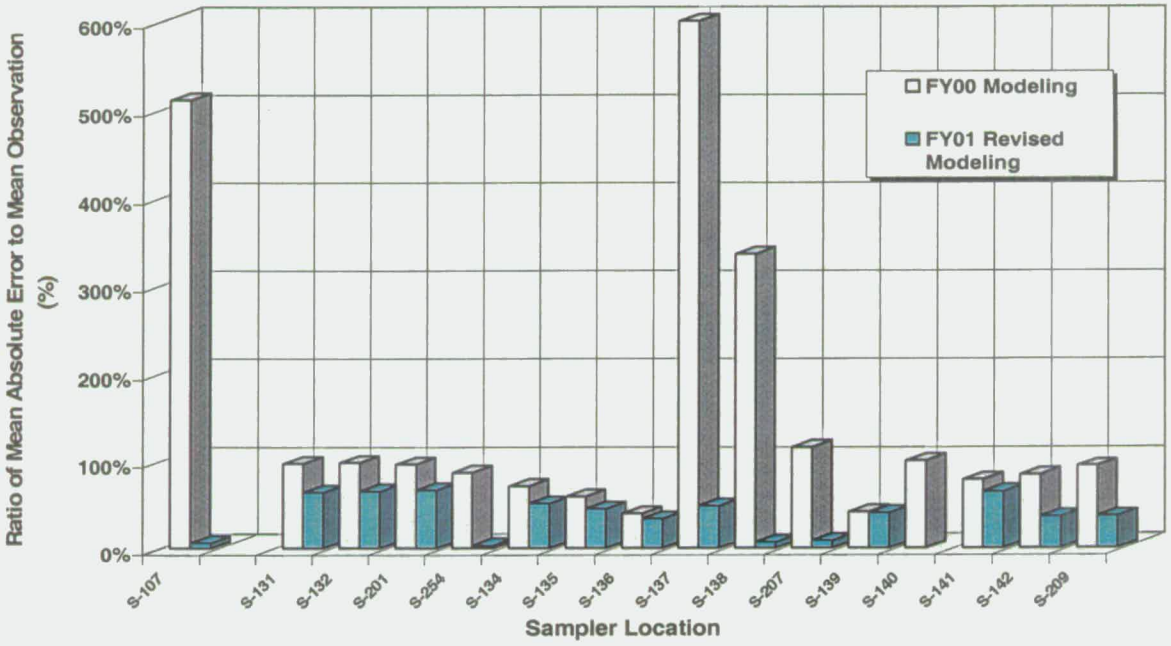

Figure 3-8. Pu-239/240 Error Ratios for FY00 and FY01 Revised Simulations

51

value of the difference between each measured and modeled annual average concentration) to the measured concentration at that sampler for Pu-239/240. For FY00, the ratio was 100% or less of the measured values at the upwind samplers but much larger at samplers in the dominant downwind direction. In contrast, FY01 modeling results show a reduction in the error ratio at upwind samplers due to the addition of background concentrations, while the ratio was decreased substantially at downwind locations due to changes in the emissions methodology.

3.4 Revised Pre-Closure Wind Erosion Results

The final revisions to the emission estimating method described in Section 3.3 were implemented and Pu-239/240 and Am-241 emissions resulting from wind erosion of the existing Site (pre-closure) were modeled. Deposition of actinides was also calculated as described in Radian, 2000, Section 2.3. The results are summarized in Table 3-1 and illustrated in Figures 3-9 through 3-12.

In addition to calculating airborne concentrations of actinides (in units of activity per unit volume of air, e.g., pCi/m^3), results have also been converted to effective dose equivalent (EDE). EDE, measured in units of Sieverts or millirem (mrem), represents the amount of radiation energy absorbed per gram of tissue, weighted by its potential to do damage and the susceptibility for harm to different tissues in the human body.

Conversion from activity to EDE depends not only on the isotope and the type of radiation it emits, but also on assumptions about exposure pathways and scenarios. To simplify this conversion, conversion factors from EPA air regulations were used that are based on standard assumptions about exposure pathways and scenarios. Title 40 of the Code of Federal Regulations (CFR), Part 61 contains requirements governing emissions of hazardous air pollutants from certain source types. DOE facilities such as RFETS are subject to the standards of Subpart H, which limits radionuclide emissions from the facility to those amounts that would result in an annual dose to the public of no more than 10 mrem. Appendix E to 40 CFR 61 gives a table (Table 2) of radionuclide concentrations in air to demonstrate compliance with the Subpart H standard. If a person was exposed to air containing a given isotope at the concentration levels listed in Table 2 for a full year (under the standard exposure assumptions inherent in these values), they would receive a 10 mrem EDE. Therefore, the Table 2 concentration levels can be used to convert between radionuclide concentrations (in curies per cubic meter [Ci/m^3] or pCi/m^3) and EDE (in mrem) for annual scenarios.

For the isotopes of interest in this study, the concentration levels from Appendix E, Table 2 are:

- Am-241 1.9×10^{-3} pCi/m^3
- Pu-239/240 2.0×10^{-3} pCi/m^3

Each of these isotopic concentrations equates to a 10 mrem per year (mrem/yr) EDE rate for the purposes of this modeling study.

For modeling, emissions in units of activity per unit area per unit time ($pCi/m^2/s$) were input for a given isotope, and the concentration results (in units of pCi/m^3) were then converted to units of mrem. The conversion factor for each isotope used the previously listed concentration values, plus the appropriate conversion between a 10 mrem and 1 mrem level.

Table 3-1. Results Summary—Pre-Closure Wind Erosion Scenario

Isotope	Maximum Estimated Annual Concentration (pCi/m^3)[a]		Factor for Conversion of pCi/m^3 to mrem	Maximum Estimated Annual EDE (mrem)	
	On Site	Off Site		On Site	Off Site
Pu-239/240	8.0×10^{-5}	3.5×10^{-6}	5,000	0.40	0.018
Am-241	1.6×10^{-5}	5.3×10^{-7}	5,263	0.08	0.003

Notes:

Am = americium
mrem = millirem
pCi/m^3 = picocuries per cubic meter
Pu = plutonium

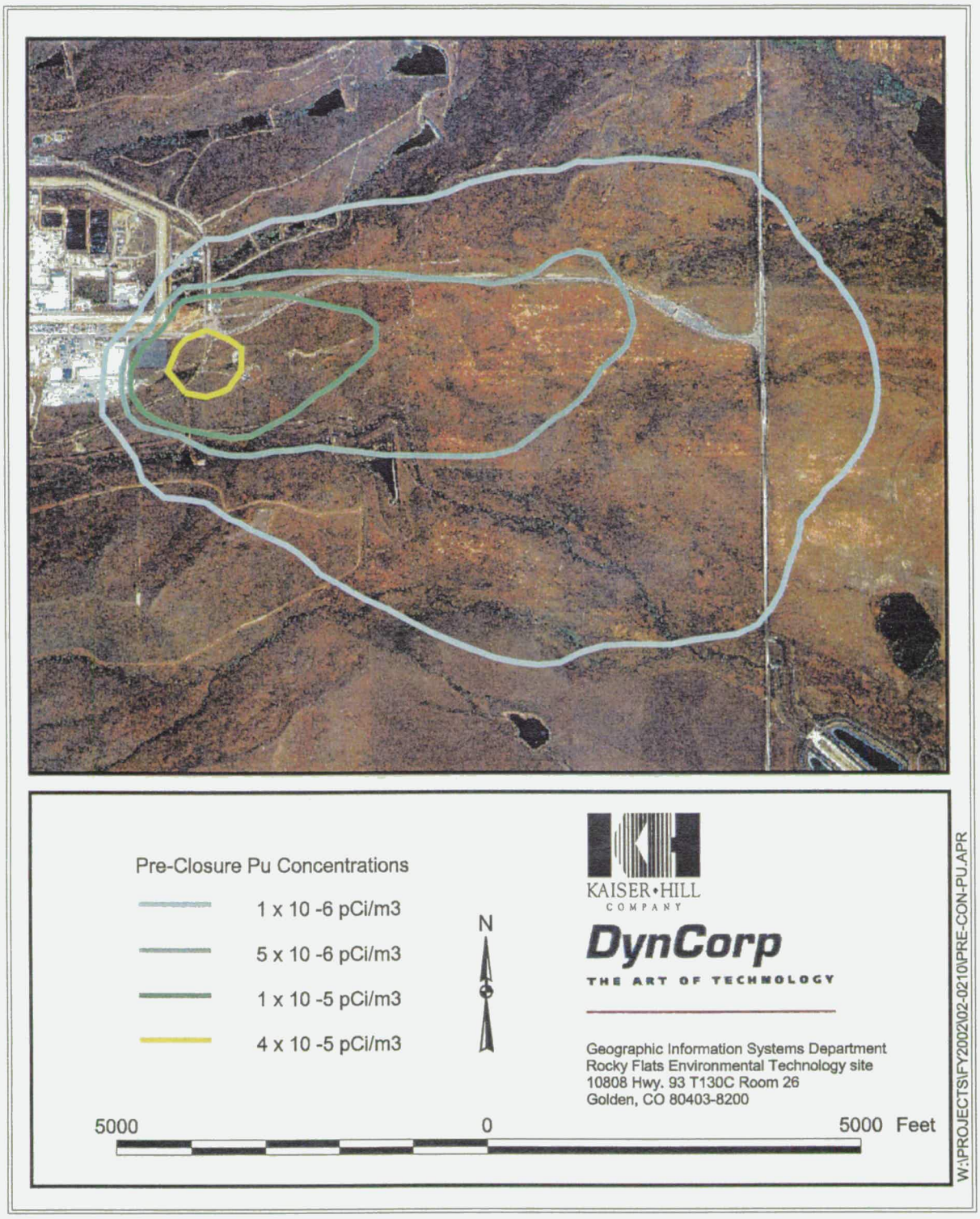

Figure 3-9. Predicted Pre-Closure Annual Average Pu-239/240 Concentrations

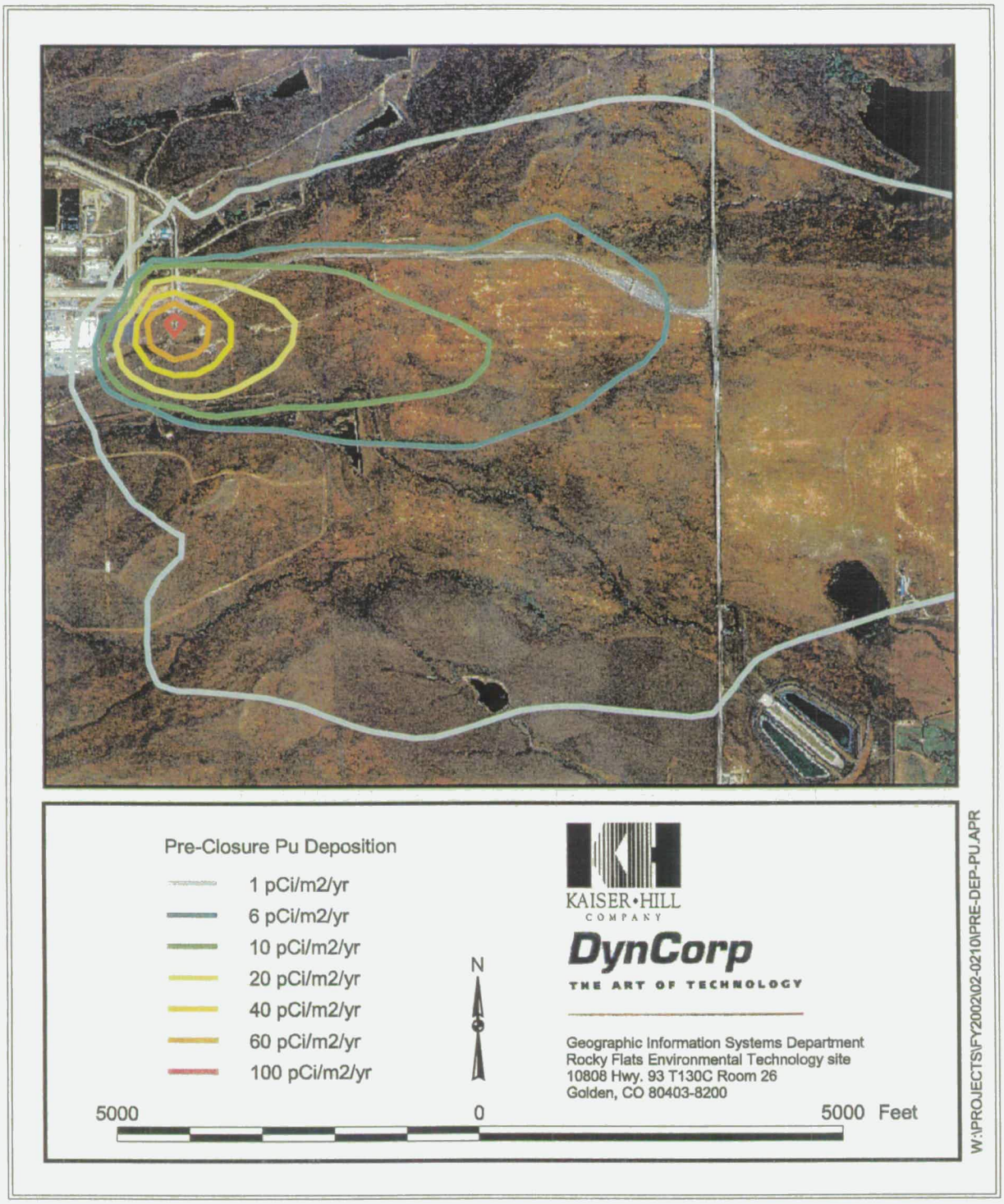

Figure 3-10. Predicted Pre-Closure Annual Pu-239/240 Deposition

55

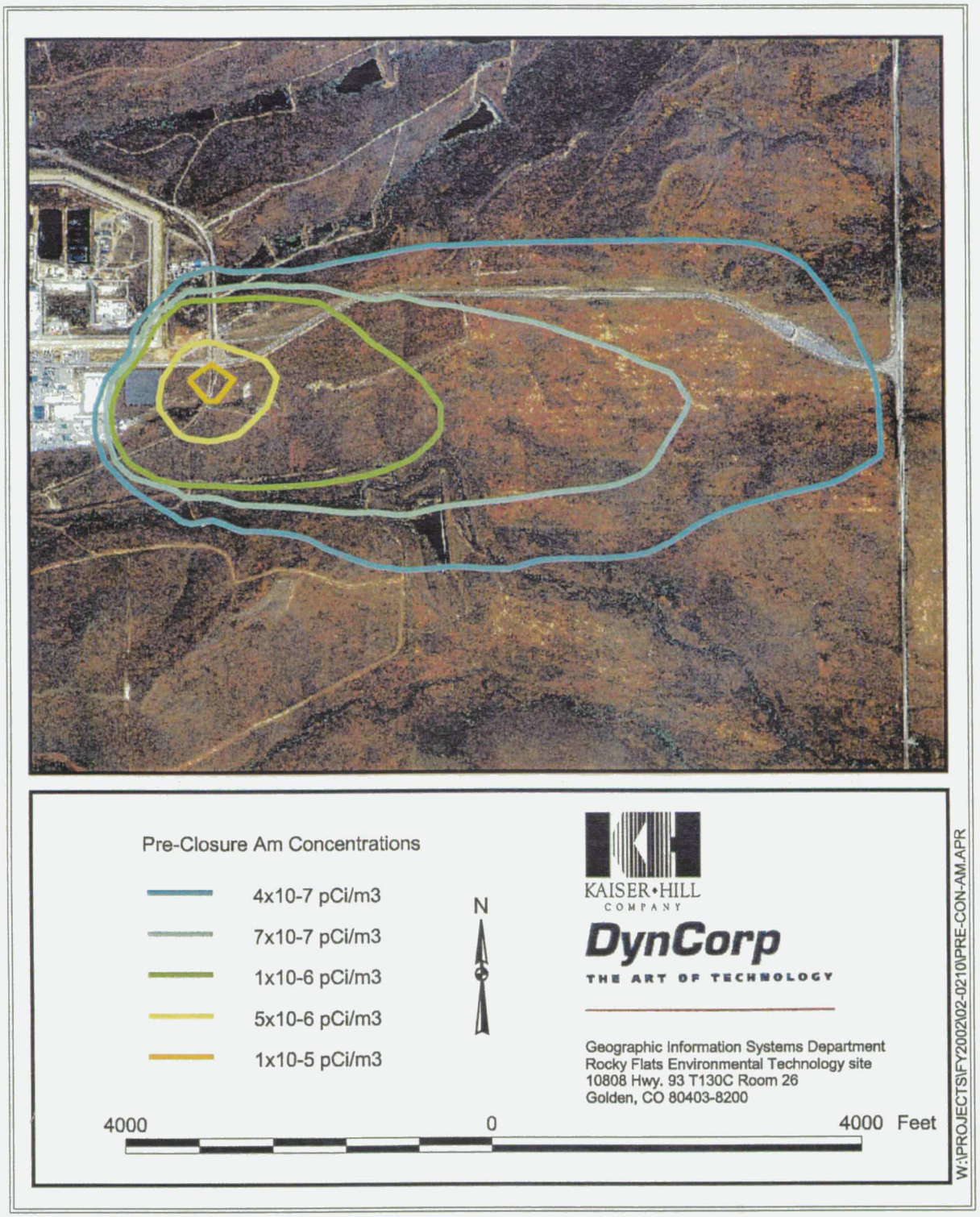

Figure 3-11. Predicted Pre-Closure Annual Average Am-241 Concentrations

56

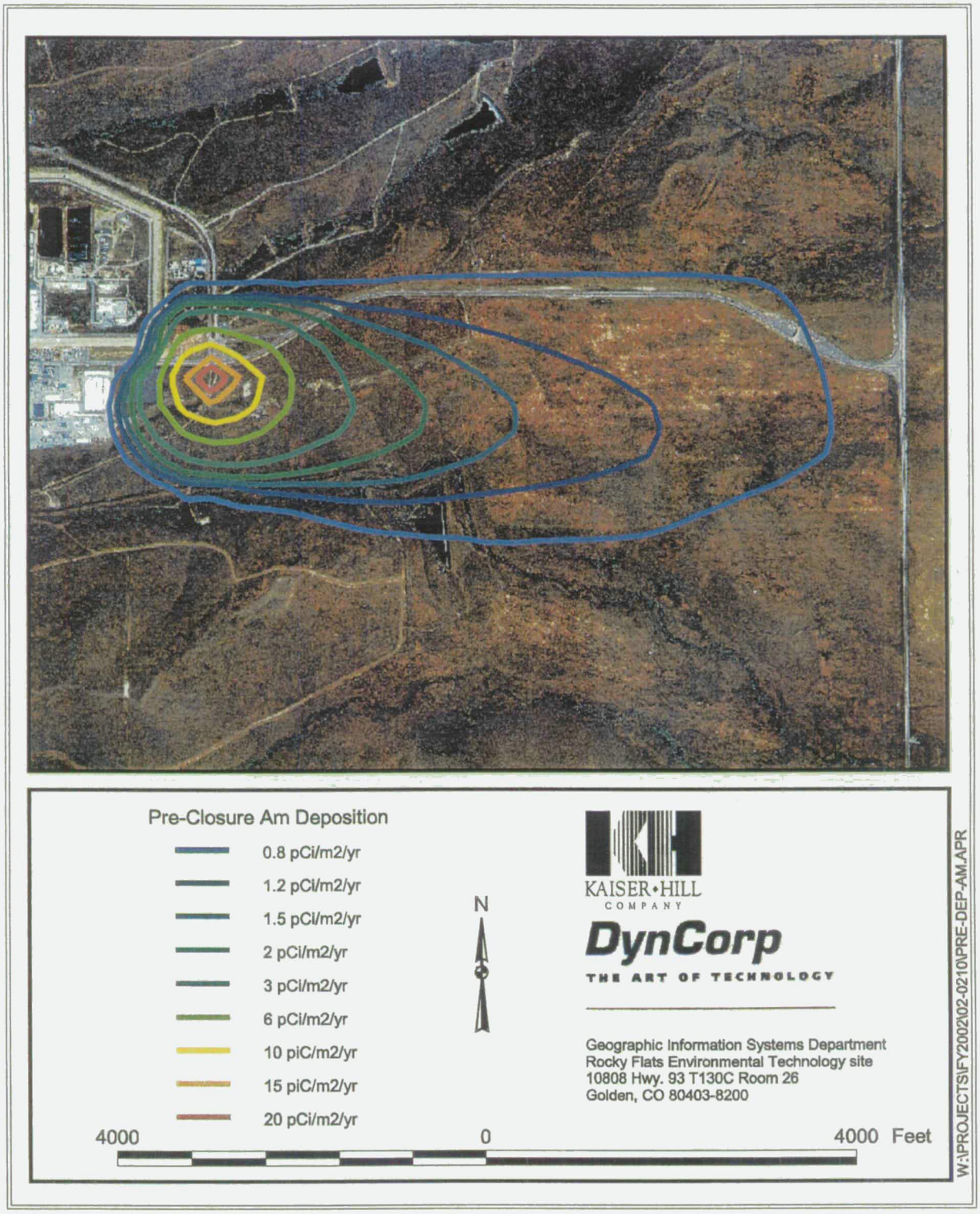

Figure 3-12. Predicted Pre-Closure Annual Am-241 Deposition

57

4.0 POST-CLOSURE WIND EROSION

The post-closure scenario modeled in FY00 was revised using the emission estimating and modeling methods described in Sections 2.0 and 3.0 of this report. Source inputs represented cleanup of soil contamination to the Rocky Flats Cleanup Agreement (RFCA) Surface Soil Action Levels that have been established for actinides at the Site. Post-closure conditions were assumed to include the removal of paved surfaces and building structures, especially in the Industrial Area, therefore allowing for wind erosion from all areas of the Site. This section describes the results of the modeling analysis.

4.1 Scenario Description and Emission Estimation

Closure of the Site will occur after D&D of all existing structures that were associated with historical operation of RFETS. D&D will include the removal of pavement in the Industrial Area, thereby allowing for wind erosion and other natural resuspension mechanisms to act upon these formerly paved, nonerodible surfaces. Radioactive emissions to the atmosphere through wind erosion under post-closure conditions will depend on the activity levels that remain in the soil.

Surface Soil Action Levels for Am-241 and Pu-239/240 that have been established for Tier I, post-closure, open-space land use are shown in Table 6-1 (DOE et al., 1996). Tier I levels are based on an annual multipathway EDE limit of 85 mrem to a hypothetical future resident. The values shown in Table 6-1 were used to determine which sources that had been created for pre-closure wind erosion modeling would be retained for post-closure modeling. Emissions for the post-closure scenario were estimated in the same manner as those for the pre-closure scenario described in Sections 2.0 and 3.0.

Table 4-1. Surface Soil Action Levels for Post-Closure

Radionuclide	Tier I Open-Space Land Use Level (pCi/g)
Pu-239/240	1,429
Am-241	215

Notes:
Am = americium
pCi/g = picocuries per gram
Pu = plutonium

4.2 Modeling Methods

The modeling assumptions and inputs for the post-closure scenario were the same as those used for the revised pre-closure wind erosion scenario, with two primary exceptions. First, the area sources used to represent actinide emissions were expanded to include the areas that were considered nonerodible in the pre-closure scenario, because these areas will be unpaved after closure of the Site. Second, area sources that represented emissions higher than the Surface Soil Action Levels shown in Table 6-1 were removed. Specifically, area sources for Am-241 representing activity levels of 250, 500, and 1,000 pCi/g were removed for the post-closure modeling because these sources were above the Tier I open-space cleanup level for Am-241 of 215 pCi/g.

No area sources were removed for Pu-239/240 because the Tier I open-space cleanup level is higher than any modeled soil activity contour for Pu-239/240. As with Am-241, however, the spatial extent of several Pu-239/240 area sources was expanded with the inclusion of the formerly nonerodible areas.

Figures 4-1 and 4-2 show the post-closure actinide isopleths that were used for modeling.

4.3 Modeling Results

Maximum predicted post-closure concentrations and EDEs are summarized in Table 4-2 for the two actinides modeled. Concentration and deposition isopleths are shown in Figures 4-3 through 4-6.

Table 4-2. Results Summary—Post-Closure Wind Erosion Scenario

Isotope	Maximum Estimated Annual Concentration (pCi/m^3)		Factor for Conversion of pCi/m^3 to mrem	Maximum Estimated Annual EDE (mrem)	
	On Site	Off Site		On Site	Off-Site
Pu-239/240	1.9×10^{-4}	3.9×10^{-6}	5,000	0.95	0.020
Am-241	3.0×10^{-5}	5.7×10^{-7}	5,263	0.16	0.003

Notes:
Am = americium
EDE = effective dose equivalent
mrem = millirem
pCi/m^3 = picocuries per cubic meter
Pu = plutonium

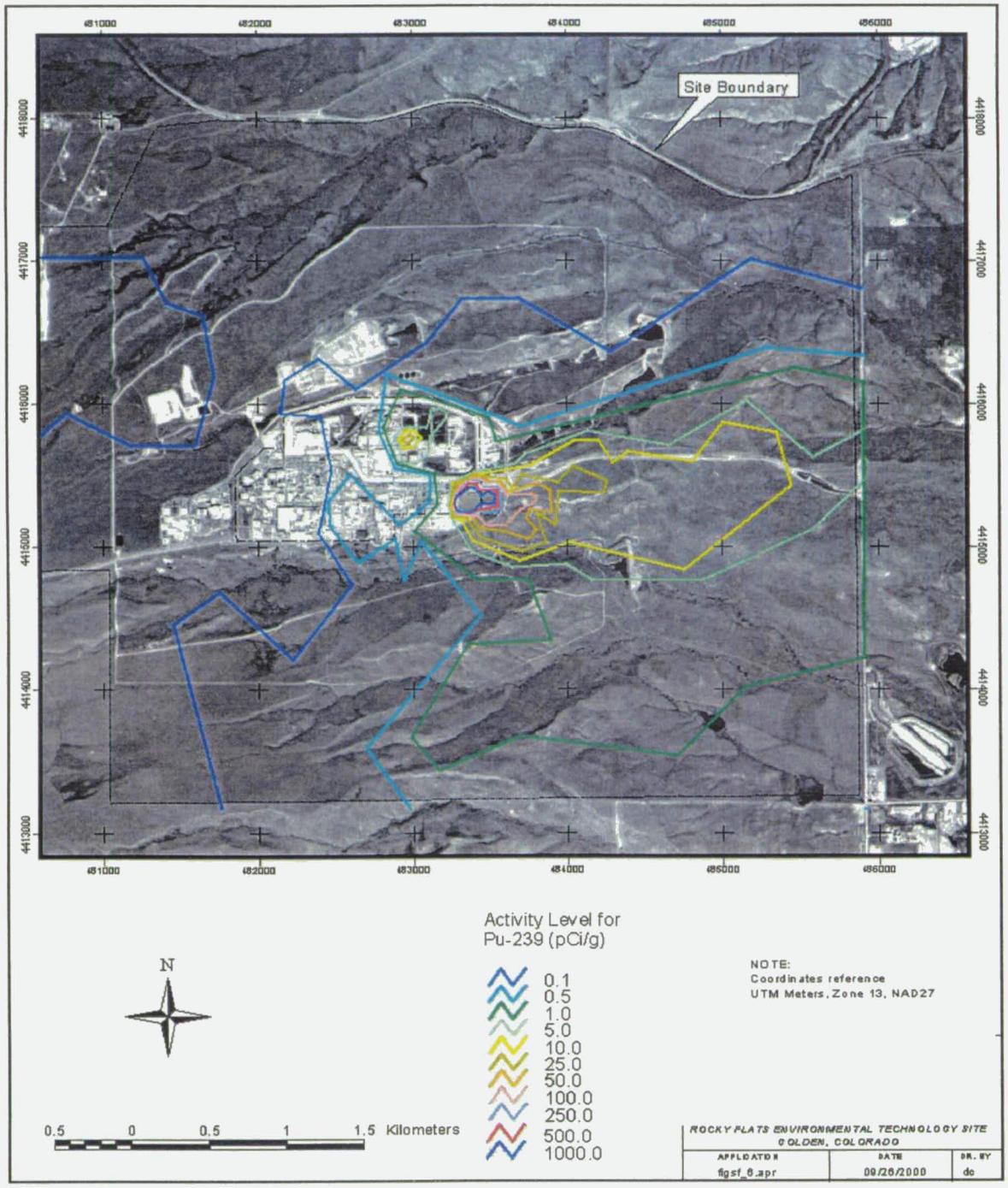

Figure 4-1. Post-Closure Pu-239/240 Source Areas Based on Surficial Soil Concentrations

60

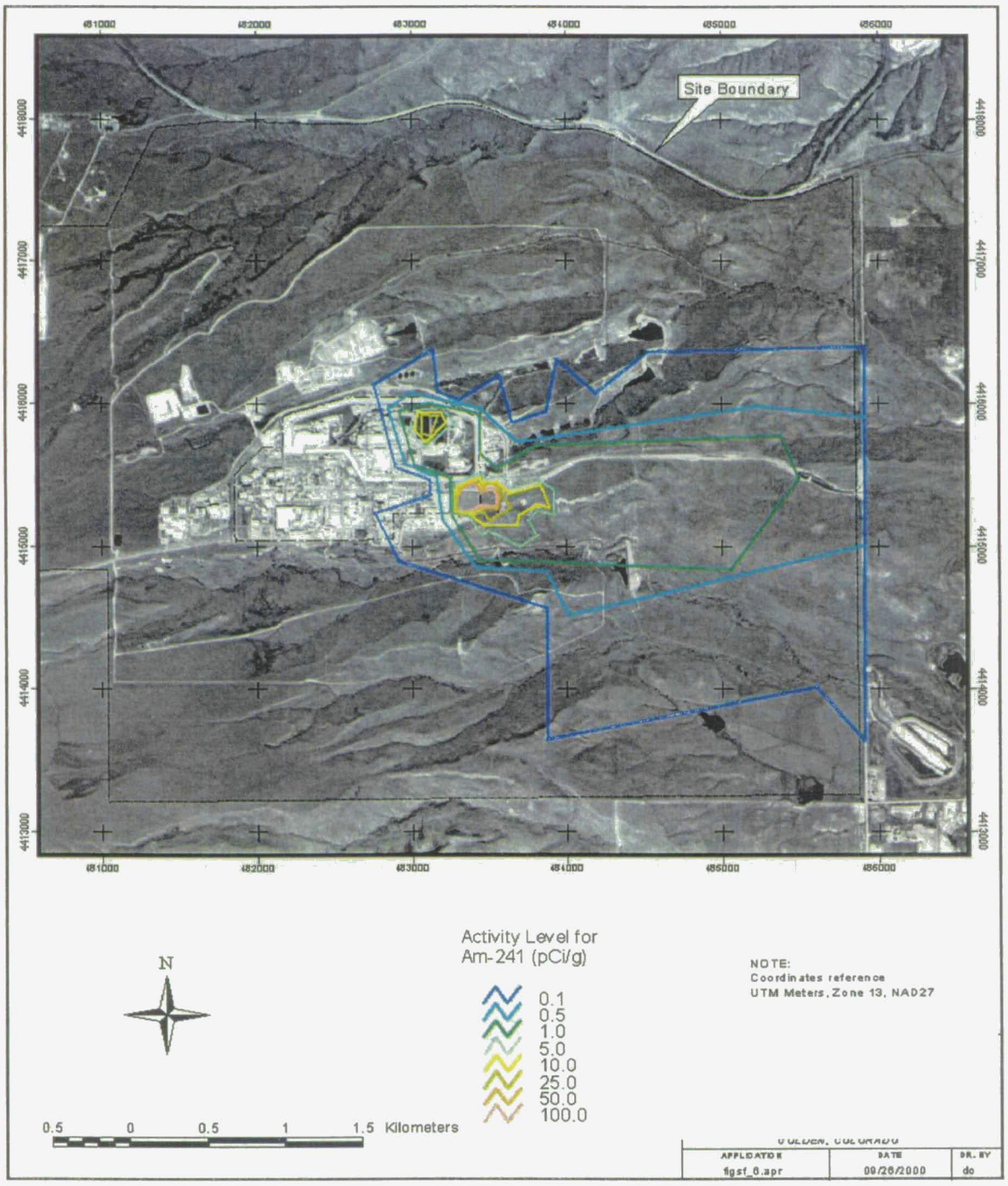

Figure 4-2. Post-Closure Am-241 Source Areas Based on Surficial Soil Concentrations

61

When the Pu-239/240 results summarized in Table 4-2 are compared with the results of the pre-closure scenario (Table 3-1), it is apparent that the predicted impacts for post-closure are of a greater magnitude, with the highest predicted impacts located nearer to the 903 Pad area. The difference between the pre-closure and post-closure model runs can be explained by the additional sources that were included with the post-closure modeling. These additional sources were added in the former Industrial Area, which had been treated as nonerodible (i.e., not a source of resuspension emissions) for the pre-closure analysis. The additional post-closure sources with the highest actinide emissions were added in the immediate vicinity of the 903 Pad.

The estimated annual concentrations of Am-241 for the post-closure modeling were also of a greater magnitude than for the pre-closure run, with the highest predicted impacts located nearer to the 903 Pad. The difference between the pre-closure and post-closure runs can again be explained by the additional sources that were included in the post-closure scenario. Although several sources of Am-241 in the Industrial Area were eliminated from the post-closure modeling because they were above the applicable Surface Soil Action Level, other sources (formerly treated as nonerodible) were added in the same area. These additional sources brought about higher estimated impacts for the post-closure modeling.

Maximum post-closure concentrations of Pu-239/240 and Am-241 would increase by a factor of 2 to 2½ over the pre-closure impacts. At the fenceline, the increase would be more limited—an increase of 10% is projected at the off-Site maximum impact point for Pu-239/240 and the increase for Am-241 is projected to be negligible.

Remediation of the 903 Pad area and cleanup of soil contamination under buildings within the Industrial Area are important components of Site closure. Remediation projects will decrease actinide concentrations in Site soils, thereby decreasing the total actinides in the Site environment. However, removal of buildings and pavement will increase the soil surface areas available for wind erosion. Although only small amounts of actinides will be left in Site surface soils, particles and actinides will be resuspended from a significantly larger source area, with resulting increases in impacts to air from this small emission source. The maximum concentrations predicted would still be substantially less than the EPA air dose limit of 10 mrem.

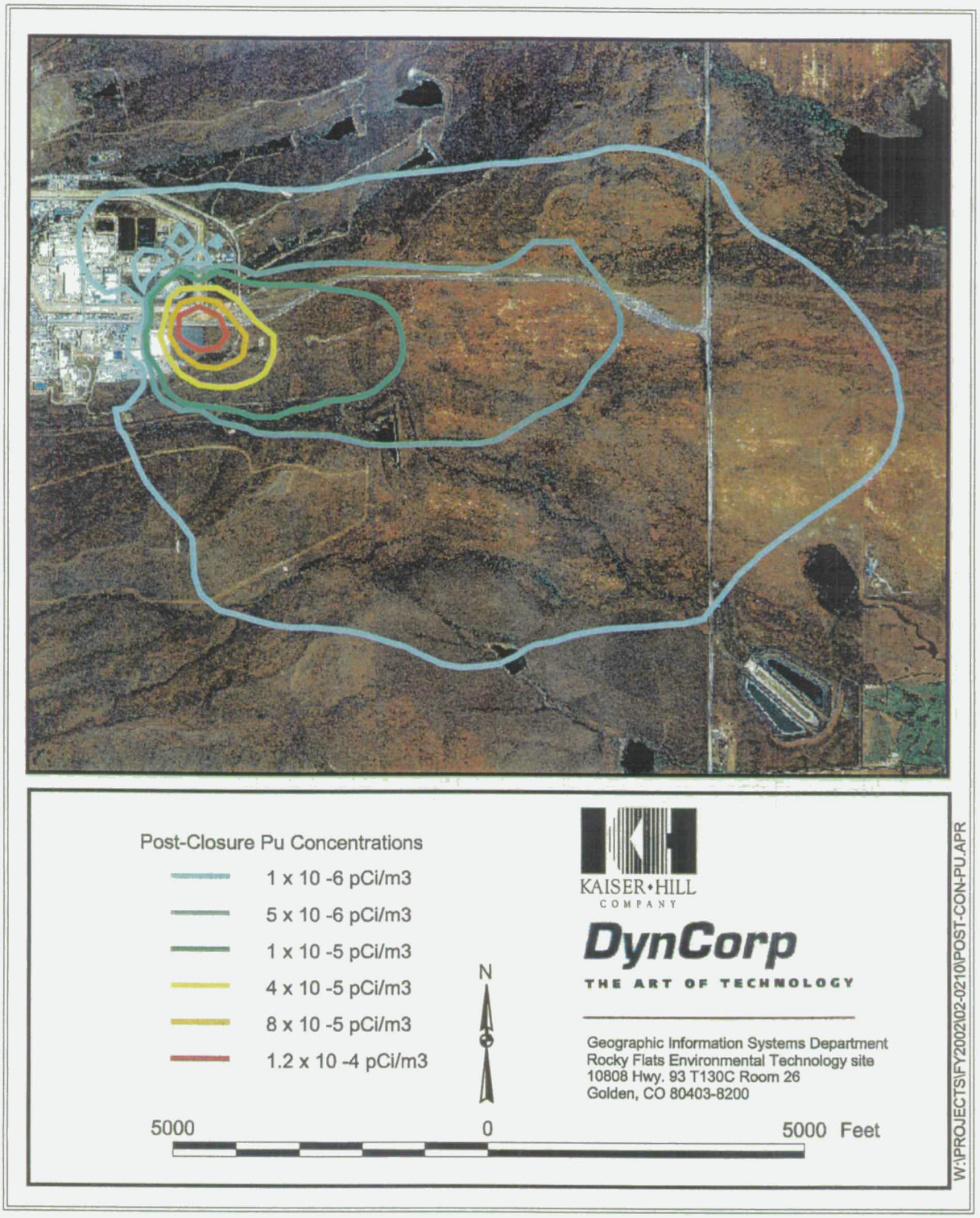

Figure 4-3. Predicted Post-Closure Annual Average Pu-239/240 Concentrations

63

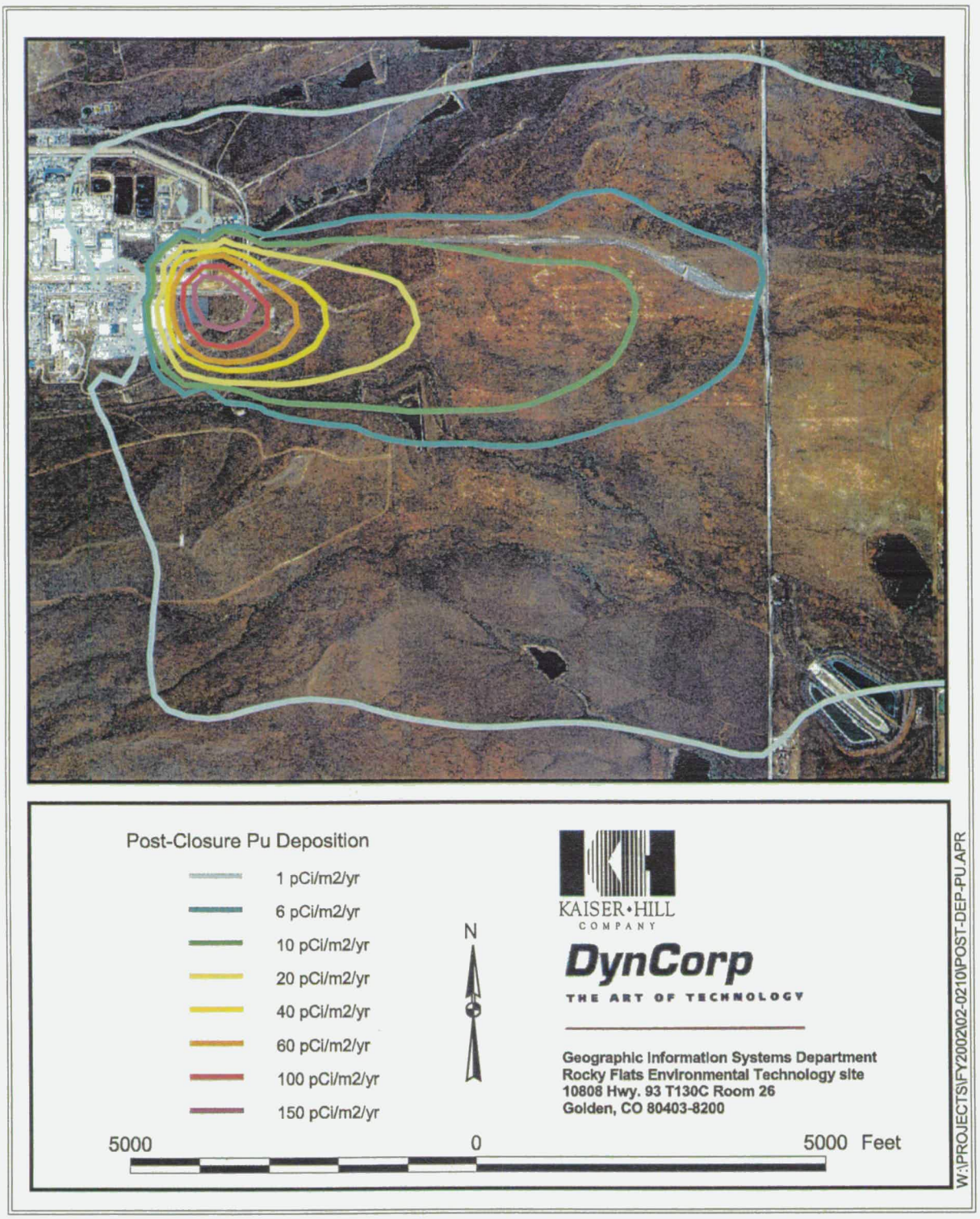

Figure 4-4. Predicted Post-Closure Annual Pu-239/240 Deposition

64

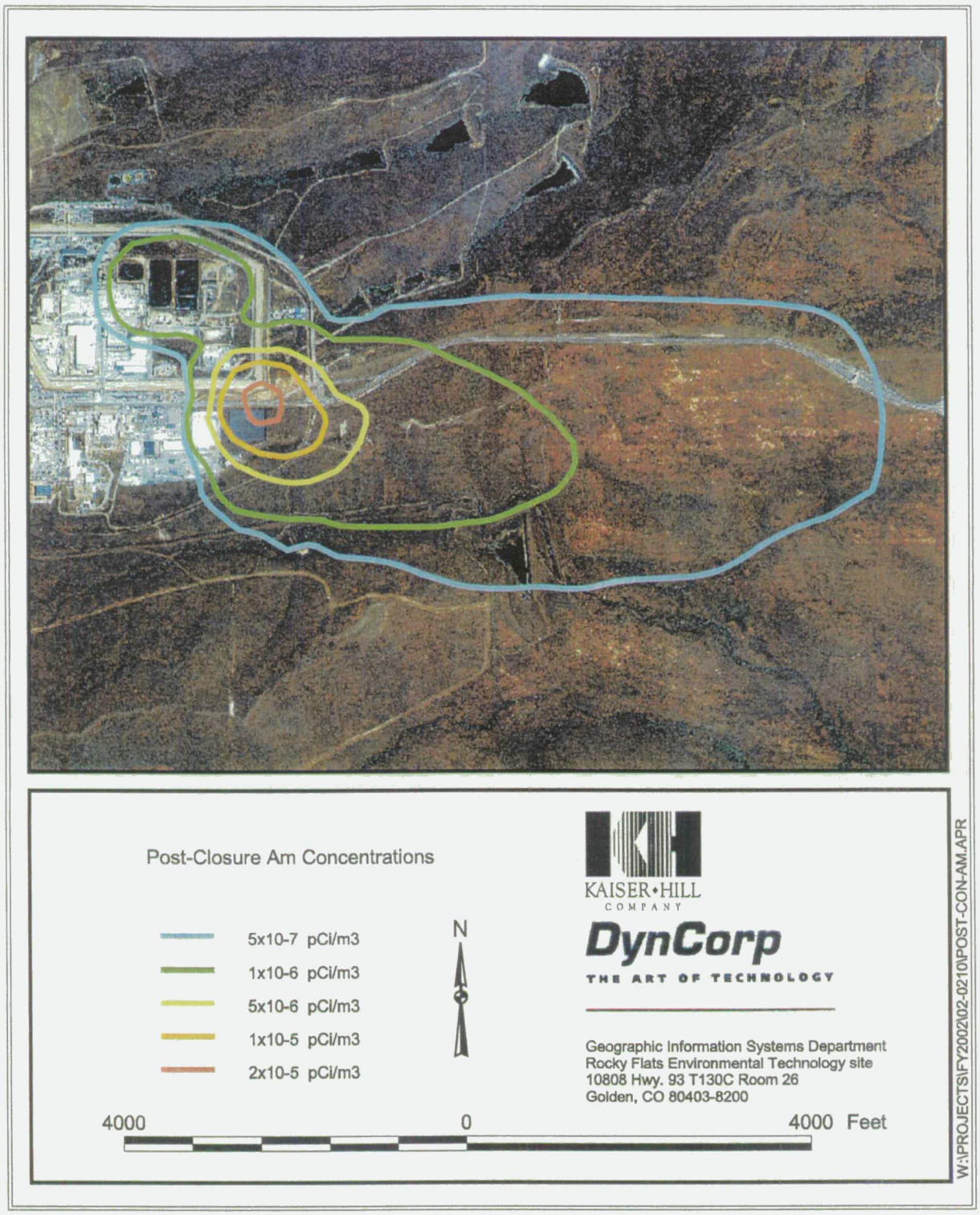

Figure 4-5. Predicted Post-Closure Annual Average Am-241 Concentrations

65

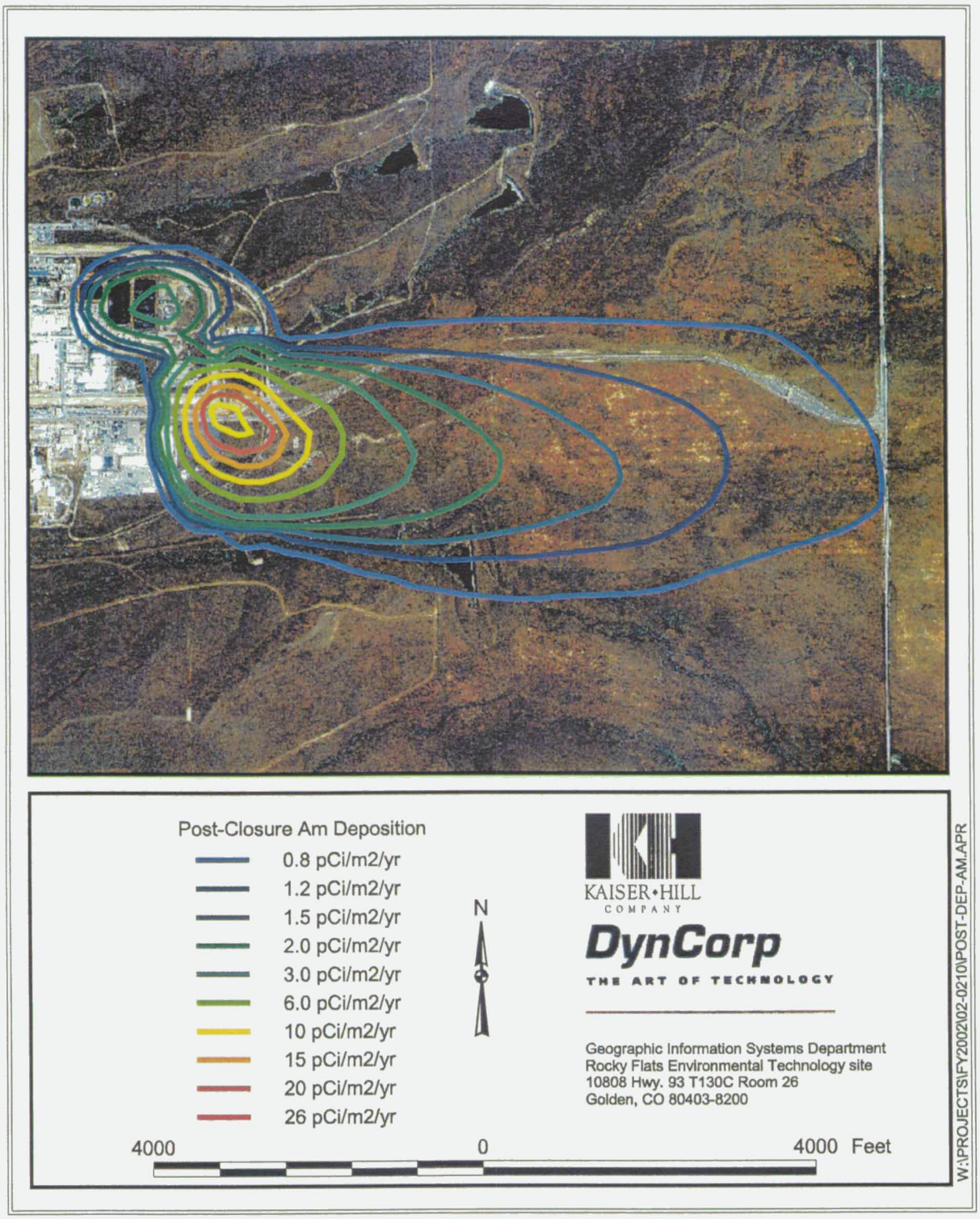

Figure 4-6. Predicted Post-Closure Annual Am-241 Deposition

66

5.0 POST-FIRE WIND EROSION

Unplanned fires may occur at the Site due to lightening strikes, as occurred as recently as July 2000, or due to ignition of flammable vegetation by other means. Planned fires may also be used at the Site for weed control and to decrease the potential for wildfires. In FY00, a post-fire wind erosion scenario was modeled that represented a reasonable worst-case situation in which a fire begins in a period of maximum fuel load and minimum post-fire recovery potential on an area with significant actinide contamination. The wind tunnel sampling in FY00 provided data with which to improve and update this scenario, as described in this section.

The 903 Pad area was again chosen as the modeling location for the post-fire wind erosion scenarios. Wildfires resulting from presumed lightning strikes were modeled under two discrete sets of assumptions, representing a spring fire with a relatively rapid recovery period and a fall fire, with a slower recovery to baseline wind erosion conditions.

5.1 Post-Fire Emission Estimates

This section describes emission estimation for the post-fire wind erosion scenarios.

5.1.1 Scenario Description

Immediately following the hypothetical fire, the ground surface was assumed to be bare soil overlain with ash and interspersed with stubble left from incomplete combustion of plant material. Wind erosion potential was assumed to increase after the fire due to removal of the vegetative cover. The erosion potential was assumed to decrease gradually with time until the pre-fire (baseline) erosion potential was restored. The rate of recovery after a fire would depend on factors such as the time of year that the fire occurred, the fire intensity, and the amount and frequency of rainfall occurring after the fire. Scenarios were modeled representing gradual recovery from a spring fire and from a fall fire, assuming both pre-closure and post-closure contaminant levels.

Though vegetation density may return to its pre-burned state in a matter of weeks under optimal conditions, as observed following the April 2000 Site test burn, it may take up to a full year or more for vegetation to recover under dry conditions. Full restoration of protection from wind erosion probably requires a layer of thatch, which is composed of dead grasses and vegetation that are pushed over and matted down by rain, wind, and snow during the fall and winter months. This is because the presence of bare soil between plants enhances the overall resuspension potential, as the bare areas should facilitate the transfer of soil particles onto plant surfaces by mechanisms such as rainsplash, in addition to providing a direct source for soil resuspension.

5.1.2 Emission Source Locations

The hypothetical spring and fall fires were assumed to be ignited by lightning striking near the 903 Pad itself. The fires were assumed to move east across the Pad Field and downslope to the South Interceptor Ditch (SID), pushed by westerly winds. As shown in Figure 5-1, the fires were assumed to consume an area bounded by the SID to the south, the 904 Pad road to the west, the East Access road to the north, and a fenceline to the distant east, where the fires were assumed to be stopped by emergency responders.

Because the area selected for the simulated wildfire includes the 903 Pad, the post-fire source areas were modeled for two configurations that differed according to the status of the pad. One configuration simulated the current conditions at the Site, with the 903 Pad covered in asphalt and not available as a source area for post-fire wind erosion. The other configuration was the post-closure, post-remediation condition in which the 903 Pad was assumed to be unpaved and revegetated. In this post-closure condition, the surface of the former 903 Pad would provide an additional area subject to post-fire wind erosion.

For each configuration, the burned area was divided into two smaller areas, one with a higher average soil contamination level (under or near the 903 Pad), and the other with a lower average soil conctamination level. Each source area was digitized and a series of points was determined that created polygons that approximated each area's shape. The polygons were input to the ISCST3 model as area sources and are shown in Figure 5-1. The average contamination levels for Pu-239/240 and Am-241 within each area were determined by examining the surface soil activity maps described in Section 2.1. As in the FY00 modeling, pre-fire emissions were modeled from the area of the hypothetical fire to provide a base case against which to compare the post-fire model results.

5.1.3 Emission Estimation

For the base case, emissions of Pu-239/240, Am-241, and particulate matter were estimated as described in Section 2.0. For the post-fire scenarios, the mechanism for resuspension of soil and ash particles and, thereby, actinides from the burned area is the same as that for chronic wind erosion. Potential and actual emissions of particulate matter and actinides from the hypothetical burned area were generally calculated and tracked as described in Section 2.0 of this report. The major differences were that erosion potential was assumed to be greater for the unprotected (unvegetated) soil than for normal, undisturbed grassland and the rates of deposition and erosion potential generation due to small-scale disturbances were also assumed to increase. The wind tunnel studies of the April 2000 test burn area were used to characterize the increase in erosion potential that would follow a fire.

Figure 5-1. Source Areas for Post-Fire Scenarios

69

Potential Emissions From Burned Areas

Wind tunnel studies were conducted on the southwestern Buffer Zone test burn area immediately following the April 6, 2000 burn, approximately four weeks later (May 2 and 3), and again after 10 weeks (June 21 and 22). Tests were also conducted on an adjacent unburned area in April and June. PM_{10} erosion potentials were normalized to a 10-m wind speed of 95 mph. The results are shown in Figure 5-2.

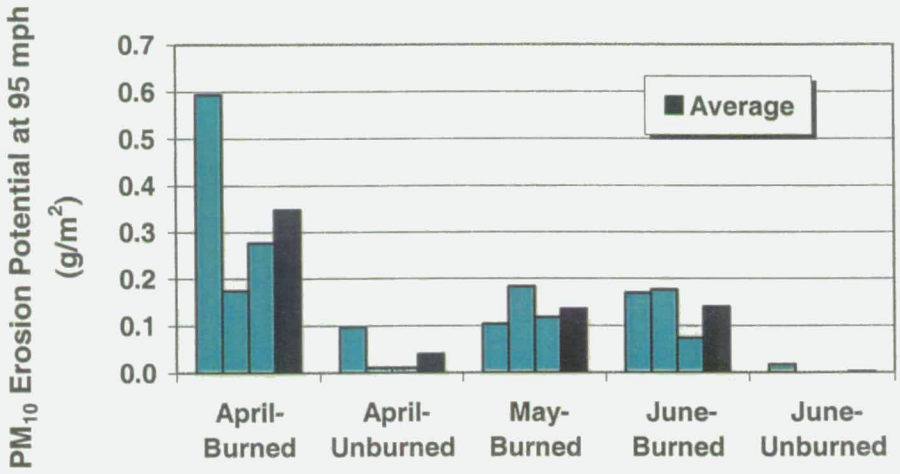

Figure 5-2. Normalized Wind Tunnel Results

The April and June unburned area data formed the basis of the emission estimates for unburned grassland that were described in Section 2.0 of this report. The average erosion potential for the unburned area from the two test periods was approximately 0.03 g/m^2. This value was used as the baseline erosion potential for the hypothetical fire scenarios.

Figure 5-2 shows that the average normalized PM_{10} erosion potentials for the burned area were approximately equal in May and June. Observations taken at the time of the tests indicated that the ground was relatively wet during the May tests but quite dry in April and June. As a result, the May results were excluded from the calculation of post-fire recovery to baseline conditions. To maintain conservatism in the emission estimates, the soil was assumed to be dry except during and for a short period following precipitation events (as described in Section 2.3.3) during which no emissions would occur. Under actual conditions, emissions may occur at a reduced rate for an additional period of time

following precipitation events as the soil continues to dry, as characterized by the May test conditions.

Potential emissions for the post-fire cases were calculated by defining weekly multipliers that were applied to the wind erosion equation described in Section 2.3.1 (Equation 5). The weekly multipliers were developed from the wind tunnel data shown in Figure 5-2 as follows:

- Two post-fire scenarios were defined—one based on a spring fire and a 12-month recovery to baseline erosion potential, the second based on a fall fire and an 18-month recovery period (through a second winter to ensure a layer of thatch).

- The April and June burned area PM_{10} erosion potentials were averaged (see Figure 5-2) to define a single erosion potential characteristic of each period. The April data were used to define erosion potential for the first week following the hypothetical spring fire. The June data defined erosion potential during the 11th week following a spring fire. The baseline erosion potential rate (0.03 g/m^2) was assumed to represent the 52nd week following a spring fire.

- Power and logarithmic curves were plotted using these three data points. The logarithmic curve fit the data better for the period of interest ($R^2 = 0.997$) and defined a slower (and therefore more conservative) decrease in erosion potential over time. The resulting equation was used to fill in erosion potentials for the other weeks.

- Weekly erosion potentials were converted to weekly multipliers by dividing each erosion potential by the baseline erosion potential of 0.03 g/m^2. The weekly multipliers were applied to the chronic wind erosion equation for undisturbed conditions that was defined in Section 2.3.1 (Equation 5) to generate potential TSP emissions for each 15-minute period in the 1996 meteorological data set. These values defined potential emissions for the spring fire case (the spring fire was assumed to occur on April 1, so the highest multiplier was applied to the first week in April, with subsequent multipliers "wrapping" back to the January through March period to complete a year-long data set for modeling).

- For the fall fire, a logarithmic curve was fitted to two points to define multipliers for a longer, slower recovery than was assumed for the spring fire. The average April burned area PM_{10} erosion potential was multiplied by 1.5 and this value was set as the erosion potential for the first week following the fall fire. The baseline erosion potential (0.03 g/m^2) was set equal to the

erosion potential in week 78. The resulting curve was used to fill in erosion potentials for the intervening weeks, which were converted to weekly multipliers by dividing each by the baseline erosion potential.

- The fall fire was assumed to occur September 1. The weekly multipliers were applied to Equation 5 to generate potential TSP emissions for each 15-minute period in the 1996 meteorological data set. As with the spring fire, the multipliers were "wrapped" around to the January through August period to complete a year-long data set for modeling.

As described in Section 2.3.3, the 15-minute potential emissions were adjusted using the albedo and precipitation flags developed for the base case. These factors accounted for periods when no emissions would occur because of snow cover or rain.

The fall fire initial erosion potential was set to 1.5 times the measured average erosion potential for the April wind tunnel trials based on additional wind tunnel data taken in August 2000. In early July 2000, the Site experienced a small wildfire in the east portion of the Buffer Zone. A series of wind tunnel tests were performed in August, approximately seven weeks following the wildfire. The mid-summer fire was considered representative of conditions that would be encountered with an early fall fire—the vegetation was fully developed and the ground was dry. Logarithmic curves developed previously for the hypothetical fall and spring fires, as well as a third curve developed for a 2-year recovery period, were used to project initial erosion potentials for the first week following the wildfire. Calculated initial erosion potentials were then compared to the measured April average erosion potential for the test burn area. The mid-summer fire was found to have an initial erosion potential between 1.27 and 1.43 times the initial test burn erosion potential. These values were rounded up to 1.5 for use with a hypothetical fall fire.

The changes in erosion potential following the hypothetical spring and fall fires are illustrated in Figure 5-3. The weekly multipliers were also averaged by month for use in other portions of the post-fire modeling analysis. The monthly multipliers are shown in Table 5-1.

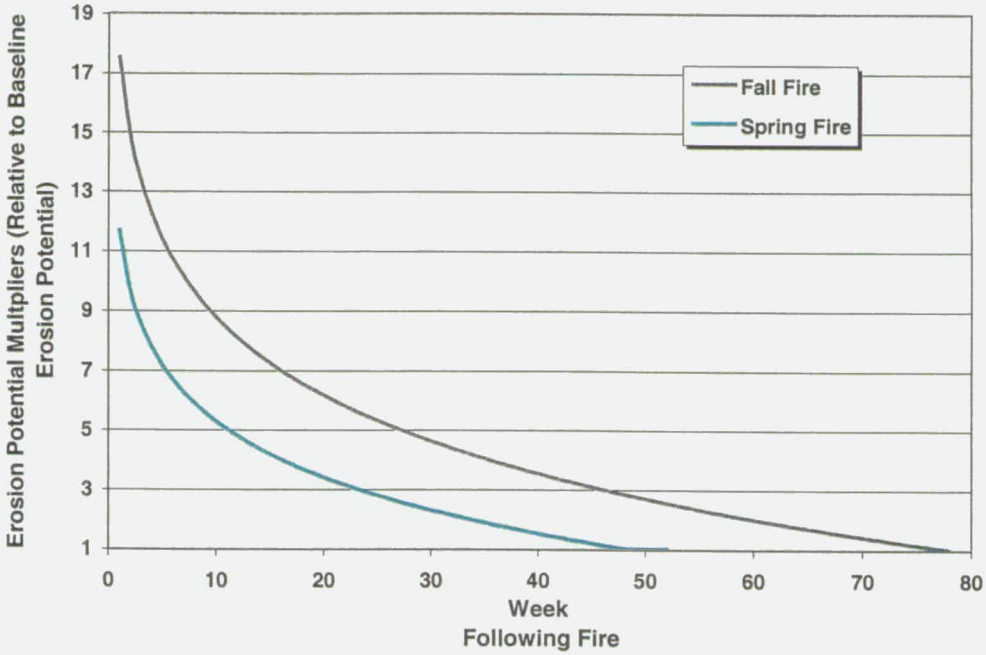

Figure 5-3. Erosion Potential Multipliers for Post-Fire Scenarios

Table 5-1. Monthly Erosion Potential Multipliers for Hypothetical Spring and Fall Fires

Month	Spring Fire Multipliers	Fall Fire Multipliers
January	1.61	6.46
February	1.34	5.71
March	1.10	5.09
April	9.41	4.56
May	6.49	4.09
June	5.16	3.68
July	4.27	3.30
August	3.61	2.96
September	3.07	14.49
October	2.63	10.47
November	2.25	8.62
December	1.91	7.38

Use of Equation 5 for the Post-Fire Case

The occurrence of a grass fire may alter the size distribution of soil particles subject to wind erosion. Ranville et al. (2000) performed a series of experiments involving Rocky Flats soil samples to learn whether soil aggregates were stable under varying conditions (see Radian, 2000, Section 5.2.3). The effect of a fire was simulated by treating the soil with hydrogen peroxide (H_2O_2), which partially destroyed the organic fraction of soil that acts as a glue to create aggregates. The result was a shift in mass to smaller size fractions and a much more dramatic shift to smaller size fractions for Pu-239/240 activity. While a typical grass fire may not develop enough heat to have as drastic an effect on particle sizes as the H_2O_2 treatment, any shift towards smaller sizes would tend to increase downwind particulate matter concentrations by decreasing deposition from the plume, since smaller particles will remain airborne for longer distances.

Ranville et al. used size cuts at 2 μm, 10 μm, 25 μm, and 53 μm in their experiments, as well as larger and smaller fractions. These size fractions represent particles with aerodynamic equivalent diameters of approximately 3.26 μm, 16.78 μm, 33.54 μm, and 71.11 μm, respectively. (Aerodynamic equivalent diameter is the diameter of a spherical particle with the same settling velocity as the particle in question, but with a density of 1 g/cm^3.) The actual soil particles used in Ranville et al.'s study were assumed to have densities of 2.65 g/cm^3 or 1.8 g/cm^3, depending on the size fraction, as described in Radian, 2000.

The 25 μm data were assumed to represent TSP, usually assumed to include particles smaller than approximately 30 μm aerodynamic equivalent diameter. Similarly, the 10 μm cut was assumed to approximate inhalable particles (e.g., PM_{10}). For non-disaggregated soil, the study showed than the 10 μm and smaller fraction comprised approximately 55% of the soil less than 25 μm diameter. These data are fairly consistent with the 39% PM_{10}/TSP ratio used in developing the baseline emission equation for undisturbed grassland (Equation 5).

In contrast, hydrogen peroxide treatment, which dissolved the organic matter, raised the small particle percentage to 77% of the 25 μm mass fraction. Based on this information, continued use of a 39% PM_{10}/TSP ratio to scale up the wind tunnel PM_{10} data to TSP should err on the high side (higher emissions) for a post-fire scenario. This is because any tendency of the fire to disaggregate the soil and produce more smaller particles at the expense of larger particles would mean that the measured wind tunnel PM_{10} data would have captured a larger percentage of the total TSP erosion potential than would be the case for the unburned area data. Should a measured PM_{10} erosion potential of 1 g/m^2 represent 70% of the TSP erosion potential, for example, the calculated TSP erosion potential would be only 1.43 g/m^2 (1 g/m^2 x 100%/70%), compared with 2.56 g/m^2 calculated using the 39% factor (1 g/m^2 x 100%/39%).

Deposition Inputs—Particulate Matter

As explained in Section 2.3, actual particulate matter emissions due to wind erosion were calculated for each time step of the simulation as the smaller of the potential particulate matter emissions or the amount of particulate matter available to be eroded. The available erodible material is renewed throughout the year through deposition of particulate matter and through small-scale disturbances of the soil. A fire would be expected to increase particulate matter emissions, which, in turn, could result in increased deposition of particulate matter back onto the burned area.

Immediately above the burned area, the particulate matter in the air would be a mixture of particulate matter derived from the area of the hypothetical fire and particulate matter originating from elsewhere. A model developed by Argonne National Laboratory deals with a similar situation in which the total "mass loading" in the air over an area of soil contamination is partitioned between "clean" particulate matter originating outside the contaminated area and contaminated soil blown off the area of contamination. The Residual Radioactivity model (RESRAD) accounts for this partitioning through an area factor that varies with the size of the contaminated area and the annual average wind speed. The area factor formulation was developed through repeated dispersion model simulations and curve fitting (Chang et al., 1998).

The RESRAD Version 5.82 area factor formulation was used to determine the fraction of the normal particulate matter in the air over the hypothetical fire location that would originate from the burned area and the fraction that would originate from elsewhere. A 4 m/s wind speed was assumed (4 m/s was the annual average 10-m wind speed measured at the Site meteorological tower in 1996 and is a good approximation of longer-term average 10-m wind speeds at the Site). For the pre-closure case, where the 903 Pad area was not included in the modeled source, the fractions were 14.68% from the burned area and 85.32% from elsewhere. For the post-closure case, where the burned area was assumed to include the area formerly occupied by the 903 Pad, the corresponding fractions were 14.74% and 85.26%.

For the post-fire scenarios, the amount of particulate matter in the air that was used to calculate deposition was again based on 1996 CDPHE TSP data, as described in Section 2.3.5. The expected increase in the particulate matter in the air over the burned area was calculated by scaling up the fraction originating from the burned area itself by the monthly multipliers shown in Table 5-1 (i.e., it was assumed that particulate matter concentration would increase linearly with the potential emissions) and adding that to the fraction that originates from elsewhere. The resulting increased TSP concentrations are shown for the spring and fall fire cases in Figure 5-4.

As explained previously, a fire may also change the size distribution of particles that are resuspended from the burned area. Annual average particulate matter deposition

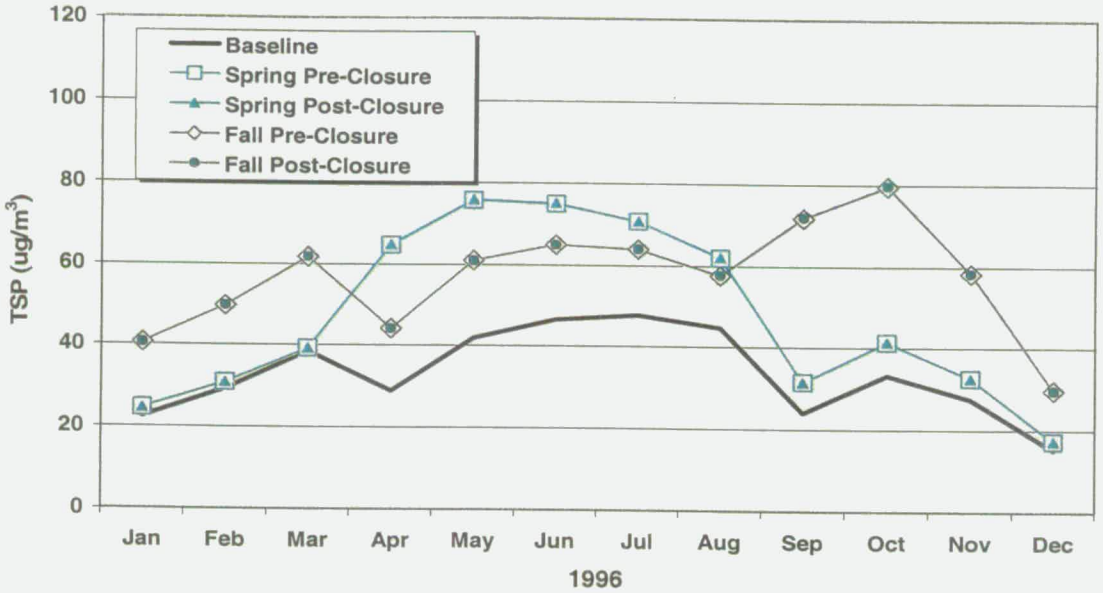

Figure 5-4. Calculated Monthly Variation in Post-Fire TSP Concentrations

velocities were recalculated using size fraction data characteristic of disaggregated soil from Ranville et al., 2000. Deposition velocities were calculated using the 25 μm and smaller fraction. Compared to the original average mass deposition velocity of 1.97 cm/s used for baseline modeling, the <25 μm fraction had an average mass deposition velocity of 1.283 cm/s (65% of original). This deposition velocity was assumed to characterize post-fire particulate matter originating from the burned area.

Monthly particulate matter deposition velocities were calculated for the post-fire simulations as weighted averages of post-fire and "normal" deposition velocities based on the percentage of total post-fire airborne particulate matter assumed to originate from the burned area vs. from the surrounding unburned areas (i.e., the percentage after consideration of the scaled-up contribution from the burned area). The monthly particulate matter deposition velocities used for the post-fire scenarios are shown in Table 5-2 (compared with 1.97 cm/s for baseline modeling).

Deposition Inputs—Activity

As described in Section 2.4.1, deposition of Pu-239/240 and Am-241 onto the source areas must also be calculated. For the pre-fire base case, annual average Pu-239/240 and Am-241 concentrations were calculated over the fire simulation source areas shown in Figure 5-1 using the same data and methods described in Section 2.4.1. The average airborne concentrations of Pu-239/240 and Am-241 were increased for the post-fire simulations by assuming that the portion of particulate matter originating from the burned areas would carry actinide activity at the same concentration levels as that in the surface

Table 5-2. Revised Particulate Matter Deposition Velocities for Post-Fire Scenarios

Month	Pre-Closure Spring Fire Deposition Velocities (cm/s)	Pre-Closure Fall Fire Deposition Velocities (cm/s)	Post-Closure Spring Fire Deposition Velocities (cm/s)	Post-Closure Fall Fire Deposition Velocities (cm/s)
January	1.820	1.607	1.820	1.606
February	1.841	1.628	1.840	1.627
March	1.860	1.648	1.860	1.647
April	1.543	1.667	1.543	1.666
May	1.606	1.685	1.605	1.684
June	1.645	1.702	1.645	1.702
July	1.678	1.720	1.677	1.719
August	1.706	1.737	1.705	1.736
September	1.731	1.477	1.731	1.477
October	1.755	1.526	1.754	1.526
November	1.777	1.558	1.777	1.557
December	1.799	1.584	1.799	1.583

Notes:

cm/s = centimeters per second

soil of those areas. Particulate matter originating from outside the burned area was assumed to carry the "normal" annual average actinide concentration appropriate for the air over the hypothetical fire area (i.e., the same concentrations used for the pre-fire base cases). (Since a portion of the "normal" actinide loading in the air over the burned area would also originate from within that area, this resulted in conservatively high estimated airborne actinide concentrations for modeling.) Revised Pu-239/240 and Am-241 concentrations were calculated separately for the pre- and post-closure cases and for the high concentration and low concentration source areas shown in Figure 5-1.

Deposition velocities were also adjusted for use with the revised airborne activity concentrations using the same approach outlined previously for particulate matter deposition velocities. Annual average activity deposition velocities were recalculated using size fraction data characteristic of Pu-239/240 in disaggregated soil from Ranville et al., 2000. Deposition velocities were calculated using the 25 μm and smaller fraction. Compared to the original average activity deposition velocity of 2.433 cm/s used for baseline modeling, the <25 μm fraction had an average activity deposition velocity of 0.809 cm/s (33% of original) and was assumed to characterize the post-fire activity distribution in particulate matter originating from the burned area.

Monthly activity deposition velocities were calculated for the post-fire simulations as weighted averages of post-fire and "normal" deposition velocities based on the percentage of total post-fire airborne particulate matter assumed to originate from the burned area vs. from the surrounding unburned areas (i.e., the percentage after

consideration of the scaled-up contribution from the burned area). The monthly activity deposition velocities used for the post-fire scenarios are shown in Table 5-3 (compared with 2.433 cm/s for baseline modeling).

Table 5-3. Revised Activity Deposition Velocities for Post-Fire Scenarios

Month	Pre-Closure Spring Fire Deposition Velocities (cm/s)	Pre-Closure Fall Fire Deposition Velocities (cm/s)	Post-Closure Spring Fire Deposition Velocities (cm/s)	Post-Closure Fall Fire Deposition Velocities (cm/s)
January	2.081	1.578	2.079	1.576
February	2.129	1.628	2.128	1.626
March	2.174	1.675	2.173	1.673
April	1.429	1.719	1.427	1.717
May	1.576	1.762	1.574	1.760
June	1.669	1.803	1.667	1.801
July	1.745	1.845	1.743	1.843
August	1.811	1.885	1.809	1.883
September	1.872	1.274	1.870	1.272
October	1.927	1.389	1.925	1.387
November	1.980	1.463	1.978	1.461
December	2.031	1.524	2.030	1.522

Notes:

cm/s = centimeters per second

Small-Scale Generation of Erosion Potential

No information is available on the possible effect of a fire on the rate at which erosion potential is renewed through freeze/thaw, burrowing animal activity, the activities of larger animals such as deer, rainsplash, etc. For the post-fire simulations, it was assumed that the rate would initially double for mass. The multiplier was then assumed to decrease from 2 to 1 over a 12-month period for the spring fire and over an 18-month period for the fall fire. Monthly multipliers were calculated assuming a logarithmic decrease. Revised activity generation was calculated for Pu-239/240 and Am-241 by multiplying the revised particulate matter generation rate by the surface soil activity level for each source area and actinide.

Initial Erodible Particulate Matter and Activity

Sensitivity analyses conducted for the baseline modeling showed that these parameters had little effect on the annual average results. The initial erodible particulate matter was set to the predicted January erosion potential from the logarithmic curve projections described previously for each scenario. This represented an increase from the initial

erodible particulate matter value used for the base case of 0.128 g/m^2 TSP to 0.138 g/m^2 for the spring fire and 0.538 g/m^2 for the fall fire. As with the baseline modeling, the initial erodible particulate matter value was multiplied by the surface soil actinide activity level for each source to define initial activity levels.

5.2 Modeling Methods

For the post-fire scenarios, actinide (Pu-239/240 and Am-241) and particulate matter concentrations resulting from wind erosion of an area recovering from a wildfire were estimated and compared to wind erosion impacts from the same area in an undisturbed state. The post-fire scenario was modeled for two configurations that differed according to the status of the 903 Pad, representing a current, pre-closure scenario and a post-closure, post-remediation scenario. The post-fire recovery modeling was further separated into two cases that represented a spring fire and a fall fire, with different rates of vegetation recovery.

Except as described below, the modeling methods were the same as those employed for the revised wind erosion modeling described in Section 2.0. The ISCST3 model was employed with the same receptor grid and 1996 meteorological data. Wind erosion emissions were simulated using ground-based area sources. Concentrations were calculated by ISCST3 and included the effects of particle settling on plume depletion; however, deposition was not calculated.

For the pre-fire base cases, the source variables for particle size categories, mass fractions, particle density, and activity fractions were the same as used for previous wind erosion modeling. This allowed for proper accounting of plume depletion for the modeling of the pre-fire case. For the fire recovery modeling, the plume depletion parameters were derived from soil aggregation/disaggregation research conducted using Site soils (Ranville et al., 2000). Mass and activity fraction data for the 25 μm and smaller fractions were taken directly from Ranville et al., 2000.

The particle size categories, mass, and activity fraction data used in the post-fire modeling are shown in Table 5-4. Mean particle diameters were calculated as described in Radian, 2000.

Table 5-4. Particle Size Data Used for Fire Recovery Dispersion Modeling

Particle Size Category	Lower-Upper Bound for Physical Particle Size Category (μm)	Mean Aerodynamic Equivalent Diameter for Particle Size Category (μm)	Particle Density (g/cm^3)[a]	Plutonium Activity Fraction[b]	Mass Fraction[b]
1	1-2	2.53	2.65	0.414	0.334
2	2-10	11.01	2.65	0.508	0.436
3	10-25	25.79	1.8	0.079	0.230

[a] Foster et al., 1985.
[b] Ranville et al., 2000.
Notes:
μm = micrometers
g/cm^3 = grams per cubic centimeter

5.3 Modeling Results

This section presents the results of the post-fire wind erosion modeling. Pre- and post-burn impacts are summarized in Tables 5-5 and 5-6. For the actinide results, concentration values have also been converted to EDE, as described in Section 3.4.

Table 5-5. Particulate Matter Results Summary—Post-Fire Recovery Scenarios

Pollutant	Maximum Estimated Annual Concentration (μg/m^3)	
	On Site	Off Site
Pre-Closure Base Case		
Particulate matter (TSP)	2.45	0.064
Pre-Closure Spring Fire Recovery		
Particulate matter (TSP)	7.35	0.144
Pre-Closure Fall Fire Recovery		
Particulate matter (TSP)	10.85	0.219
Post-Closure Base Case		
Particulate matter (TSP)	2.50	0.065
Post-Closure Spring Fire Recovery		
Particulate matter (TSP)	7.47	0.147
Post-Closure Fall Fire Recovery		
Particulate matter (TSP)	11.06	0.225

Notes:
TSP = Total suspended particulate
μg /m^3 = micrograms per cubic meter

80

Table 5-6. Activity Results Summary—Post-Fire Recovery Scenarios

Isotope	Maximum Estimated Annual Concentration (pCi/m^3)[a]		Factor for Conversion of pCi/m^3 to mrem	Maximum Estimated Annual EDE (mrem)	
	On Site	Off Site		On Site	Off Site
Pre-Closure Base Case					
Pu-239/240	1.2×10^{-4}	6.6×10^{-7}	5,000	0.60	0.003
Am-241	4.8×10^{-5}	2.1×10^{-7}	5,263	0.25	0.001
Pre-Closure Spring Fire Recovery					
Pu-239/240	9.2×10^{-4}	3.6×10^{-6}	5,000	4.60	0.018
Am-241	3.7×10^{-4}	1.1×10^{-6}	5,263	1.94	0.006
Pre-Closure Fall Fire Recovery					
Pu-239/240	1.5×10^{-3}	6.1×10^{-6}	5,000	7.50	0.031
Am-241	5.8×10^{-4}	2.0×10^{-6}	5,263	3.05	0.011
Post-Closure Base Case					
Pu-239/240	1.7×10^{-4}	9.5×10^{-7}	5,000	0.85	0.005
Am-241	4.9×10^{-5}	2.5×10^{-7}	5,263	0.26	0.001
Post-Closure Spring Fire Recovery					
Pu-239/240	1.3×10^{-3}	5.2×10^{-6}	5,000	6.50	0.026
Am-241	3.8×10^{-4}	1.4×10^{-6}	5,263	2.00	0.007
Post-Closure Fall Fire Recovery					
Pu-239/240	2.1×10^{-3}	8.8×10^{-6}	5,000	10.50	0.044
Am-241	6.0×10^{-4}	2.3×10^{-6}	5,263	3.16	0.012

Notes:

Am = americium
EDE = effective dose equivalent
mrem = millirem
pCi/m^3 = picocuries per cubic meter
Pu = plutonium

5.3.1 Spring Fire Results

Figures 5-5 through 5-13 show the results of the spring fire modeling. The spring fire simulation resulted in a projected 5- to 8-fold increase in annual actinide concentrations relative to the base case results. Particulate matter concentrations were projected to increase by smaller amounts (2- to 3-fold increase). Post-closure concentrations of both actinides and particulate matter were predicted to be slightly higher than pre-closure concentrations because the modeled source areas were larger for the post-closure scenarios due to the inclusion of the area formerly occupied by the 903 Pad.

Maximum spring fire increases in Pu-239/240 and Am-241 concentrations were added to the results for the baseline wind erosion simulations described in Sections 3.0 and 4.0 of this report plus regional background concentrations to determine the maximum total

81

concentrations of these actinides that could result under the modeled scenarios. Maximum total annual on-Site concentrations of Pu-239/240 and Am-241 were approximately equal to the post-fire concentrations shown in Table 5-5. Maximum total annual off-Site concentrations were estimated to be:

- Pre-closure Pu-239/240: 6.0×10^{-6} pCi/m^3 (0.030 mrem)
- Pre-closure Am-241: 1.4×10^{-6} pCi/m^3 (0.007 mrem)
- Post-closure Pu-239/240: 7.5×10^{-6} pCi/m^3 (0.038 mrem)
- Post-closure Am-241: 1.6×10^{-6} pCi/m^3 (0.008 mrem)

5.3.2 Fall Fire Results

Figures 5-14 through 5-22 show the results of the fall fire modeling. The fall fire simulation resulted in a projected 9- to 13-fold increase in annual actinide concentrations relative to the base case results. Particulate matter concentrations were projected to increase by smaller amounts (3- to 5- fold increase). Post-closure concentrations of both actinides and particulate matter were predicted to be slightly higher than pre-closure concentrations because the modeled source areas were larger for the post-closure scenarios due to the inclusion of the area formerly occupied by the 903 Pad.

Maximum fall fire increases in Pu-239/240 and Am-241 concentrations were added to the results for the baseline wind erosion simulations described in Sections 3.0 and 4.0 of this report plus regional background concentrations to determine the maximum total concentrations of these actinides that would result under the modeled scenarios. Maximum total annual on-site concentrations of Pu-239/240 and Am-241 were approximately equal to the post-fire concentrations shown in Table 5-5. Maximum total annual off-Site concentrations were estimated to be:

- Pre-closure Pu-239/240: 7.5×10^{-6} pCi/m^3 (0.038 mrem)
- Pre-closure Am-241: 2.1×10^{-6} pCi/m^3 (0.011 mrem)
- Post-closure Pu-239/240: 1.1×10^{-5} pCi/m^3 (0.055 mrem)
- Post-closure Am-241: 2.5×10^{-6} pCi/m^3 (0.013 mrem)

5.4 Conclusions

The post-fire resuspension scenarios showed that over the course of a year, recovery from a spring fire would result in a 5- to 8-fold increase in actinide impacts from the burned area. A fall fire, representing a reasonable worst-case vegetation recovery scenario, would increase actinide impacts from the burned area 9- to 13-fold. In both cases, particulate matter increases would be less than projected actinide increases. These post-fire increases are higher than those predicted in the FY00 modeling, where a 5-fold increase in actinide impacts was estimated. However, the base case impacts have been reduced from those estimated in the FY00 modeling due to the revised emissions

methodology and the total predicted post-fire impacts have therefore decreased relative to the earlier modeling.

The post-closure vegetative recovery scenarios showed somewhat higher concentrations than the pre-closure scenarios. The reason is that the area of the 903 Pad itself would become a source subject to wind erosion after the asphalt covering is removed.

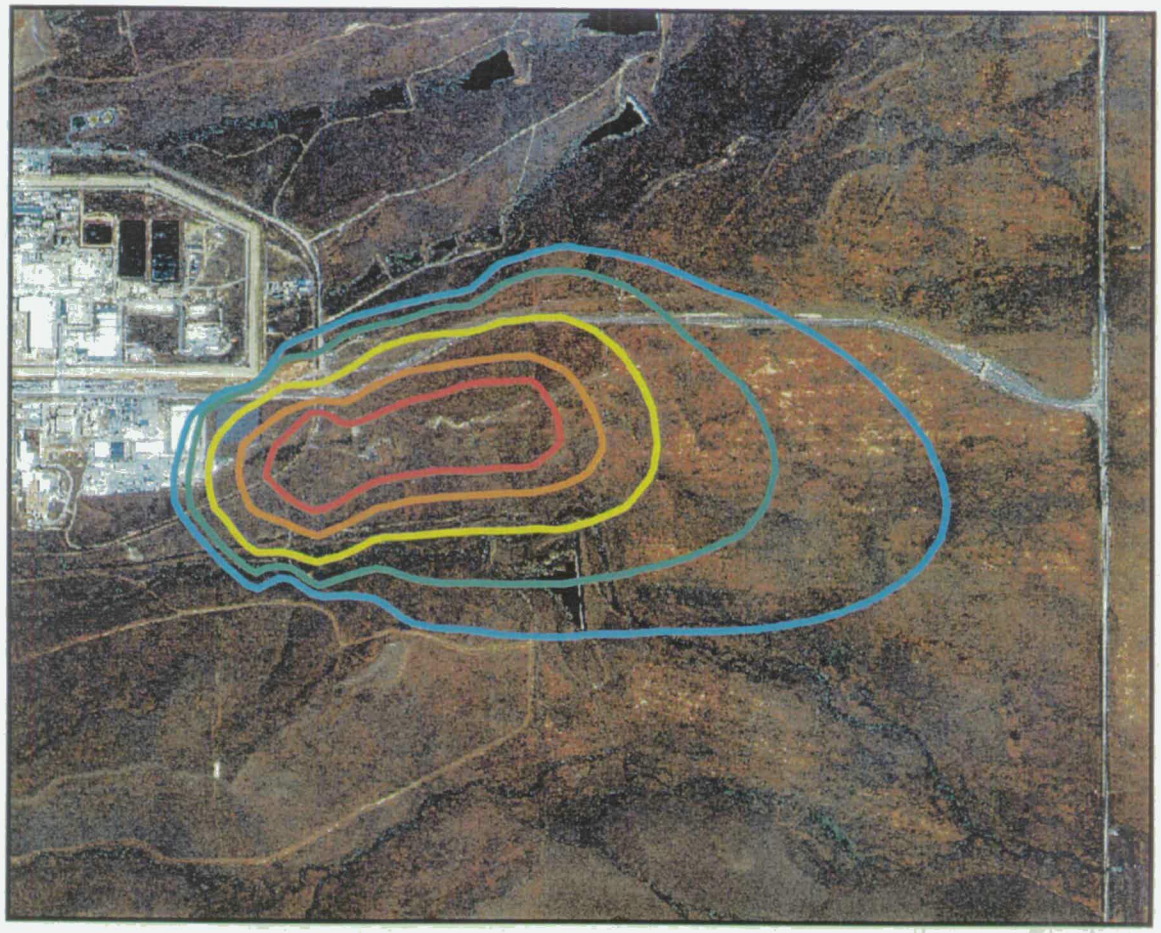

Particulate Matter Concentrations -
Pre-Closure, Post-Fire Base Case

0.1 ug/m3
0.2 ug/m3
0.6 ug/m3
1.4 ug/m3
2.0 ug/m3

N

KAISER•HILL COMPANY

DynCorp
THE ART OF TECHNOLOGY

Geographic Information Systems Department
Rocky Flats Environmental Technology site
10808 Hwy. 93 T130C Room 26
Golden, CO 80403-8200

4000 0 4000 Feet

W:\PROJECTS\FY2002\02-0210\BASE\PRE-MASS.APR

Figure 5-5. Pre-Closure Base Case:
Predicted Annual Average Particulate Matter Concentrations

84

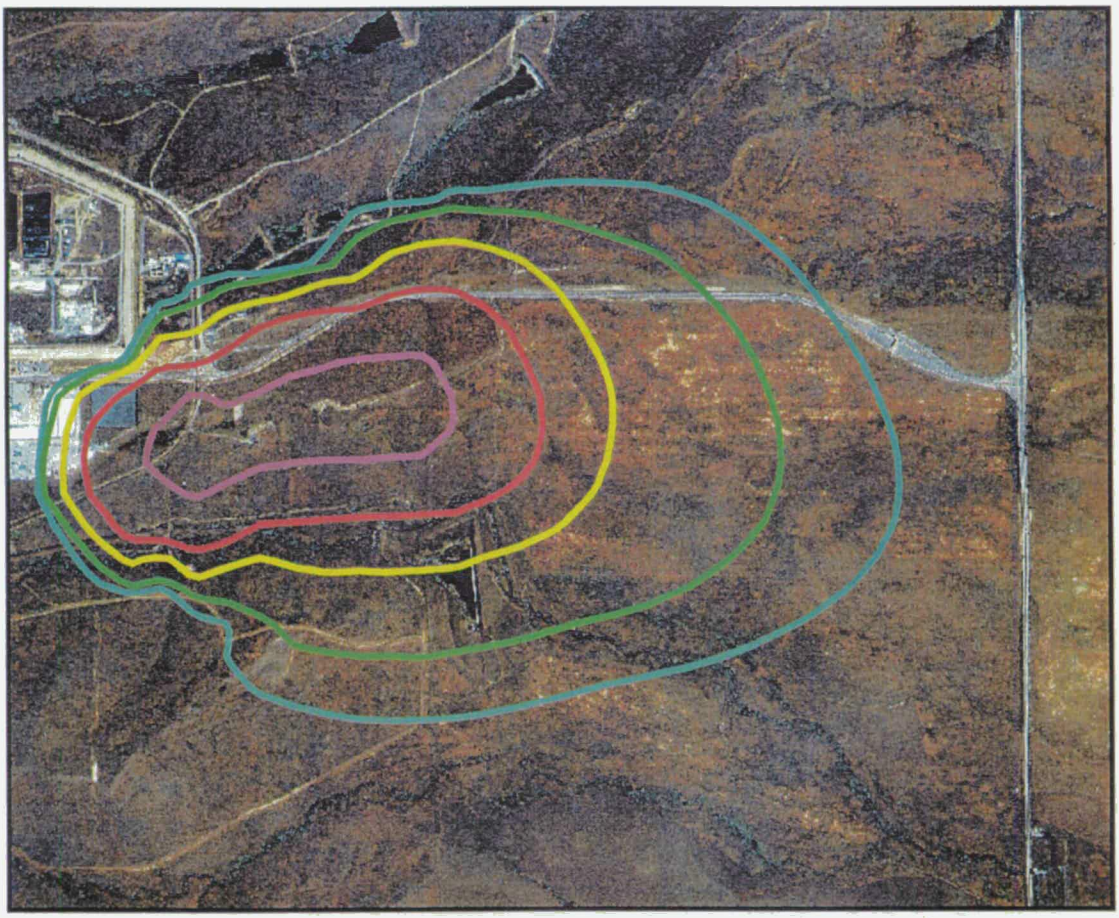

Particulate Matter Concentrations
Following Spring Fire - Pre-Closure

0.2 ug/m3
0.3 ug/m3
0.7 ug/m3
2.0 ug/m3
6.0 ug/m3

N

KAISER•HILL COMPANY

DynCorp
THE ART OF TECHNOLOGY

Geographic Information Systems Department
Rocky Flats Environmental Technology site
10808 Hwy. 93 T130C Room 26
Golden, CO 80403-8200

4000 0 4000 Feet

W:\PROJECTS\FY2002\02-0210\MASS\PRE-MASS-SPRING.APR

Figure 5-6. Pre-Closure Spring Fire:
Predicted Annual Average Particulate Matter Concentrations

85

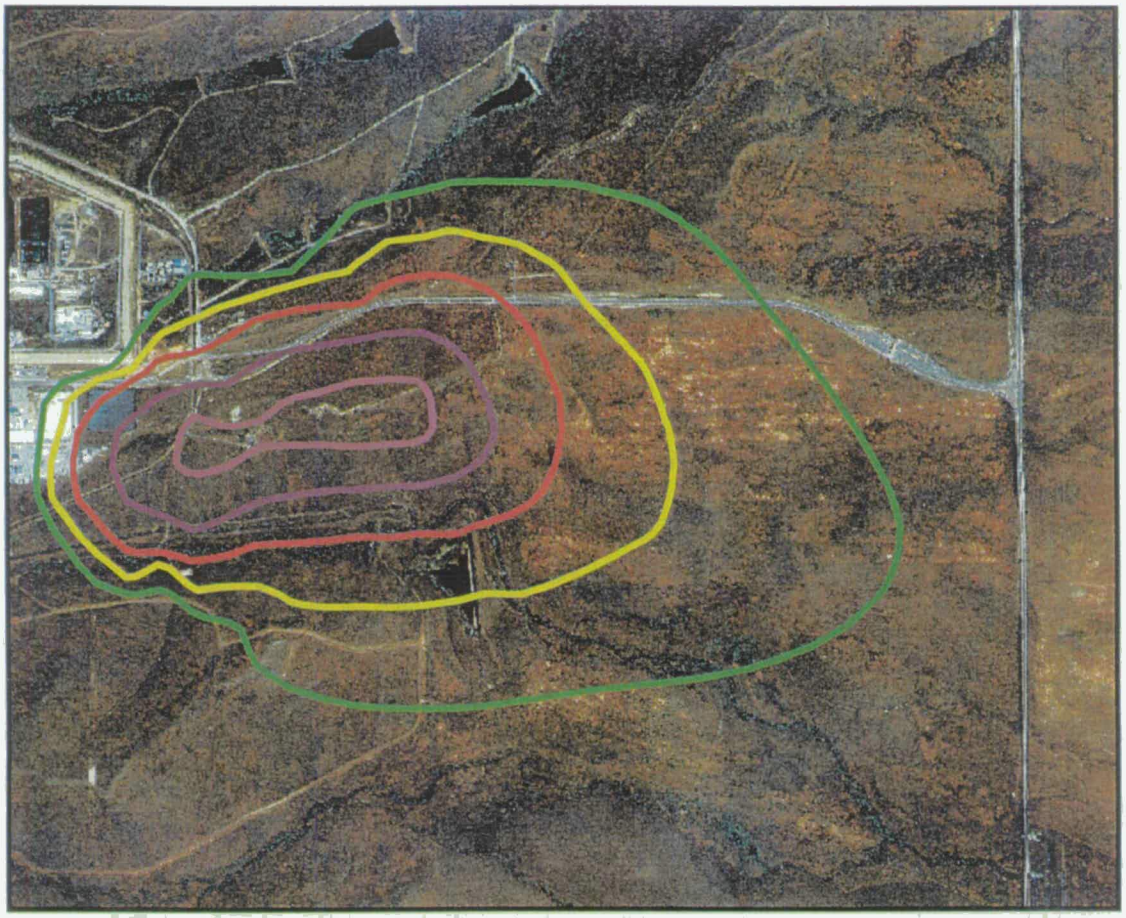

Particulate Matter Concentrations
Following Fall Fire - Pre-Closure

0.3 ug/m3
0.7 ug/m3
2.0 ug/m3
6.0 ug/m3
10.0 ug/m3

N

KAISER•HILL COMPANY

DynCorp
THE ART OF TECHNOLOGY

Geographic Information Systems Department
Rocky Flats Environmental Technology site
10808 Hwy. 93 T130C Room 26
Golden, CO 80403-8200

4000 0 4000 Feet

W:\PROJECTS\FY2002\02-0210\MASS\PRE-MASS-FALL.APR

Figure 5-7. Pre-Closure Fall Fire:
Predicted Annual Average Particulate Matter Concentrations

86

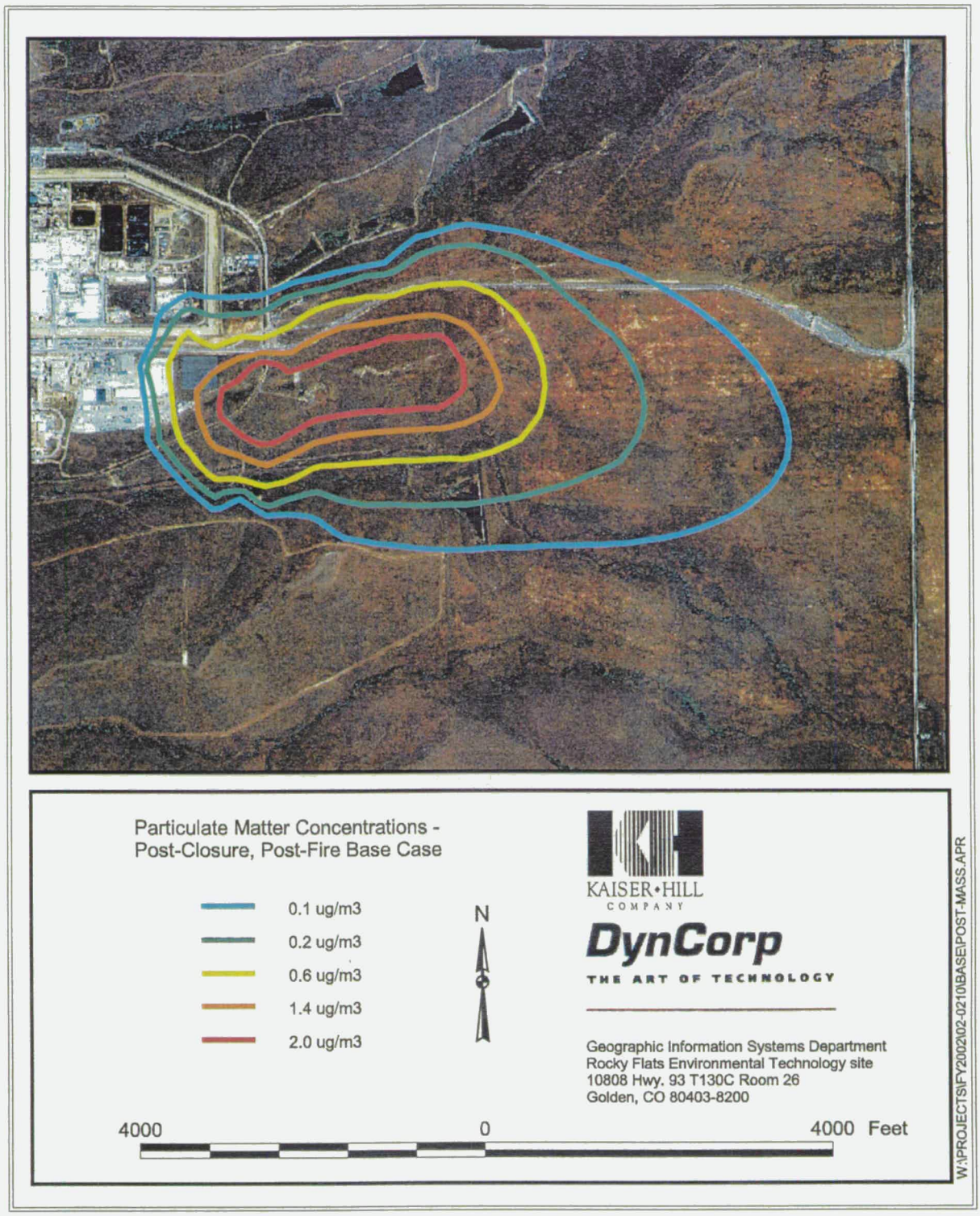

Figure 5-8. Post-Closure Base Case:
Predicted Annual Average Particulate Matter Concentrations

87

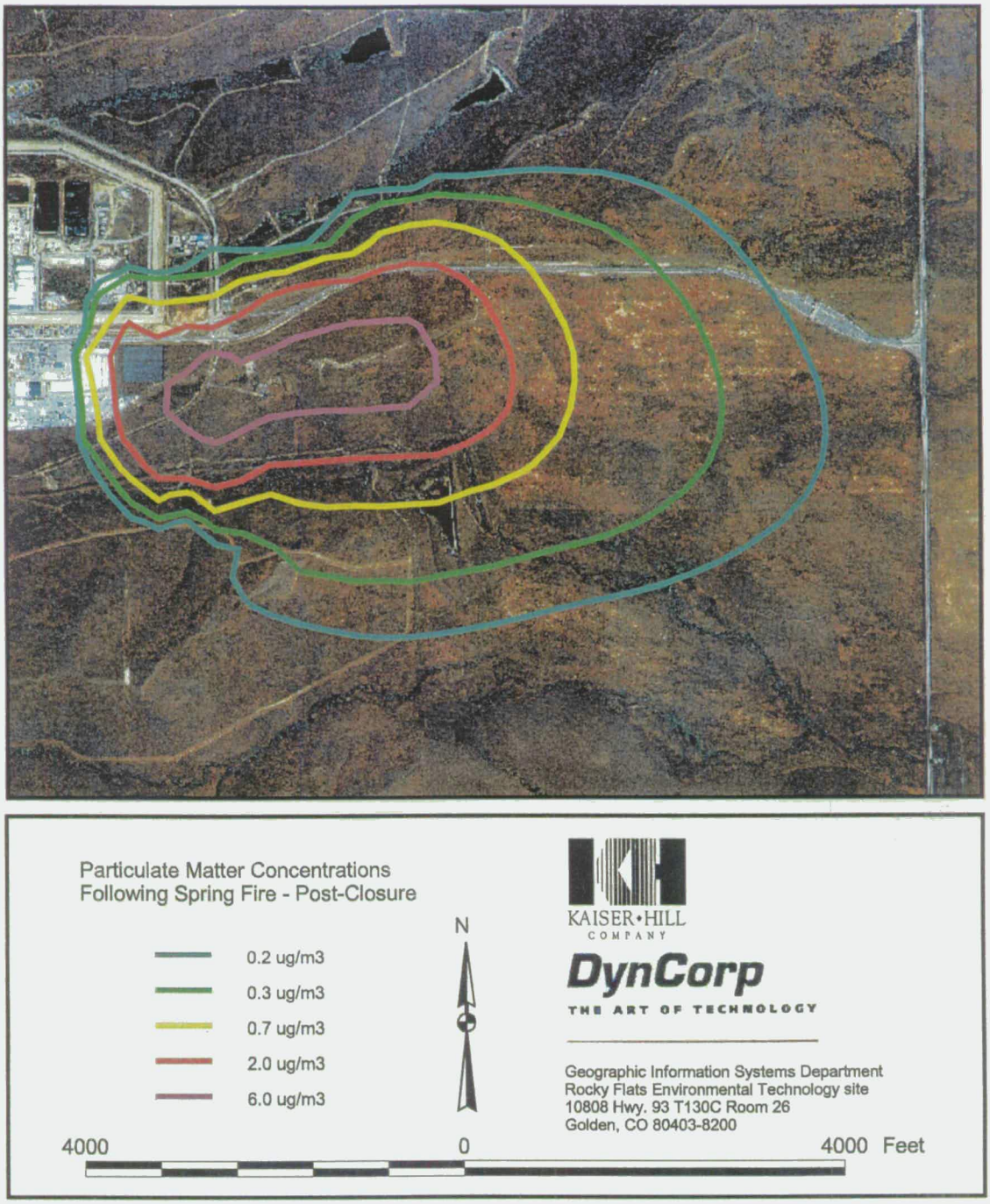

Figure 5-9. Post-Closure Spring Fire: Predicted Annual Average Particulate Matter Concentrations

88

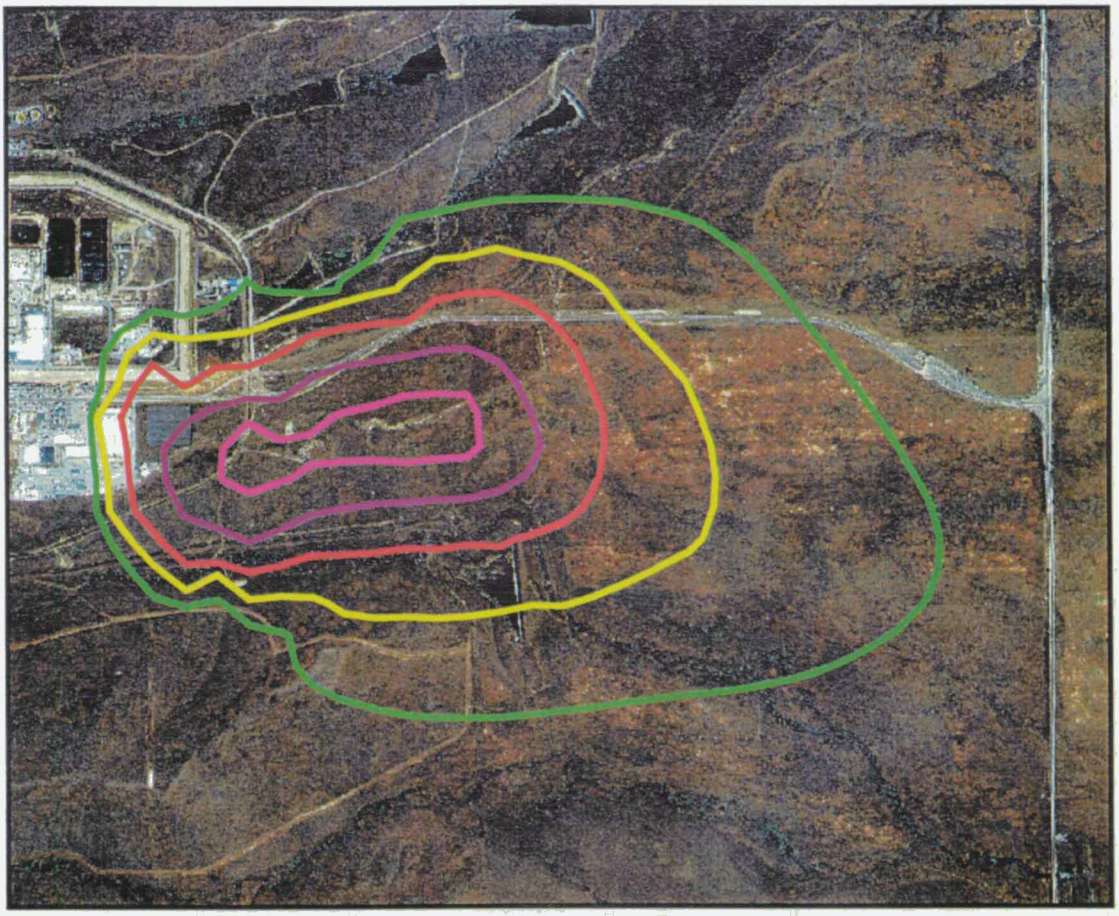

Particulate Matter Concentrations
Following Fall Fire - Post-Closure

0.3 ug/m3
0.7 ug/m3
2.0 ug/m3
6.0 ug/m3
10.0 ug/m3

N

KAISER•HILL COMPANY

DynCorp
THE ART OF TECHNOLOGY

Geographic Information Systems Department
Rocky Flats Environmental Technology site
10808 Hwy. 93 T130C Room 26
Golden, CO 80403-8200

4000 0 4000 Feet

W:\PROJECTS\FY2002\02-0210\MASS\POST-MASS-FALL.APR

Figure 5-10. Post-Closure Fall Fire:
Predicted Annual Average Particulate Matter Concentrations

89

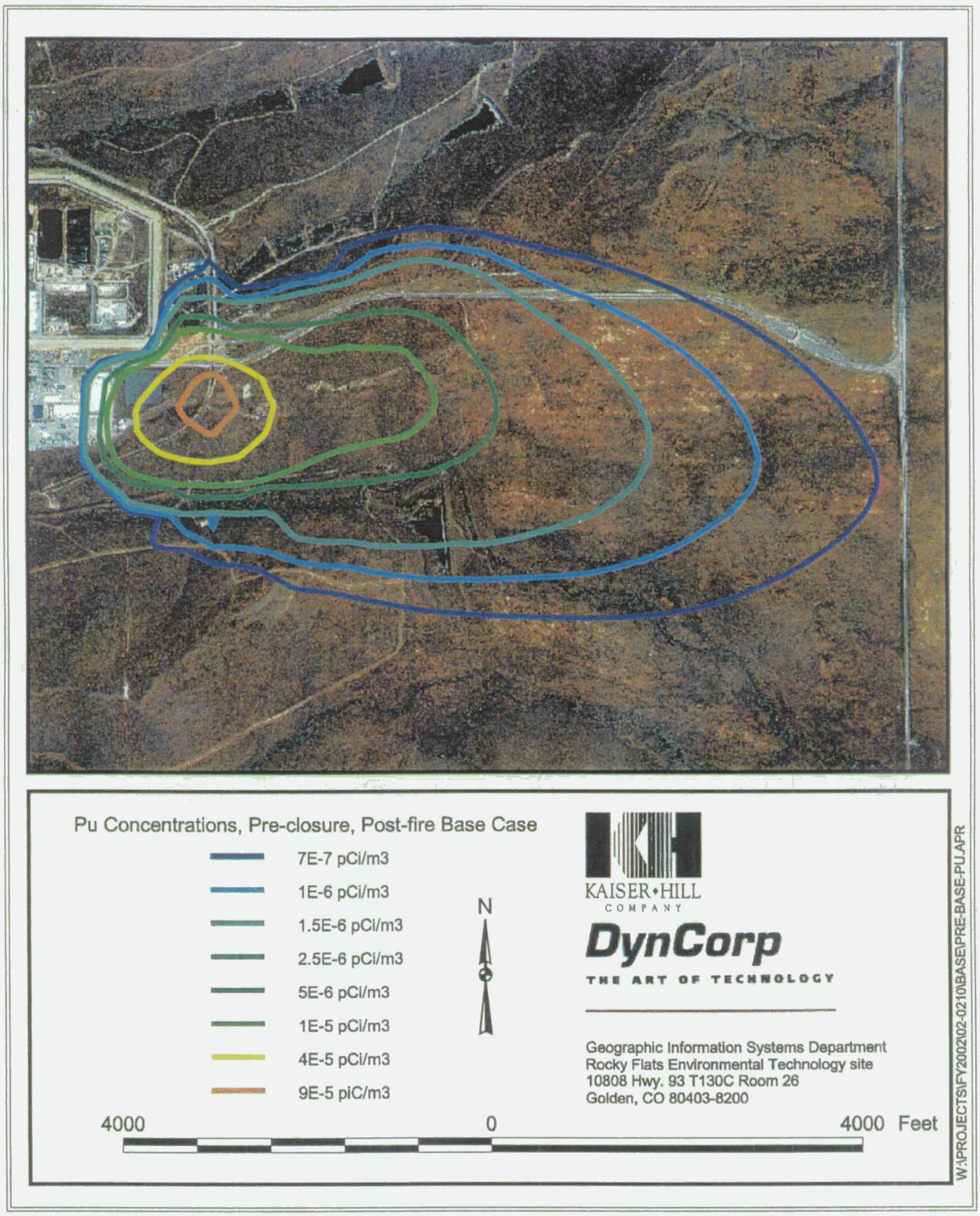

Figure 5-11. Pre-Closure Base Case: Predicted Annual Average Pu-239/240 Concentrations

90

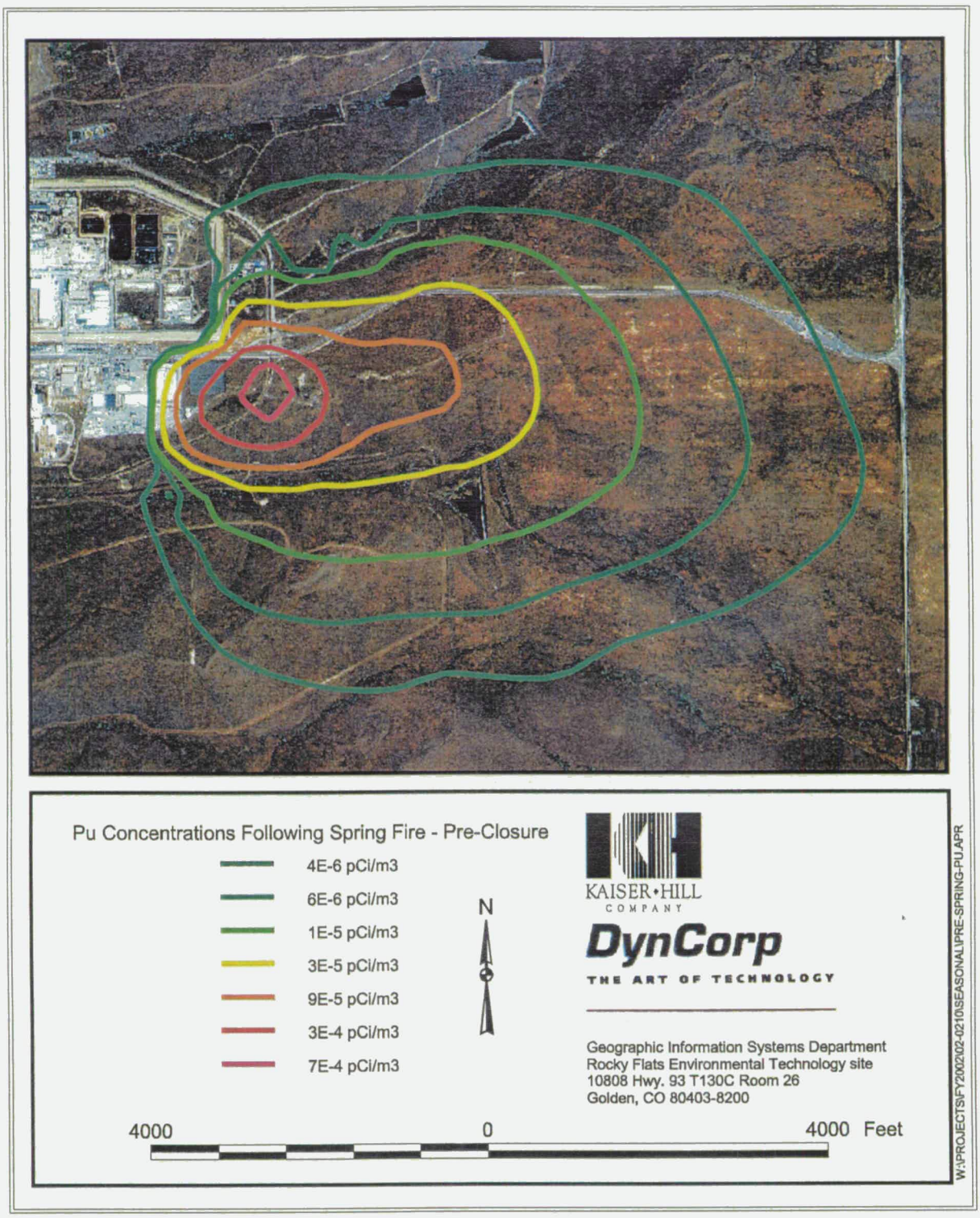

Figure 5-12. Pre-Closure Spring Fire: Predicted Annual Average Pu-239/240 Concentrations

91

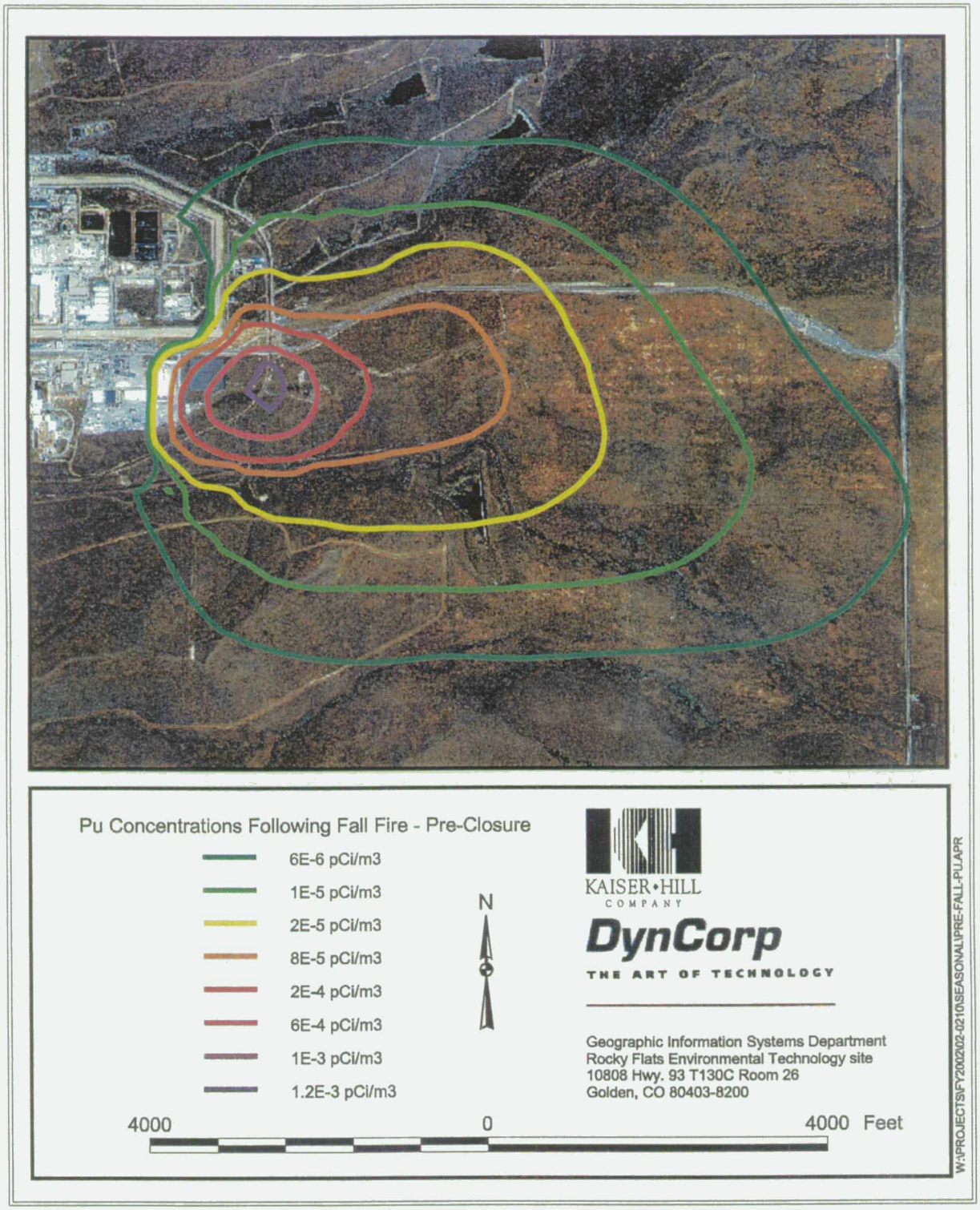

Figure 5-13. Pre-Closure Fall Fire:
Predicted Annual Average Pu-239/240 Concentrations

92

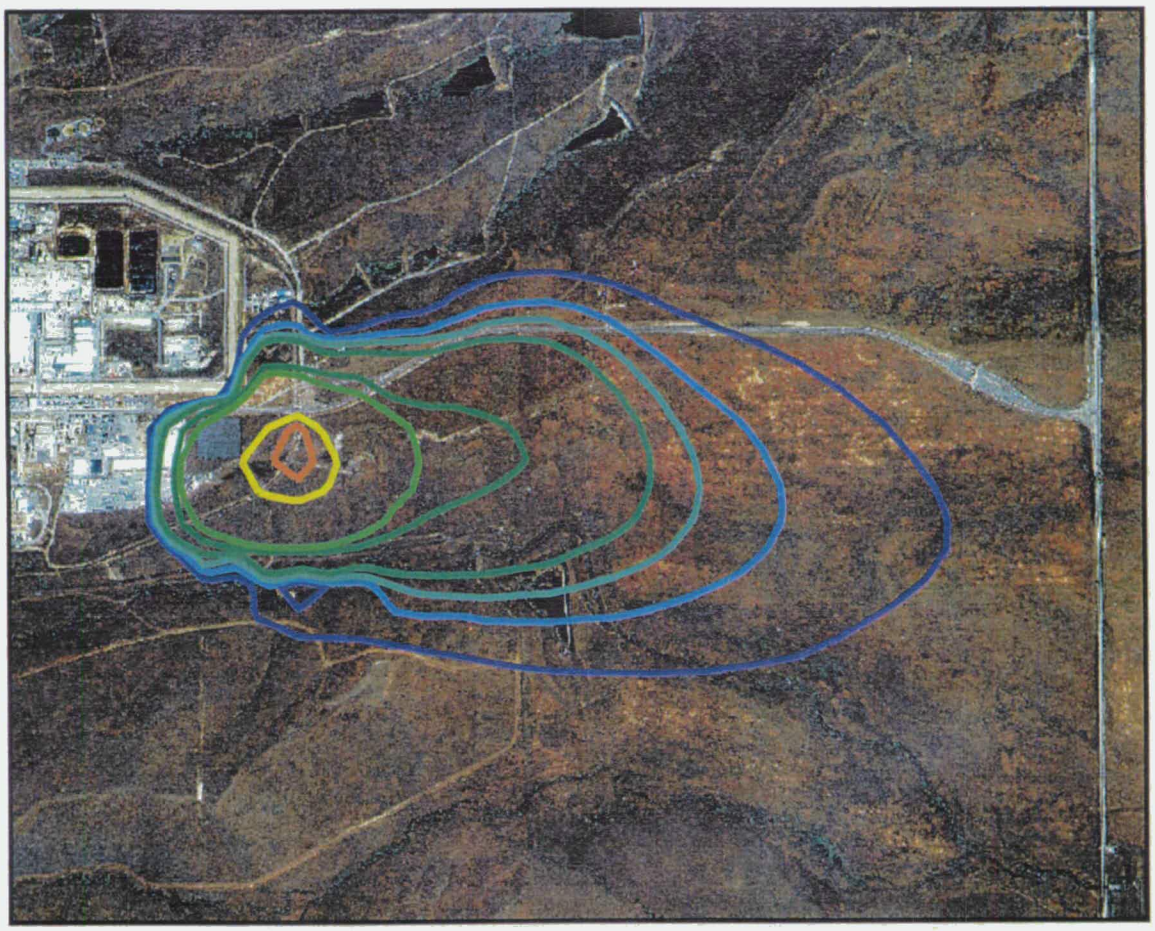

Am Concentrations - Pre-Closure, Post-Fire Base Case

- 3E-7 pCi/m3
- 5E-7 pCi/m3
- 7E-7 pCi/m3
- 1E-6 pCi/m3
- 3E-6 pCi/m3
- 5E-6 pCi/m3
- 3E-5 pCi/m3
- 4E-5 pCi/m3

N

KAISER•HILL COMPANY

DynCorp
THE ART OF TECHNOLOGY

Geographic Information Systems Department
Rocky Flats Environmental Technology site
10808 Hwy. 93 T130C Room 26
Golden, CO 80403-8200

4000 0 4000 Feet

W:\PROJECTS\FY2002\02-0210\BASE\PRE-BASE-AM.APR

Figure 5-14. Pre-Closure Base Case: Predicted Annual Average Am-241 Concentrations

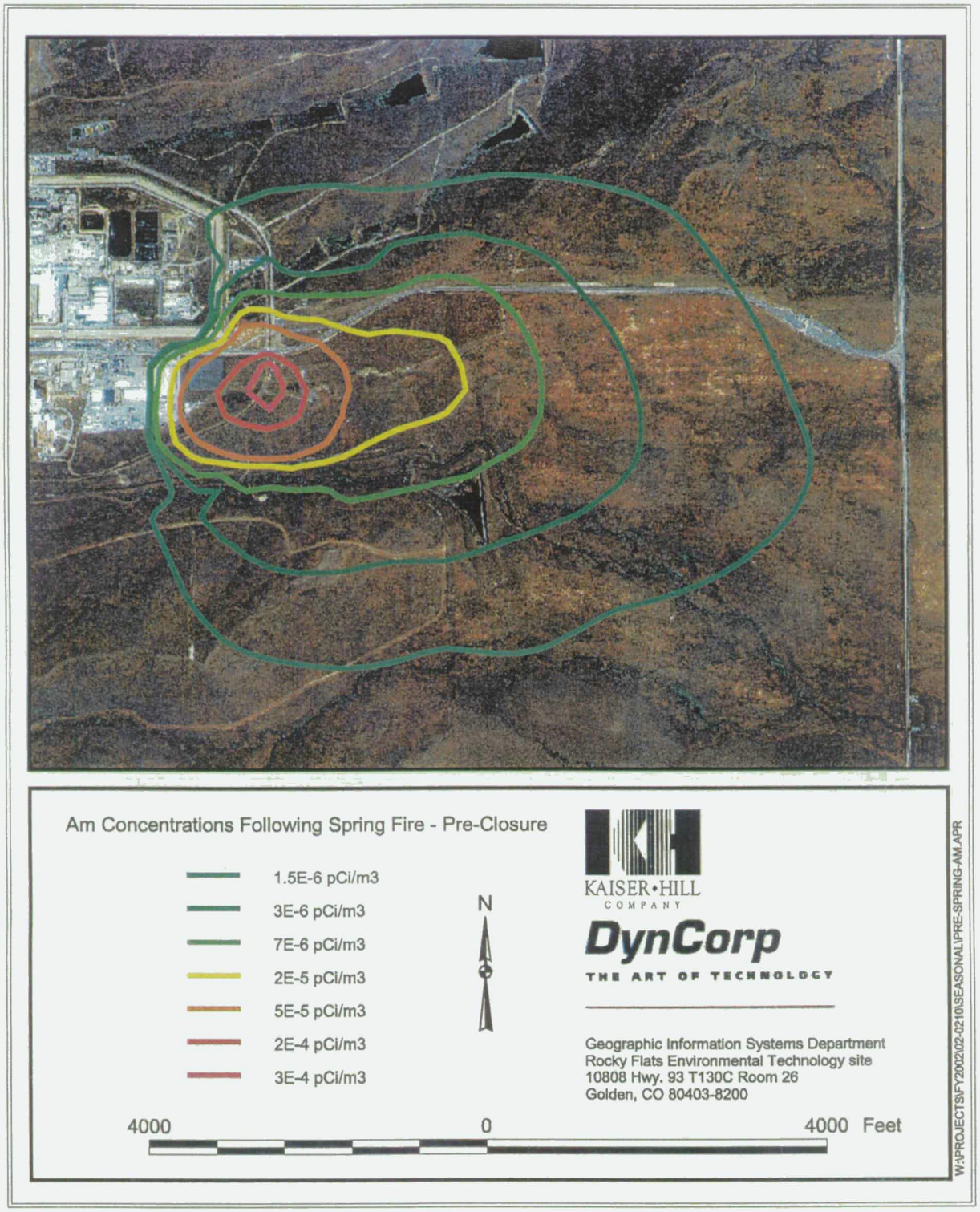

Figure 5-15. Pre-Closure Spring Fire: Predicted Annual Average Am-241 Concentrations

94

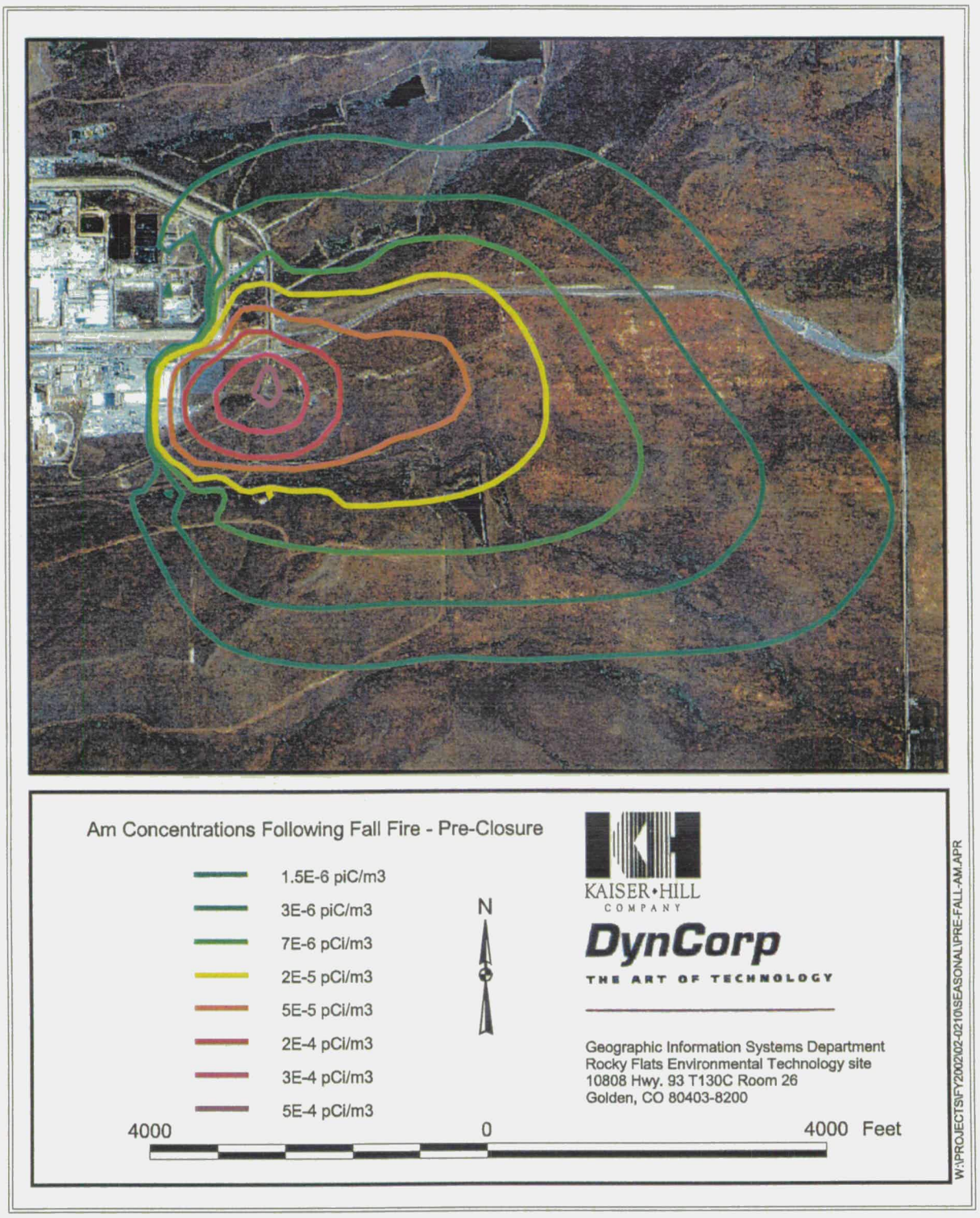

Figure 5-16. Pre-Closure Fall Fire: Predicted Annual Average Am-241 Concentrations

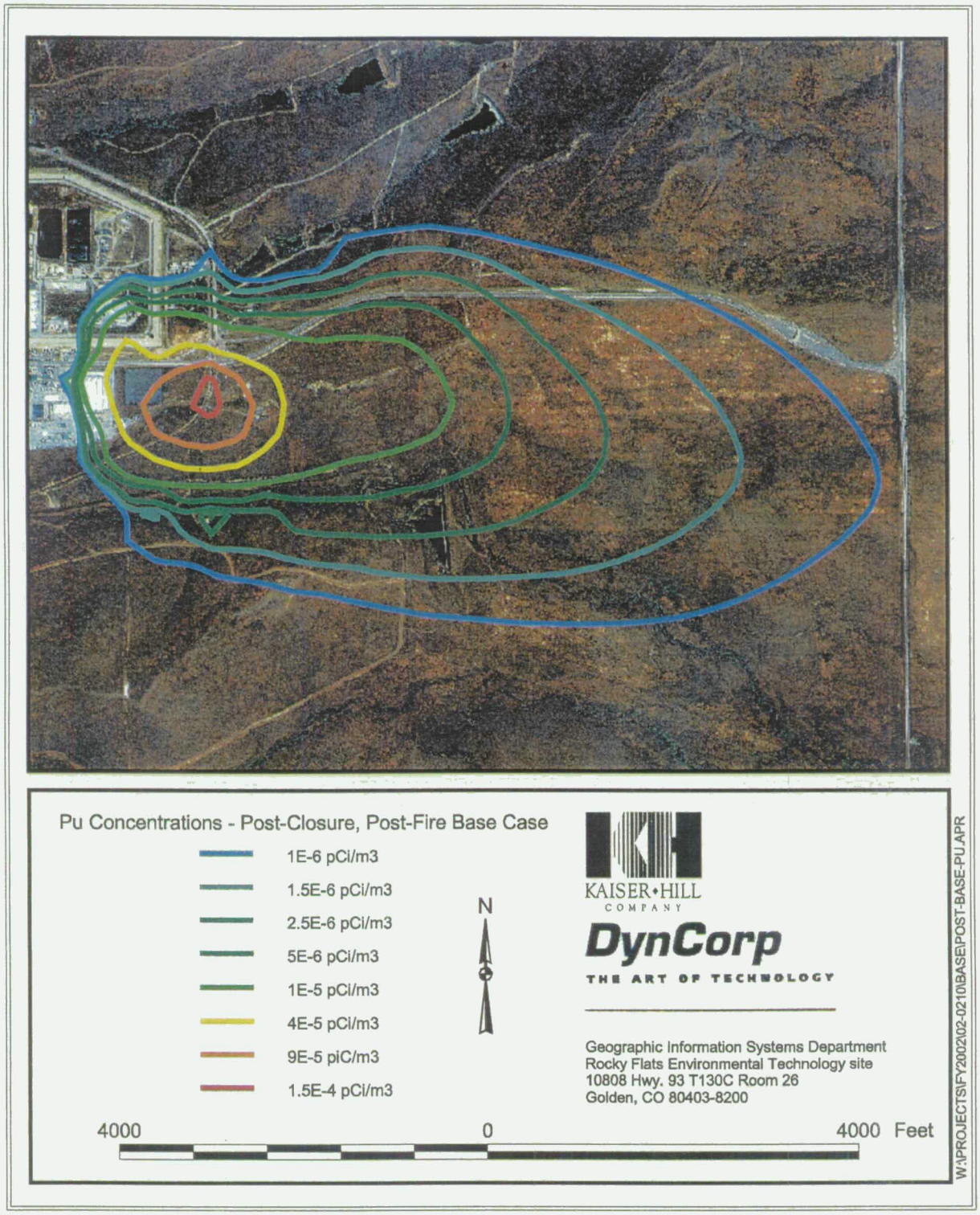

Figure 5-17. Post-Closure Base Case: Predicted Annual Average Pu-239/240 Concentrations

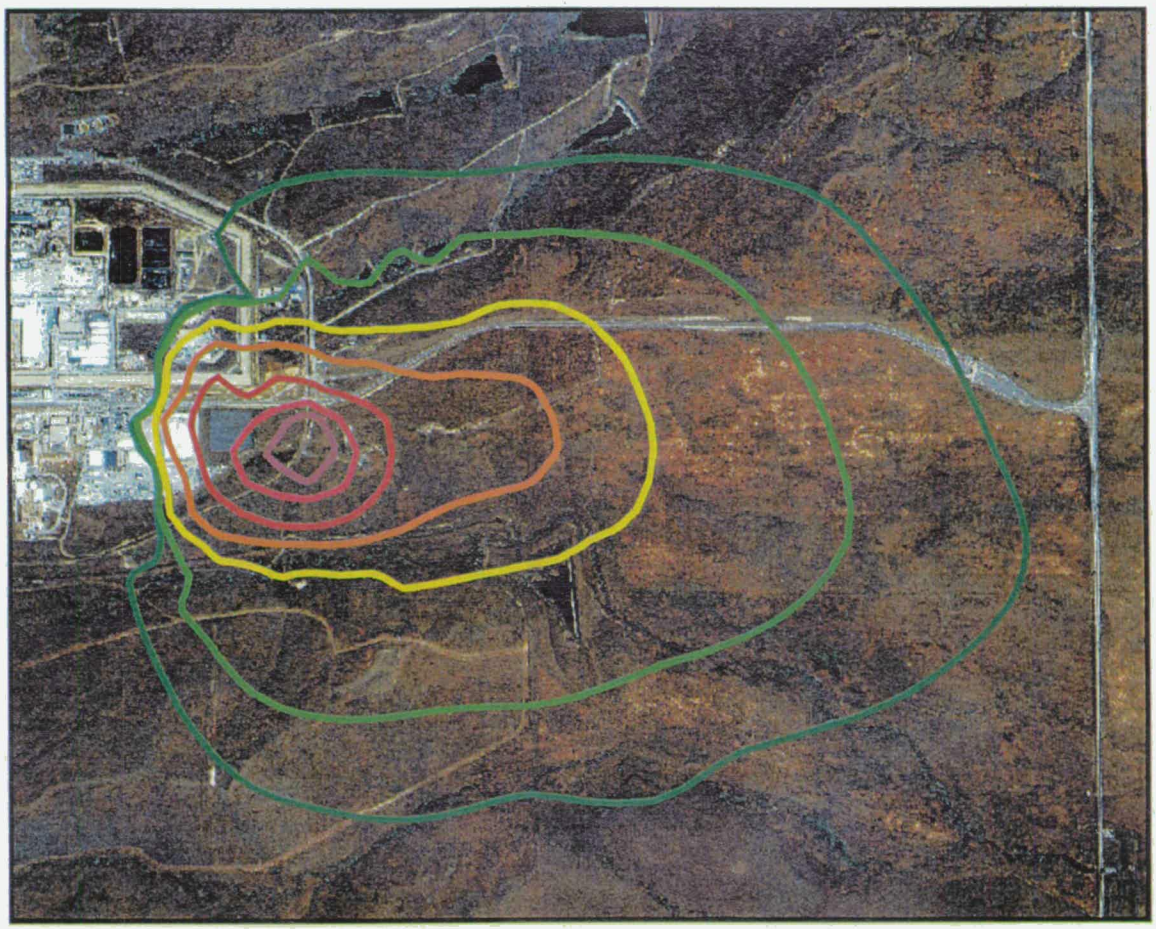

Pu Concentrations Following Spring Fire - Post-Closure

6E-6 pCi/m3
1E-5 pCi/m3
3E-5 pCi/m3
9E-5 pCi/m3
3E-4 pCi/m3
7E-4 pCi/m3
1E-3 pCi/m3

N

KAISER•HILL COMPANY

DynCorp
THE ART OF TECHNOLOGY

Geographic Information Systems Department
Rocky Flats Environmental Technology site
10808 Hwy. 93 T130C Room 26
Golden, CO 80403-8200

4000 0 4000 Feet

W:\PROJECTS\FY2002\02-0210\SEASONAL\POST-SPRING-PU.APR

Figure 5-18. Post-Closure Spring Fire: Predicted Annual Average Pu-239/240 Concentrations

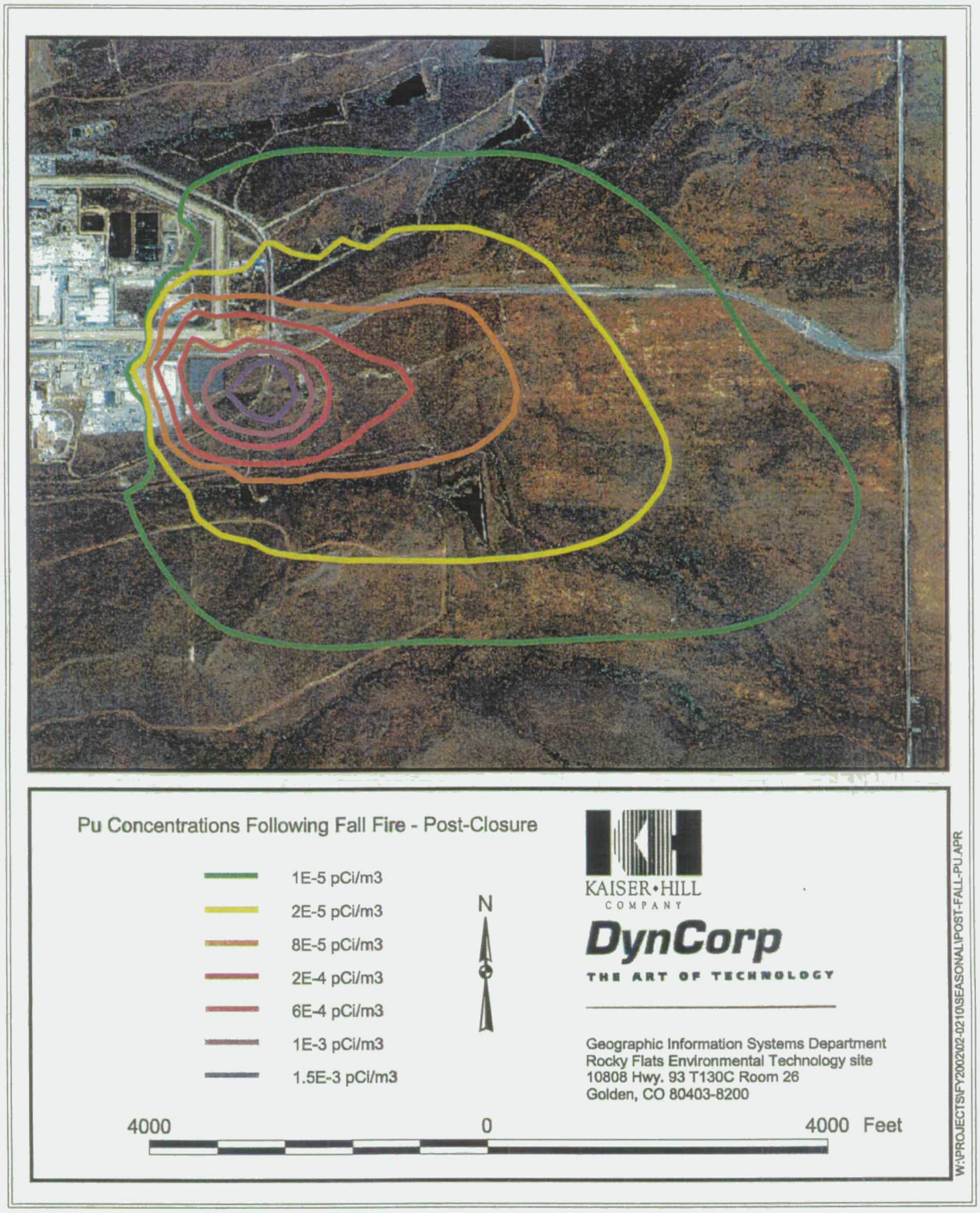

Figure 5-19. Post-Closure Fall Fire: Predicted Annual Average Pu-239/240 Concentrations

98

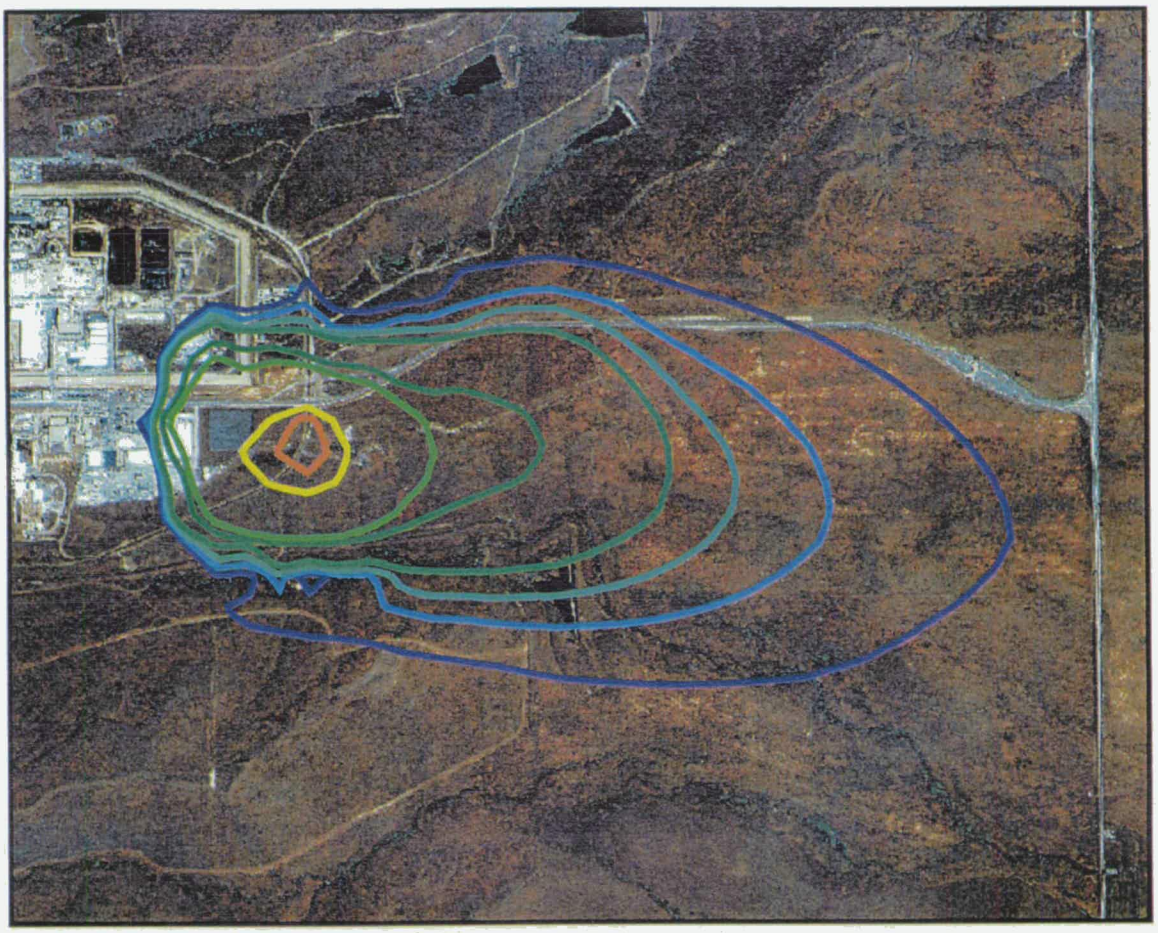

Am Concentrations - Post-Closure, Post Fire Base Case

- 3E-7 pCi/m3
- 5E-7 pCi/m3
- 7E-7 pCi/m3
- 1E-6 pCi/m3
- 3E-6 pCi/m3
- 5E-6 pCi/m3
- 3E-5 piC/m3
- 4E-5 pCi/m3

N

KAISER•HILL COMPANY

DynCorp

THE ART OF TECHNOLOGY

Geographic Information Systems Department
Rocky Flats Environmental Technology site
10808 Hwy. 93 T130C Room 26
Golden, CO 80403-8200

4000 0 4000 Feet

W:\PROJECTS\FY2002\02-0210\BASE\POST-BASE-AM.APR

Figure 5-20. Post-Closure Base Case: Predicted Annual Average Am-241 Concentrations

99

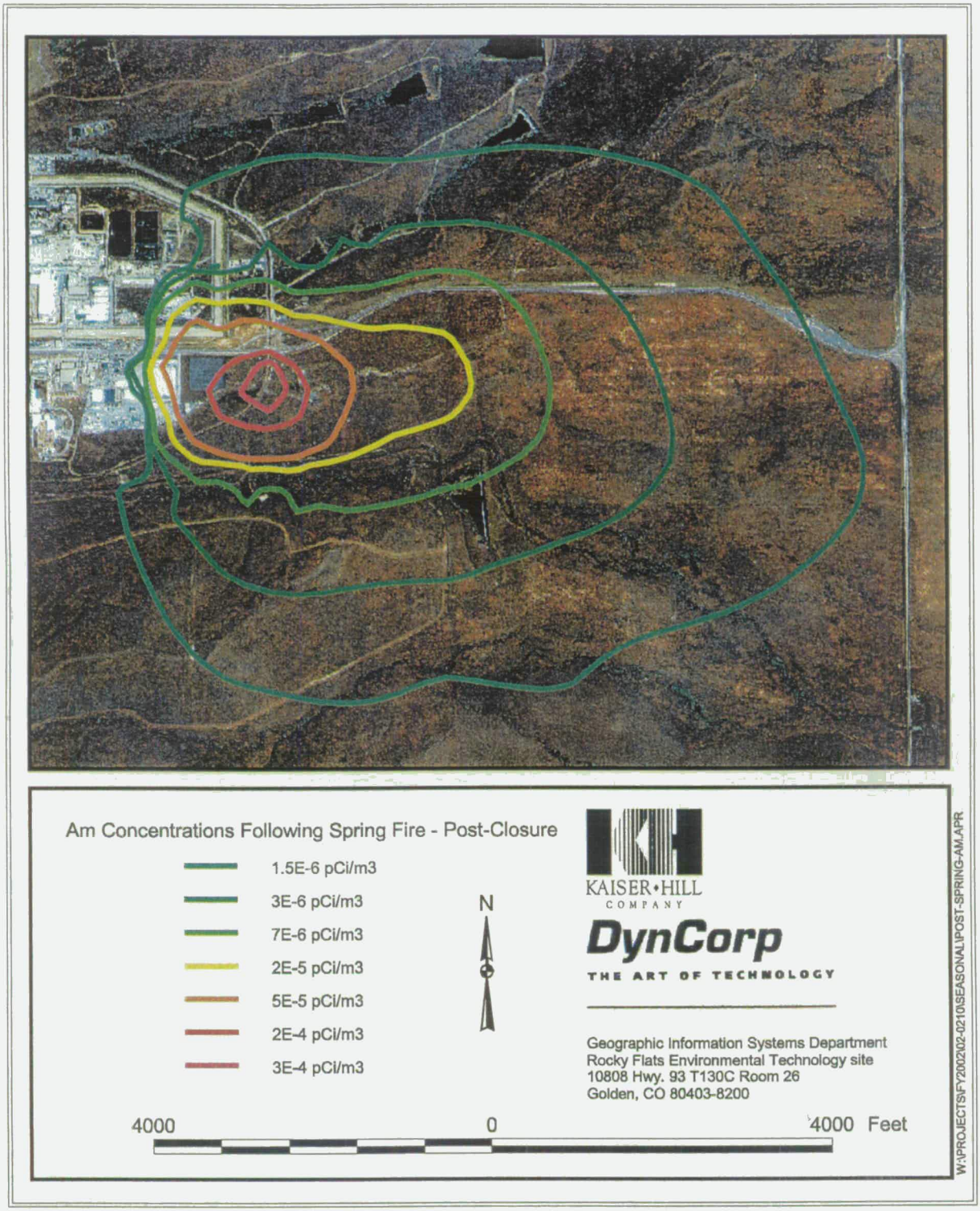

Figure 5-21. Post-Closure Spring Fire: Predicted Annual Average Am-241 Concentrations

100

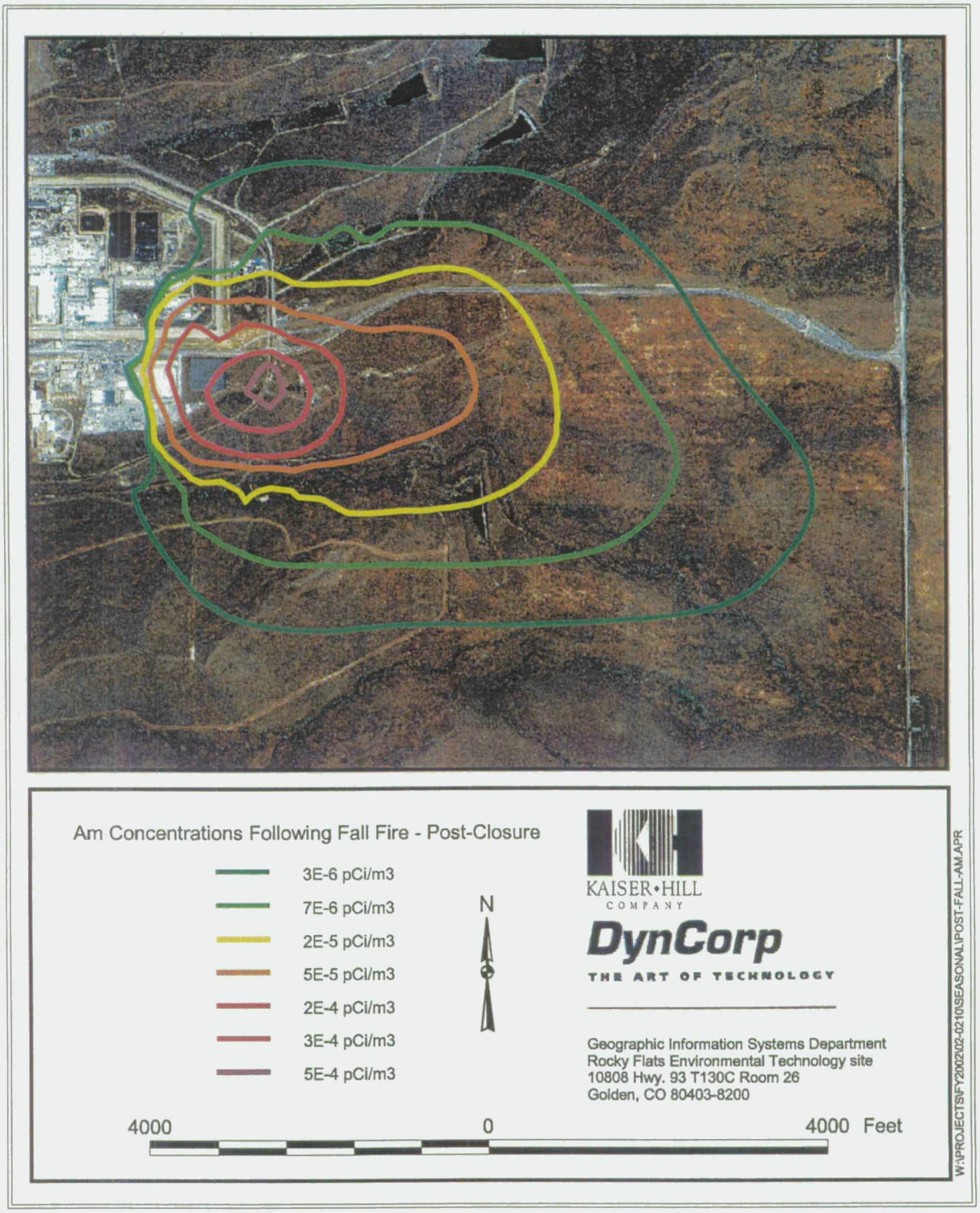

Figure 5-22. Post-Closure Fall Fire:
Predicted Annual Average Am-241 Concentrations

101

6.0 FY01 AIR PATHWAY DISCUSSION AND CONCLUSIONS

This section summarizes the findings of the FY01 air pathway work and discusses the information provided by the improved emission estimating technique.

6.1 Air Pathway Findings

The emission estimating technique developed in FY99 and FY00 for wind erosion at the Site was revised based on wind tunnel studies performed in 2000. The revised technique more accurately reflects the current vegetation state of Site surfaces and accounts for both limitations in erodible particulate matter mass and dilution of actinide concentrations by particulate matter originating outside the contaminated areas. Comparisons to measured actinide concentrations showed significant improvement in the model results relative to previous years. Modeled actinide emissions from undisturbed areas at the Site, when added to regional background concentrations, now provide a good fit to measured data at all locations.

Modeling of chronic wind erosion emissions of Pu-239/240 and Am-241 under current Site conditions showed maximum concentrations and deposition of actinides to the east of the primary source areas on Site, reflecting the prevailing direction of higher speed winds at the Site. Post-closure wind erosion impacts are expected to exhibit similar patterns but the impacts will increase slightly because removal of buildings and pavement will increase the soil surface areas available for wind erosion. Although only small amounts of actinides will be left in Site surface soils, particles and actinides will be resuspended from a significantly larger source area, with resulting increases in impacts to air from this small emission source. Maximum post-closure concentrations of Pu-239/240 and Am-241 would still be substantially less than the annual EPA air dose limit (10 mrem).

Wind erosion following a fire in the 903 Pad area was predicted to cause as much as a 5- to 13-fold increase in annual actinide concentrations when compared to unburned conditions. Particulate matter concentrations were predicted to increase by smaller amounts. The increases in particulate matter and actinide concentrations would vary with the location of the fire and with the time of the year that the fire occurred. A fall fire would cause greater concentration increases than a spring fire because vegetation would recover more slowly over the winter months than during the spring and summer.

The worst-case, pre-closure fire was predicted to result in an annual Pu-239/240 EDE of approximately 7.5 mrem and an Am-241 EDE of 3.05 mrem. These concentrations represent a receptor located within the burned area itself. At the Site fenceline, predicted worst-case, post-fire concentrations totaled 0.038 mrem Pu-239/240 and 0.011 mrem Am-241. Post-closure impacts would be somewhat higher for a fire in the same location:

10.5 mrem Pu-239/240 and 3.16 mrem Am-241 for a receptor located within the burned area and 0.055 mrem Pu-239/240 and 0.013 mrem Am-241 for a fenceline receptor.

6.2 Discussion of Revised Wind Erosion Modeling Methods

The wind erosion emission estimating method combined with the ISCST3 model provide a valuable tool for exploring future wind erosion scenarios. The basic technique has been verified against measured data for undisturbed conditions and performs well. While the hypothetical post-fire and post-closure scenarios cannot be similarly verified, the modeling method is expected to account for most important variables in a fairly realistic manner, again providing a useful tool for exploring future emission scenarios.

The sensitivity analyses showed several interesting interactions. The analyses indicated that dilution of contaminated surface soil with "clean" particulate is probably a very important effect in limiting total actinide emissions. It is interesting to note that the wind tunnel tests that followed the July 2000 wildfire showed direct evidence of such dilution in the top soil layer, which represents the particles most available for wind erosion.

An important variable about which little is known is the rate at which erosion potential is renewed by small-scale soil disturbances such as freeze/thaw, rainsplash, animal activity, etc. While most of the particulate matter that is available for wind erosion from undisturbed areas is probably derived from deposition of airborne particulate matter, the majority of the actinide content of airborne emissions is derived through soil disturbances. As a result, improved understanding of this process and alternative ways to estimate generation rates would be useful in providing a better understanding of air transport of actinides from the Site.

Under undisturbed conditions, the analyses indicated that sufficient erodible material may be generated on an annual basis through deposition or soil disturbance to supply the relatively low erosion potential that characterizes vegetated areas of the Site. In contrast, emissions from a burned surface would be significantly limited by the rate at which erodible material is renewed. This observation parallels previous erosion studies that have shown that emissions decrease from a surface over time unless the surface is disturbed. The erodible material is exhausted and no additional emissions occur until the erodible material can be resupplied.

This effect is important in limiting emissions following a fire. For example, the simulations indicated that fall fire particulate matter emissions would have been double what was predicted if unlimited erodible material had been available. Similarly, spring fire particulate matter emissions would have increased by 1.5 times the predicted amount. These emission increases would generally have translated into comparable increases in particulate matter and actinide concentrations.

The post-fire simulations also revealed additional interactions that may influence actinide concentrations in the real world. Changes in assumed particle size distribution affected not only the predicted deposition and concentration patterns downwind from the source areas but also altered the amount of particulate matter and actinide available for erosion. Increased emissions from the burned areas increased mass loading over them, creating a feedback loop that further enhanced particulate matter emissions but that may have decreased actinide emissions through dilution. Predicted emissions were limited for the spring fire case because the summer period, during which the ground was assumed to be relatively bare and erosion potential highest, had lower wind speeds than fall and winter, by which time substantial vegetative recovery was predicted. These types of interactions indicate that airborne actinide concentrations following a fire event cannot be accurately predicted by taking into account the potential increase in erosion potential alone.

7.0 REFERENCES CITED

Chang, Y. S., Yu, C. and S. K. Wang, 1998. *Evaluation of the Area Factor Used in the RESRAD Code for the Estimation of Airborne Contaminant Concentrations of Finite Area Sources.* Report ANL/EAD/TM82. Argonne National laboratory, Argonne, Illinois.

DOE, EPA and CDPHE, 1996. *Final Rocky Flats Cleanup Agreement*. July.

EG&G, 1994. *OU3 Wind Tunnel Study, Volume 1: Test Report, Volume I1: Field Data Sheets.* DOE Prime Contract No. DE-AC04-90DP62349, Subcontract No. ASC218973GG, MRI Project No. 3155-M. Golden, Colorado.

EPA, 1989. *National Technical Guidance Series Air Pathway Analysis Procedure for Superfund Applications. Vol. II: Estimates of Baseline Air Emissions at Superfund Sites.* EPA-450/1-89-002a.

EPA, 1995. *User's Guide for the Industrial Source Complex (ISC3) Dispersion Models, Volume I and II (EPA-454/B-95-003a).* Office of Air Quality Planning and Standards, Research Triangle Park, North Carolina.

EPA, 2000. *Compilation of Air Pollutant Emission Factors*. Volumes I and II. Office of Air Quality Planning and Standards, Research Triangle Park, North Carolina.

Hulse, S.E., S.A. Ibrahim, F.W. Whicker, and P.L. Chapmant, 1999. *Comparison of* ^{241}*Am,* ^{239,240}*Pu and* ^{137}*Cs Concentrations in Soil Around Rocky Flats.*

Langer, G., 1986. *Dust Transport- Wind Blown and Mechanical Resuspension, July 1983 to December 1984 (RFP-3914).* Rockwell International, Golden, Colorado. September.

MRI, 2001a. *Effect of Controlled Burning on Soil Erodibility by Wind, Final Test Report.* MRI Project No.110056.

MRI, 2001b. Effect of Wildfires on Soil Erodibility by Wind, Final Test Report. MRI Project No. 110056.1.004

Radian International, 1999. *Air Transport and Deposition of Actinides at the Rocky Flats Environmental Technology Site.*

Radian International, 2000. *Air Transport and Deposition of Actinides for the Actinide Migration Evaluation at Rocky Flats Environmental Technology Site, FY00 Report.*

Ranville, M., Harnish, R. A., Winkler, S. and B. D. Honeyman, 2000. *Soil Aggregation and Its Influence on ^{239,240}Pu Particle-Size Distributions of Soils Collected from Rocky Flats, Colorado.* Department of Chemistry and Geochemistry, Division of Environmental Science and Engineering, Colorado School of Mines, Golden, Colorado. July.

APPENDIX A

Effects of Prescribed Grass Fire on Wind Erosion Rates from Surface Soil at Rocky Flats, CO

Effects of Prescribed Grass Fire on Wind Erosion Rates from Surface Soil at Rocky Flats, Colorado

Patrick Haines and Susan Templeman
URS/Radian, 8181 East Tufts Ave., Denver, Co 80237
patrick.haines@rfets.gov

Martha Hyder
Wind River Environmental Group LLC, 3785 S. Poplar Street, Denver, CO 80237
martha.hyder@rfets.gov

Chatten Cowherd, Jr. and Mary Ann Grelinger
Midwest Research Institute, 425 Volker Boulevard, Kansas City, MO 64110
ccowherd@mriresearch.org

ABSTRACT

Removal of plants and plant litter by fire significantly increases the erosion potential of the underlying soil for some period of time. By using a portable wind tunnel to simulate high winds across test plots within a prescribed burn area, the effects of fire on soil erosion potential may be quantified as a function of wind speed and elapsed time following the fire.

A portable wind tunnel was used to generate high winds and collect soil particles eroded from a 50-acre study area that underwent a controlled burn in April 2000. Wind tunnel studies of the burned area and neighboring control areas were performed following the test burn, and again at intervals of 25 and 73 days following the fire. Soil erosion rates at incremented wind speeds were determined using optical particle counters and gravimetric analysis of dust samples. Shallow soil samples were collected from areas around the wind tunnel study plots for analysis in a soil dustiness test chamber.

The study was directed at answering the following questions:

- What increase in soil erosion potential may be expected as a result of grassland fire?
- What is the recovery rate of soil protective elements (vegetation and litter) for an area denuded by fire, as indicated by soil erosion potential?
- What algorithms may be employed to estimate increases in fugitive dust emissions resulting from post-fire increases in soil erosion potential?
- How may such algorithms be employed in common atmospheric dispersion models?

INTRODUCTION

The U.S. Department of Energy's Rocky Flats Environmental Technology Site (Site) has several areas of actinide-contaminated soil as a result of spills and releases during the Site's nuclear weapons production era. Most such areas are well vegetated, which has stabilized potential wind-driven resuspension of actinide-contaminated soil particles. The Site is currently

undergoing cleanup and closure, and as plans are being made for post-closure use, the increase in actinide emissions that might result following removal of vegetation by fire has become an issue of great interest. The Site has experienced three small lightening-caused grass fires in the past 10 years, so fires represent reasonably foreseeable occurrences.

In Spring 2000, the Site conducted a test burn to evaluate a proposed program of prescribed burning for weed control and prairie restoration. The test burn, which covered approximately 50 acres in the Site's buffer zone (the large, undeveloped area surrounding the Site's industrial area), presented an opportunity to gather data on post-fire resuspension rates and subsequent recovery for use in estimating emissions and impacts from wildfires at the Site. A portable wind tunnel was used to generate high winds and collect soil particles eroded from soil surfaces following the test burn, and again at intervals of 25 and 73 days following the test burn. Wind tunnel tests were performed by Midwest Research Institute (MRI) on representative portions of the test-burn area and also on an adjacent, unburned grassy area within the Rocky Flats site.

Because removal of standing plants and plant litter by fire significantly increases the erosion potential of the underlying soil for some period of time, one goal of the study was to evaluate the length of time it takes for a burned surface to regain protection against wind erosion comparable to pre-burn conditions. The objectives of the study also included determining how dust resuspension increases from one wind speed plateau to the next and how resuspension rates decay in time at a given wind speed. The wind tunnel tests determined wind erosion emission rates that will be used in the future to model short-term and annual particulate matter and actinide emissions from potential fires at the Site. The methods and results of the study are described below.

TEST EQUIPMENT AND PROCEDURES

The prescribed burn was conducted on April 6, 2000 and wind tunnel testing was initiated the day after the burn. Wind tunnel tests were performed by MRI using a portable reference wind tunnel, described in the *Air/Superfund National Technical Guidance Study Series, Volume II, Estimates of Baseline Air Emissions at Superfund Sites.*[1] Two TSI DustTRAK monitors were used to provide real-time concentrations of PM_{10} (particles less than or equal to 10 micrometers [μm] in aerodynamic diameter) in the tunnel effluent. Laboratory dustiness tests were run on bulk surface soil samples from burned areas to characterize the soil texture and to investigate the effects of soil moisture on erosion potential.

Wind Tunnel Trials

Field tests of the prescribed burn area at Rocky Flats were performed over one-week periods beginning April 7, May 2, and June 19, 2000. During each test, the wind tunnel was moved three times over the test area, to collect additional particulate on the back-up filter in the effluent sampling train and to improve the detection and precision of the PM_{10} erosion potential estimates.

The primary test device used in the evaluation was MRI's portable reference wind tunnel, shown in Figure 1. Although the portable wind tunnel does not generate the larger scales of turbulent motion found in the atmosphere, the turbulent boundary layer formed within the tunnel simulates the smaller scales of atmospheric turbulence. It is the smaller scale turbulence that penetrates the wind flow in direct contact with the erodible surface and contributes to the particle entrainment mechanisms. The wind tunnel method relies on a straightforward mass balance technique for calculation of particulate emission rates. Previous wind erosion studies using the MRI reference wind tunnel have led to the U.S. Environmental Protection Agency (EPA) recommended emission factors for industrial wind erosion presented in *Compilation of Air Pollutant Emission Factors (AP-42).*[2]

For each run, the open-floored test section was placed directly over the surface to be tested. Air was drawn through the tunnel at controlled velocities, increasing at 2 meter per second [m/s] (5 mile per hour [mph]) increments, to a maximum velocity of about 40 mph at the tunnel centerline. This corresponded to a wind speed between 97 and 145 mph at a 10 meter (m) height; the equivalent 10-m speed varied with the roughness height of the surfaces tested in each trial.

Typically, each time the wind speed was increased, a PM_{10} concentration spike was observed. Furthermore, upon each successive increase, the peak value of the spike increased and the rate of decay decreased. The PM_{10} concentration values for each wind speed plateau were observable in the "real-time" concentration histories, recorded by the DustTRAK monitors (described below). For higher wind speed plateaus, the duration of sampling was increased to allow additional time for the spike to decay. An example of the concentration spikes that occurred during wind tunnel testing on the burned area can be seen in Figure 2.

A pitot tube was used to measure the centerline wind speed in the open-floored test section. The volumetric flow rate through the wind tunnel was determined from a published relationship between the maximum centerline velocity in a circular duct and the average velocity, as a function of Reynolds' number.[3] Because the ratio of the centerline wind speed in the sampling extension to the centerline wind speed in the working section was nearly independent of flow rate, the ratio could be used to determine isokinetic sampling conditions for any flow rate in the tunnel.

The surface roughness heights for the test runs were determined by fitting vertical profiles of wind speed in the test section of the wind tunnel to a logarithmic function. An average roughness height was calculated for each test series, for purposes of calculating friction velocities and 10-m equivalent wind speeds. The friction velocity, which is a measure of wind shear at the erodible surface, characterizes the capacity of the wind to cause surface particle movement.

The exit air stream from the test section was passed through a circular duct fitted with a sampling probe near the downstream end. The particulate sampling train, which was operated at 68 cubic meters per hour (m^3/hr) (40 actual cubic feet per minute [acfm]), consisted of the tapered sampling probe, cyclone pre-collector, quartz backup filter, and high-volume motor. The sampling probe was pointed into the air stream, and isokinetic sampling was achieved by fitting

the sampling probe with a nozzle of appropriate size. Sampled total airborne particulate (TP) emissions were separated into two particle size fractions by the cyclone: particles larger than PM_{10} were collected inside the cyclone, and PM_{10} was collected on the backup filter below the cyclone.

A high-volume ambient air sampler was operated at 68 m^3/hr (40 acfm) near the inlet of the wind tunnel to provide for measurement and subtraction of the contribution of the ambient background particulate level. The filter was vertically oriented, parallel to the tunnel inlet face.

At the completion of each test series, the sampling train was disassembled and taken to the field instrument van, where the collected samples of dust emissions (cyclone catch and backup filter) were carefully placed in protective containers. Dust samples from the field tests were returned to an environmentally controlled laboratory for gravimetric analysis. Quartz filters were conditioned at constant temperature (23 degrees Celsius [°C] ±1°C) and relative humidity (45% ± 5%) for 24 hours prior to weighing (the same conditioning procedure used prior to tare weighing). The particulate catch from the cyclone pre-collector was weighed in a tared poly bag.

DustTRAK Monitoring

Continuous monitoring of particulate concentration in the sampling extension provides for a greater level of detail in tracking the dynamics of the wind erosion process. For this study, two portable DustTRAK Aerosol Monitors (TSI, Inc., St. Paul, Minnesota) were used to continuously sample the air between the cyclone and the backup filter to track the PM_{10} concentrations in the tunnel effluent.

The DustTRAK monitor is a portable, battery-operated instrument that gives real-time measurements and has a built-in data logger. The operating principle of the DustTRAK is based on 90° light scattering. Light scattering (deflection) by local variations in refractive index is caused by the presence of particles whose size is comparable to the wavelength of the incident light. The theoretical detection efficiency peaks at about 0.2-0.3 μm and gradually decreases for larger particle sizes. A pump draws aerosol into the optics chamber where either solid or liquid particles are detected using a laser diode light source and a solid-state photodetector. The instrument can store measurements at programmable intervals for later trending and reporting.

The DustTRAK PM_{10} monitor was calibrated against the actual PM_{10} mass collected on the backup filter of the wind tunnel effluent sampling train during a given test run. This calibration required an integration of the real-time DustTRAK PM_{10} concentration profile (versus time) and calculation of the average DustTRAK PM_{10} concentration. The average DustTRAK PM_{10} concentration was then compared to the average PM_{10} concentration calculated from the PM_{10} mass collected on the backup filter below the cyclone.

Use of the DustTRAK monitor provided a more comprehensive analysis of surface erodibility than wind tunnel sampling alone, especially appropriate to study surfaces that do not have a well defined wind erosion threshold velocity. There are multiple contributors to wind generated particulate emissions on the burned vegetative surfaces at the Site: 1) bulk soil, 2)

settled surface dust trapped by vegetation, and 3) the vegetation itself. The particle releases from these reservoirs are all driven by different mechanisms, each with a different wind speed dependence.

The approach taken in this study was to expose each test surface to a well-defined time history of increasing wind speeds, while simultaneously monitoring the PM_{10} concentration in the tunnel effluent. Each time the wind speed was increased, a concentration spike was observed. Time integration of these spikes generated erosion mass increments of PM_{10} that when added together yielded cumulative erosion potential as a function of wind speed.

Dustiness Testing

In April and May 2000, six subareas in the controlled burn area were sampled for surface soil. The soil samples were collected to a depth of approximately 1 to 1.5 centimeters (cm) using a whiskbroom and dustpan. The areas were judged to be representative of the wind tunnel test areas.

Dustiness testing was performed on samples of surface soil to characterize the potential for release of airborne PM_{10} when the soil is disturbed. Dustiness tests were also run under varying soil moisture levels to provide information on the mitigating effect of soil moisture in reducing PM_{10} emissions. The moisture levels selected for dustiness testing were 0%, 2%, 4%, 6%, and 8%.

The MRI Dustiness Test Chamber is a laboratory device used to determine the tendency of finely divided bulk materials (e.g., soils, powders) to release fine particles. Within the chamber, the particles generated from controlled pouring of material are captured on an overhead filter with a sampling rate of 5 liters per minute. The net weight of particulate matter caught on the filter (final filter weight minus tare weight) is divided by the mass of material poured to calculate the mass emission rate in units of milligrams of dust per kilogram of material poured. This quantity is defined as the dustiness index of the test material.

TEST ANALYSIS

Because wind erosion is an avalanching process, it is reasonable to assume that the loss rate from a surface is proportional to the amount of erodible material remaining:

$$\frac{dM}{dt} = -kM \qquad (1)$$

where

M = quantity of erodible material on the surface at any time, grams per square meter (g/m^2)
k = proportionality constant, inverse seconds (s^{-1})
t = cumulative erosion time, seconds (s)

Integration of Equation 1 yields:

$$M = M_o e^{-kt} \qquad (2)$$

where

M_o = erosion potential, i.e, quantity of erodible material present on the surface before the onset of erosion, g/m^2

The loss of erodible material (g/m^2) from the exposed surface area during a test is calculated:

$$L = \frac{CQt}{A} \qquad (3)$$

where

C = average particulate concentration in tunnel exit stream (after subtraction of background concentration), g/m^3
Q = tunnel flow rate, cubic meters per second (m^3/s)
A = exposed test surface area (0.918 square meters [m^2] for the reference wind tunnel)

Alternatively, the erosion potential can be directly calculated from the cyclone and filter net mass (after correction for background).

For a specific surface, the wind erosion potential is dependent on the wind speed and on the frequency of disturbance of the erodible surface. Each time that a surface is disturbed, its erosion potential is restored. A disturbance is defined as an action that results in the exposure of fresh surface material. For this study, a disturbance occurred when the soil surface was exposed by the prescribed burn.

Whenever a surface is tested at sequentially increasing wind speeds, the measured losses from the lower speeds are added to the losses at the next higher speed and so on. This reflects the hypothesis that, if the lower speeds had not been tested beforehand, correspondingly greater losses would have occurred at the higher speeds.

In summary, the calculated test results for each test surface included:

- Roughness height: from extrapolated subthreshold velocity profile;
- Friction velocity: from measured centerline wind speed and roughness height;
- Equivalent wind speed at reference 10-m height: from measured centerline wind speed and roughness height; and
- Erosion potential (for "limited reservoir" surfaces) for a maximum wind speed: equivalent to the cumulative particle mass loss.

In addition to the wind tunnel results, 6-second concentrations were graphed and integrated over wind tunnel run time to calculate the hypothetical mass that would have been collected by each DustTRAK monitor. As discussed previously, the integrated mass (erosion

potential) for each wind speed plateau included integrated masses from each previous plateau. Finally, the average PM_{10} mass for the entire DustTRAK sampling period was compared to the actual PM_{10} mass collected on the PM_{10} backup filter.

TEST RESULTS

The results of the wind tunnel tests and erosion potential calculations are presented in Table 1. As expected, the average PM_{10} concentration in the wind tunnel effluent for the April test series was much higher for the burned areas than for the adjacent unburned areas. At the beginning of the first test series, one day after the burn, the average PM_{10} erosion potential was approximately nine times higher than found for unburned grassland adjacent to the burn area.

The PM_{10} erosion potentials, normalized to a 10-m wind speed of 95 mph, are shown graphically in Figure 3. Normalization was performed because the growth of vegetation between the prescribed burn and the later tests, on both burned and unburned plots, resulted in different surface roughness heights and consequent 10-m wind speed equivalents for the maximum wind tunnel centerline speeds. This effect is also shown in the progression of roughness heights and friction velocities between the earlier and later tests that can be seen from Table 1.

From Figure 3, the PM_{10} erosion potential of the burned area appears to decay in time with the regrowth of vegetation. Observations made at the time of each test series also indicated that the ground was somewhat moist in May but was fairly dry for both the April and June test series on the burned area. The dustiness tests that were performed with soil from the burned area showed that moisture is very effective in limiting PM_{10} erosion potential. As moisture was increased from 2% to 8%, for example, in the laboratory testing, the dustiness (potential for release of airborne PM_{10}) was seen to decrease by over an order of magnitude.

The PM_{10} erosion potential for the unburned grassland remained consistently low, in the range of 0.05 g/m^2 or less, as seen from April and June tests shown in Table 1. The PM_{10} erosion potential for the unburned areas also decreased between April and June as the vegetation grew.

Table 1 also shows erosion potential for total particulates. The results show a somewhat different pattern than found for PM_{10} and indicate that erosion potential increased with time, on both the burned and unburned areas. These results are somewhat misleading, because the results cannot be normalized in the same manner as the PM_{10} since DustTRAK data are not available for the larger particles, nor would they be reliable. However, the indicated trend may also result from changes in vegetation with time. As the vegetation grew, it would have presented a larger surface area to catch and hold deposited dust. Other researchers have found that larger particles may be more easily dislodged from vegetation surfaces than smaller particles, such as PM_{10}, which may be better protected by boundary layer effects on the leaves themselves.[4,5] As a result, the growing vegetation may constitute an effective reservoir of erodible particles, particularly in the larger size fractions that contribute to total airborne particulate.

The logging mode of the DustTRAK provided 6-second average concentration values for each of the test runs. After subtracting out a minimum value assumed to be background, these values were used to find an average concentration value from the beginning of the test run to the

end of the run time for each 10-m wind speed. The average concentration along with the tunnel volumetric flow rate, the length of time from the beginning of the test until the end of the specified wind speed plateau, and the exposed test surface area were used to determine the (cumulative) erosion potential for that wind speed.

It should be noted that the actual average PM_{10} concentration in the tunnel effluent was several times higher than the average PM_{10} concentration indicated by the DustTRAK. This reflects the fact that while the coarse mode of the PM_{10} (particles larger than 2.5 μm) constitutes much of the PM_{10} sample mass, it does not scatter light very effectively. Calibration of DustTRAK results to backup filter mass corrected for this bias.

Figure 4 shows average erosion potential values versus wind speed (mph) at a 10-m height. The same pitot tube pressure differentials for the predetermined tunnel centerline wind speeds were used for the three test periods, yet the roughness height of the surface changed over the three-month period, corresponding to increases in 10-m wind speeds, in relation to centerline values.

It is clear from Figure 4 that the erosion potential distributions (versus 10-m wind speed) decay with time after the prescribed burn. The May curve lies below the June curve because of the damp soil conditions encountered during the May testing.

DISPERSION MODELING APPROACH

Wind tunnel test results are being used to model the movement of airborne particulate matter and actinides in the Site environment. A Site-specific wind erosion equation was developed from previous wind tunnel studies performed at the Site by MRI in 1993.[6] In that approach, particulate emissions from undisturbed, vegetated surfaces at the Site were calculated as a function of the 1-hour average wind speed measured at a 10 m height, and the presence or absence of snow cover. Actinide emissions were calculated based on concentrations in the underlying soil.

Emissions were then modeled using a Site-specific implementation of EPA's Industrial Source Complex Short Term model (ISCST3) (the model uses a 1-hour time step). Comparison of model predictions to measured ambient air plutonium and americium concentrations at various locations around the Site indicated that the approach overpredicts actinide concentrations by up to an order of magnitude close to source areas and by a factor of 3 to 6 at the downwind fenceline (located 2,500 to 3,000 m east of source areas)[7]. Much of this overprediction is presumed to be caused by the inability of the present model to account for limitations in the available reservoir of erodible particles. Rather than depleting the supply of particles that can be eroded in an hour at a given wind speed, the model assumes that each subsequent hour at a similar wind speed could erode a similar mass of material.

Refinements are being made to the modeling approach to take this limitation into account. The modeling approach is also being revised to account for removal of vegetation by a fire and to incorporate the subsequent, temporary increases in erosion potentials that were the

subject of the study reported here. The refined approach is outlined below for a 1-year modeling scenario, using historical meteorological data measured at the Site.

- Track 15-Minute Wind Speed and Precipitation

  The 15-minute mean wind speeds are representative of maximum sustained winds (wind data from the Site are recorded as 15-minute averages). The 15-minute wind speed and precipitation data will be used to calculate wind erosion rates.

- Develop 15-Minute Emission Rates as a Function of Wind Speed Using Wind Tunnel Data From Undisturbed Areas

  Dispersion models for open dust sources require emission rates in units of mass per unit area per unit time (i.e., $g/m^2/s$). In contrast, particulate emissions from wind erosion are expressed in terms of mass per unit area (g/m^2) for the maximum sustained wind speed (minimum of 2 minutes) between surface disturbances. To account for these differences, the refined approach will assume that the erosion potential for a given wind speed will be exhausted within a 15-minute time step and the total particulate and actinide emissions will be averaged over the time step. It will be assumed that additional erosion for subsequent wind speeds at or below the initial wind speed will be insignificant until the erosion potential is replenished by surface disturbance; subsequent higher wind speeds will be allowed to erode an additional increment of material based on wind tunnel erosion potential data for undisturbed, vegetated surfaces.

- Eliminate Periods During and Immediately After Precipitation Events and When Snow Cover is Present

  High winds that occur in the same 4-hour period as light precipitation or within 24 hours of significant precipitation are unlikely to cause significant wind erosion. Emission rates for these periods will be reduced to zero for calculation purposes. Similarly, periods with snow cover (based on measured albedo data) will also be reduced to zero.

- Project Hourly Particle Deposition and Erosion Potential Replenishment

  A small replenishment of erosion potential will occur on an ongoing basis because of particle deposition, freeze/thaw events, etc. Hourly estimates of particle and actinide deposition will be made based on measured meteorological data and historical PM_{10}, total suspended particulate, and ambient actinide concentration data for the Rocky Flats area. A small additional increment will be added for ongoing, small-scale soil disturbances such as freeze/thaw cycles, rainsplash, and animal activity.

- Calculate Hourly Emission Rates, Taking into Account Erosion Losses from Previous Wind Events

The erosion potential will be reduced with each high wind event. If the erosion potential at 35 mph (10-m height) is x g/m^2, then that erosion potential will no longer be available for future winds of 35 mph or less until the erosion potential is restored by deposition or other means. Only winds above ~35 mph will produce future soil erosion. In addition, if a 50-mph wind event follows a 25-mph wind event, the curve will produce y g/m^2 erosion potential, but the previous wind erosion potential must be subtracted to give only $(y - x)$ g/m^2 for the 50-mph wind event.

Hourly emission rates will be calculated for each source area by treating this situation using a mass balance, "bookkeeping" approach. Beginning with an assumed initial erosion potential at the beginning of the modeling period, increases and decreases in erosion potential will be calculated for each 15-minute period based on losses due to emissions and inputs due to deposition, etc. Emissions will be constrained for each 15-minute time step so that they do not exceed the net remaining erosion potential for the applicable wind speed. The calculated 15-minute emissions will be used to develop hour-by-hour emission rates for input to ISCST3.

To model resuspension following a fire, multipliers will be developed and applied to the above-estimated emissions. The multipliers will vary based on the elapsed time following the fire and based on soil moisture conditions, as follows.

- Generate Erosion Potential Decay Curves for Each Tested Wind Speed, Soil Condition, and Time Period Following a Grass Fire

  Erosion potentials for three different elapsed times following the test burn are given in g/m^2 for each tested wind speed in Figure 4. May is assumed to represent "damp soil" erosion potential, while the April and June tests are assumed to represent dry conditions. Erosion potentials at intermediate wind speeds can be interpolated from the curves.

- Use Damp/Dry Soil Curves as Appropriate for each 15-Minute Period

  High winds that occur within 24 to 48 hours of significant precipitation should be associated with a damp soil curve for calculation of erosion potential and emissions.

- Model 1-yr Periods (Assume Full Revegetation and Restoration of Original, Reduced Erosion Potential Within 1 Year)

  Decay curves will be assumed to decline to a level represented by the unburned area tests after one year. Restoration of the full vegetation protection against wind erosion will not be complete until a new layer of thatch is laid down and covers the soil between grass clumps.

CONCLUSIONS

The results of the wind erosion tests on the Rocky Flats prescribed burn area showed that low PM_{10} emissions occurred below 40 mph (equivalent wind speed at a height of 10 m above ground). Above 40 mph, PM_{10} emissions increased with increasing wind speed. After burning, the land was observed to retain many of the characteristics that limit wind erosion—including soil crusts, rocks/pebbles that protected the surface soil, and grass clumps. Grass clumps, even when burnt, are very protective of soil erosion, but usually were not spaced closely enough on Rocky Flats land for good protection of all of the exposed area.

PM_{10} emissions were observed to increase as wind speed increased, and erosion potentials were calculated for various wind speed plateaus during each of the three months of testing. Erosion potentials from the prescribed burn area were always somewhat greater than for unburned areas, even for the June tests—approximately 2½ months after the burn. This was clearly due to the wind protection afforded by dead grass thatch that had formerly covered the unburned areas, but was not present after the prescribed burn.

Even though the burned areas had revegetated to a large extent by the June test period, bare soil that constituted an emission source was still visible between the revegetating plants. Moreover, the vegetative restoration of the prescribed burn areas included mostly tall, thin plants that did not completely protect the soil from wind erosion through late June, when the latest wind tunnel tests were conducted. During May tests, soil moisture was observed to be effective in reducing soil erosion rates from high winds at moderate temperatures. However, when rainfall wets the soil surface and temperatures are warm, the surface dries quickly in the relatively low humidity environment of Rocky Flats, so this mitigating effect is transient.

A new approach to ambient impact modeling of a grass fire is being developed for wind erosion sources to reflect a limited reservoir erosion potential (emission rate) in units of g/m^2. This approach tracks historical 15-minute mean wind speeds. The times and extent of wind erosion are dominated by the occurrence of the highest wind speeds. Wind tunnel data provide the relationship between particulate emission rates and maximum sustained winds. The modeling approach takes into account losses of erosion potential from previous high wind events, the mitigating effects of vegetation, and the role of background dust deposition.

The new approach will account for the absence of emissions during precipitation events and when snow cover is present. Increases and decreases in erosion potential will be calculated for each 15-minute period based on losses due to resuspension and input due to deposition and other natural processes (e.g., freeze/thaw). A mass balance accounting will be performed so that emissions will not exceed the net remaining erosion potential for a given source area for the applicable wind speed. Calculated 15-minute emissions will be used to develop hour-by-hour emission rates for input to ISCST3. To model resuspension following a fire, multipliers based on the elapsed time following the fire and on soil moisture conditions will be applied to the above-estimated emissions.

REFERENCES

1) U.S. Environmental Protection Agency. *National Technical Guidance Series Air Pathway Analysis Procedure for Superfund Applications*. Vol. II: *Estimates of Baseline Air Emissions at Superfund Sites*. Research Triangle Park, NC, 1989; EPA-450/1-89-002a.
2) U.S. Environmental Protection Agency. *Compilation of Air Pollutant Emissions Factors*, AP-42. Fifth Edition, Supplements A-F, Volume I: *Stationary Point and Area Sources.* Research Triangle Park, NC, 2000.
3) Owen, E.; Pankhurst, R.C. *The Measurement of Air Flow*; Pergamon Press; London, 1969.
4) Garland, J.A. *Resuspension of Particulate Matter From Grass Experimental Programme 1979-1980*. UKAEA Atomic Energy Research Establishment, Environmental and Medical Sciences Division, Harwell, England, 1982; AERE-R-10106.
5) Langer, G. *Resuspension of Soil Particles from Rocky Flats Containing Plutonium Particles*. EG&G Rocky Flats, Inc., Golden, CO, 1991.
6) Midwest Research Institute. *OU3 Wind Tunnel Study*, Vol. I: *Test Report*. Prepared for EG&G Rocky Flats, Inc., Golden, CO, 1994.
7) Radian International. *Air Transport and Deposition of Actinides at the Rocky Flats Environmental Technology Site, FY00 Report*. Prepared for Kaiser-Hill Company, L.L.C., Golden, CO, 2000.

Figure 1. MRI portable wind tunnel.

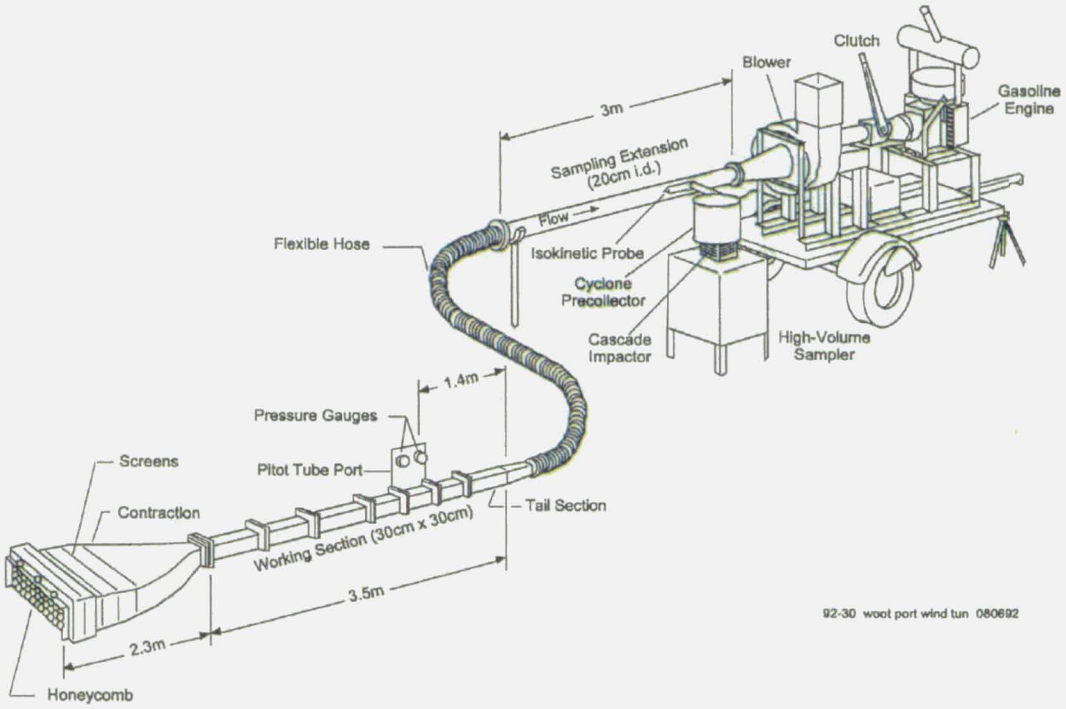

Figure 2. DustTRAK graph for run CB-8B.

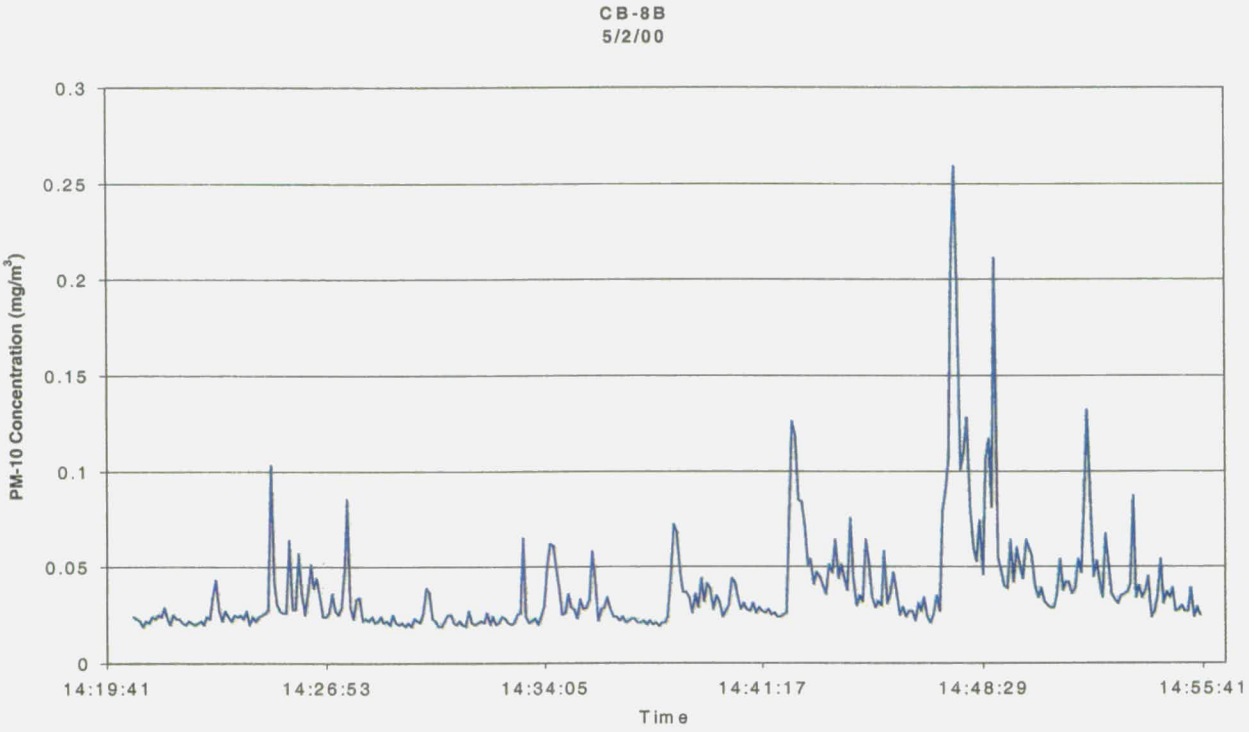

120

Figure 3. Erosion potential history for each test series.

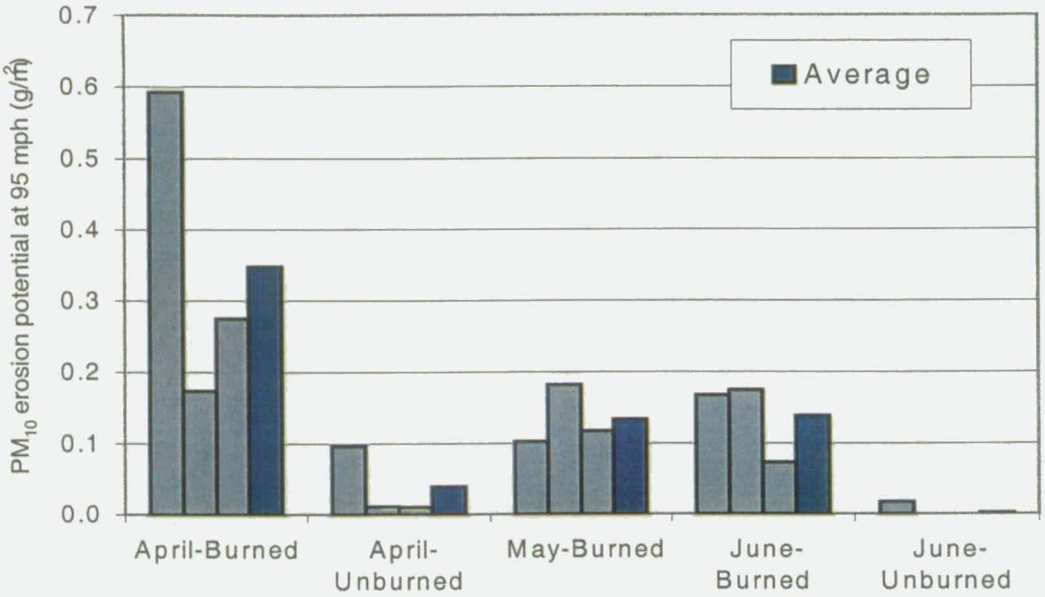

Figure 4. Erosion potential at 10-m wind speeds as determined from DustTRAK data.

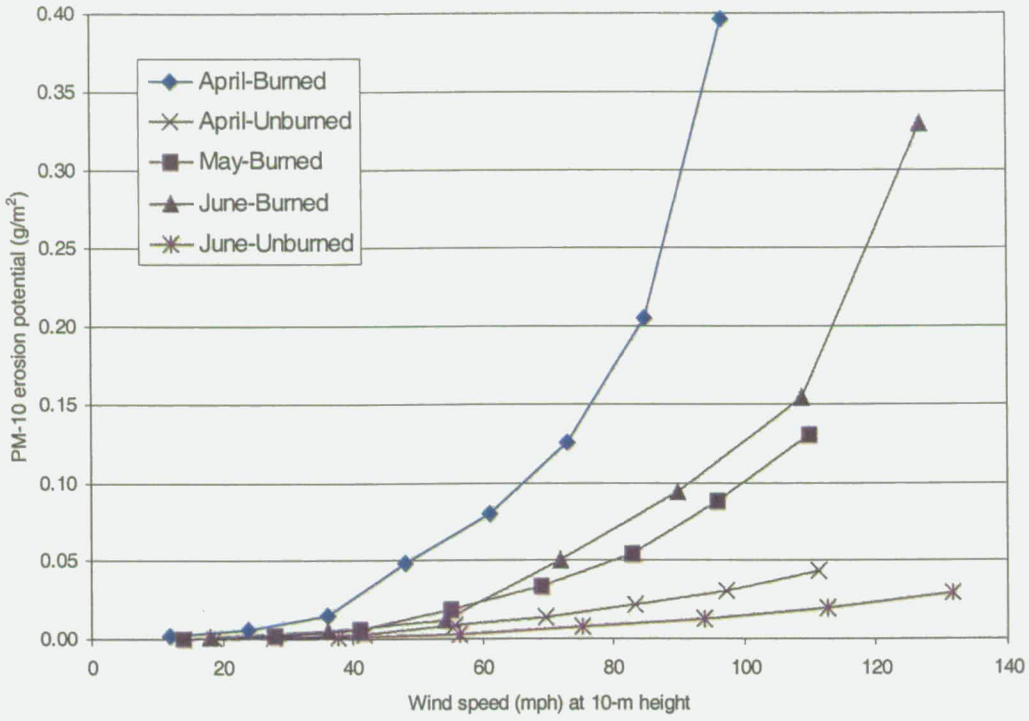

121

Table 1. Wind tunnel erosion potentials.

Date of test series	Surface condition	Average roughness height (cm)	Maximum wind speed (mph) at tunnel CL[a]	Equivalent maximum wind speed (mph) at 10-m height[b]	Corresponding friction velocity[b] (cm/s)	Erosion potential[c] (g/m^2)		
						TP	PM_{10}	PM_{10} normalized to 95 mph at 10-m height
4/7/00	Burned	0.85	40.3	97.6	244.7	1.33	0.65	0.59
4/8/00	Burned	0.66	40.3	97.6	244.7	0.61	0.19	0.17
4/8/00	Burned	0.89	40.3	97.6	244.7	0.62	0.30	0.28
4/9/00	Unburned	1.65	39.7	110.1	301.0	0.31	0.14	0.10
4/10/00	Unburned	1.76	40.3	111.9	305.8	0.13	0.02	0.01
4/11/00	Unburned	0.92	40.3	111.9	305.8	0.18	0.02	0.01
5/2/00	Burned	1.10	37.0	100.5	271.4	1.07	0.12	0.10
5/2/00	Burned	1.31	40.3	109.6	295.8	2.50	0.26	0.18
5/3/00	Burned	1.57	37.2	101.2	273.3	0.76	0.14	0.12
6/21/00	Burned	3.00	38.6	138.3	425.9	11.09	0.67	0.17
6/21/00	Burned	3.12	29.2	104.7	322.4	1.67	0.23	0.18
6/22/00	Burned	2.91	35.8	128.4	395.3	3.65	0.23	0.07
6/22/00	Unburned	3.17	39.3	145.2	452.5	0.16	0.05	0.02
6/23/00	Unburned	3.16	34.8	128.6	400.6	0.45	<0.02	<0.02
6/23/00	Unburned	3.32	37.5	138.8	432.4	0.83	<0.02	<0.02

Notes:

cm = centimeter
mph = miles per hour
CL = centerline
m = meters
cm/s = centimeters per second
g/m^2 = grams per square meter
TP = total particulate

[a] Average maximum wind speed at tunnel centerline for all three tests.
[b] Average roughness height over three runs used to calculate equivalent 10-m wind speed and friction velocity.
[c] Calculated using net mass.

122

KEYWORDS

Wind tunnel
PM_{10}
Fire
Controlled burn, prescribed burn
Fugitive dust

APPENDIX B

Wind Erosion Tracking Program

```
program winderosion (precipfile, albedofile, puout, amout, info);

(*Calculates mass, Pu, and Am emissions by 15-minute time step and hour,
  then writes hourly emission files for ISCST3*)

(*This version is for: pre-closure baseline, as originally modeled in FY01*)

type
    sourceinfo  =  record
                      name:string[8];
                      activityinc:real;
                   end;

var
    puavailable, puintrinsic, pudep, puhourlyemissions: array [1..12] of real;
    amavailable, amintrinsic, amdep, amhourlyemissions: array [1..10] of real;
    massavailable, massintrinsic, masshourlyemissions: real;
    massdep: array[1..12] of real;
    potentialmass, actualmass: real;
    actualactivity: real;
    albedoflag, precipflag: integer;
    source, quarterhour: integer;
    precipfile, albedofile, potemissions, puout, amout, info: text;
    numhours, numdays, currenthour: integer;
    month, jday, day, hour, period: integer;
    puid: array [1..12] of sourceinfo;
    amid: array [1..10] of sourceinfo;
    depvelm, depvela : real;
    totmassavail, totmasspot, totmassact, totintrinsic, totdep: real;

(*_____________________________________________________________________*)

procedure updatereservoir (thismonth:integer);

(*This procedure updates the available mass and activity reservoirs at each time
  step.  Total erodible material is calculated as the current erodible material
  + deposition input for the time step + input via small-scale soil disturbance
  (intrinsic generation)*)

var
    area: integer;

    begin    (*updatereservoir*)

(*Pu updates*)

        for area := 1 to 12 do
              begin
                    puavailable[area]:= puavailable[area] +
                        puintrinsic[area] + pudep[area];
              end;  (*for area*)

(*Am updates*)

        for area := 1 to 10 do
              begin
                    amavailable[area] := amavailable[area] +
```

```
                    amintrinsic[area] + amdep[area];
            end;  (*for area*)

(*Update mass*)

        massavailable := massavailable + massintrinsic + massdep[thismonth];

(*Update running totals for information file*)

        totmassavail := totmassavail + massintrinsic + massdep[thismonth];
        totintrinsic := totintrinsic + massintrinsic;
        totdep := totdep + massdep[thismonth];

    end;    (*procedure updatereservoir*)

(*_____________________________________________________________________*)

procedure outputemissionsdata (thismonth:integer; thisday:integer;
                               thishour:integer);

(*Writes the ISC hourly emission files for Pu and Am*)

var
    area:integer;
    amemis, puemis : real;

    begin  (*outputemissionsdata*)

(*Note that hourly emissions (g/m² or pCi/m²) must be converted to an
   emission rate (g/m²/s or pCi/m²/s)*)

        puemis := 0.0;
        amemis := 0.0;

(*Write Pu file*)

        for area := 1 to 12 do
            begin
            puemis := puhourlyemissions[area]/3600.0;
            writeln (puout, 'SO HOUREMIS 96 ',thismonth:3, thisday:3,
                     thishour:3, puid[area].name:9, puemis:13);
            end;

(*Write Am file*)

        for area := 1 to 10 do
            begin
            amemis := amhourlyemissions[area]/3600.0;
            writeln (amout, 'SO HOUREMIS 96 ',thismonth:3, thisday:3,
                     thishour:3, amid[area].name:9, amemis:13);
            end;

    end;  (*procedure outputemissionsdata*)

(*_____________________________________________________________________*)

procedure initialize;
```


126

```
(*Initialize variables*)

    begin

(*Start with basic source data-names are needed to write file that
  serves as ISC input*)

(*For pre-closure, there are 12 Pu source areas and 10 Am source areas*)

        puid[1].name := '1.000011';
        puid[2].name := '1.000012';
        puid[3].name := '1.00005';
        puid[4].name := '1.0001';
        puid[5].name := '1.0005';
        puid[6].name := '1.001';
        puid[7].name := '1.0025';
        puid[8].name := '1.005';
        puid[9].name := '1.01';
        puid[10].name := '1.025';
        puid[11].name := '1.05';
        puid[12].name := '1.1';

        amid[1].name := '1.00001';
        amid[2].name := '1.00005';
        amid[3].name := '1.0001';
        amid[4].name := '1.0005';
        amid[5].name := '1.001';
        amid[6].name := '1.0025';
        amid[7].name := '1.005';
        amid[8].name := '1.01';
        amid[9].name := '1.025';
        amid[10].name := '1.05';

(*Now initialize the incremental activity.  This is the additional activity in
  each "layer" of the stacked isopleths.  The incremental activity, when added
  to the incremental activity of the source areas "below" will yield the total
  isopleth activity*)

        puid[1].activityinc := 0.1;  (*pCi/g soil*)
        puid[2].activityinc := 0.1;   (*This is the only isopleth that isn't
                                        "stacked" in the pre-closure set*)
        puid[3].activityinc := 0.4;
        puid[4].activityinc := 0.5;
        puid[5].activityinc := 4.0;
        puid[6].activityinc := 5.0;
        puid[7].activityinc := 15.0;
        puid[8].activityinc := 25.0;
        puid[9].activityinc := 50.0;
        puid[10].activityinc := 150.0;
        puid[11].activityinc := 250.0;
        puid[12].activityinc := 500.0;

        amid[1].activityinc := 0.1;
        amid[2].activityinc := 0.4;
        amid[3].activityinc := 0.5;
        amid[4].activityinc := 4.0;
```

```
        amid[5].activityinc := 5.0;
        amid[6].activityinc := 15.0;
        amid[7].activityinc := 25.0;
        amid[8].activityinc := 50.0;
        amid[9].activityinc := 150.0;
        amid[10].activityinc := 250.0;

(*Next initial mass and activity renewal by small-scale soil disturbances*)

(*Note that all Pu isopleths are stacked except source 2 and all Am isopleths
  are stacked*)

        massintrinsic := 0.00112/4; (*Convert g/m²/hour to g/m²/15-minutes*)
                                    (*Based on average of Pu and Am g/m²/hr
                                      from intrinsicgenerationfinal2.xls*)

        puintrinsic[1] := 0.000111/4;  (*pCi/m²/15 min*)
        puintrinsic[2] := 0.000111/4;
        puintrinsic[3] := 0.000443/4;
        puintrinsic[4] := 0.000554/4;
        puintrinsic[5] := 0.00443/4;
        puintrinsic[6] := 0.00554/4;
        puintrinsic[7] := 0.0166/4;
        puintrinsic[8] := 0.0277/4;
        puintrinsic[9] := 0.0554/4;
        puintrinsic[10] := 0.166/4;
        puintrinsic[11] := 0.277/4;
        puintrinsic[12] := 0.554/4;

        amintrinsic[1] := 0.000113/4;
        amintrinsic[2] := 0.000454/4;
        amintrinsic[3] := 0.000567/4;
        amintrinsic[4] := 0.00454/4;
        amintrinsic[5] := 0.00567/4;
        amintrinsic[6] := 0.0170/4;
        amintrinsic[7] := 0.0284/4;
        amintrinsic[8] := 0.0567/4;
        amintrinsic[9] := 0.1704/4;
        amintrinsic[10] := 0.284/4;

(*Now initialize the deposition input*)

        depvela := 2.433 * 900/100;  (*Activity-weighted deposition velocity
                                       in cm/s, converted to m/15-minutes*)
        depvelm := 1.97 * 900/100;   (*Mass weighted deposition velocity*)

(*Pu and Am deposition are based on incremental air concentrations over
  each source area*)

        pudep[1] := depvela * 0.00000136; (* in pCi/m²/15-min*)
        pudep[3] := depvela * (0.00000151-0.00000136);
        pudep[4] := depvela * (0.00000168-0.00000151);
        pudep[5] := depvela * (0.00000229-0.00000168);
        pudep[6] := depvela * (0.00000263-0.00000229);
        pudep[7] := depvela * (0.00000452-0.00000263);
        pudep[8] := depvela * (0.00000539-0.00000452);
        pudep[9] := depvela * (0.00000617-0.00000539);
```

```
        pudep[10] := depvela * (0.00000639-0.00000617);
        pudep[11] := depvela * (0.00000611-0.00000639);
        pudep[12] := depvela * (0.00000574-0.00000611);

        pudep[2] := depvela * 0.00000176;  (*Not stacked*)

        amdep[1] := depvela * 0.000000262;
        amdep[2] := depvela * (0.000000330-0.000000262);
        amdep[3] := depvela * (0.000000395-0.000000330);
        amdep[4] := depvela * (0.000000792-0.000000395);
        amdep[5] := depvela * (0.000000924-0.000000792);
        amdep[6] := depvela * (0.000000978-0.000000924);
        amdep[7] := depvela * (0.00000104-0.000000978);
        amdep[8] := depvela * (0.000000980-0.00000104);
        amdep[9] := depvela * (0.000000905-0.000000980);
        amdep[10] := depvela * (0.000000903-0.000000905);

(*Mass deposition is next-it varies by month*)

        massdep[1] := depvelm * 0.0000224; (*Mass is in g/m^3 of TSP, from 1996
                                             CDPHE data in supplyside.xls;
                                             product is in g/m^2/15-minutes*)
        massdep[2] := depvelm * 0.0000292;
        massdep[3] := depvelm * 0.0000384;
        massdep[4] := depvelm * 0.0000288;
        massdep[5] := depvelm * 0.0000418;
        massdep[6] := depvelm * 0.0000464;
        massdep[7] := depvelm * 0.0000476;
        massdep[8] := depvelm * 0.0000446;
        massdep[9] := depvelm * 0.000024;
        massdep[10] := depvelm * 0.0000332;
        massdep[11] := depvelm * 0.0000274;
        massdep[12] := depvelm * 0.0000152;

(*Next step is to initialize available mass and activity at beginning of year*)
(*Assume PM10 = 0.05 g/m^2 & PM10/TSP = 0.39 at beginning of year*)

        massavailable := 0.128;  (*TSP in g/m^2*)

(*Pu and Am initial activity (in pCi/m^2)*)

        for source := 1 to 12 do
            puavailable[source] := massavailable * puid[source].activityinc;

        for source := 1 to 10 do
            amavailable[source] := massavailable * amid[source].activityinc;

    end; (*procedure initialize*)

(*_____________________________________________________________________*)

begin    (*main*)

(*open files*)

    assign (precipfile, 'pflags.prn');
    assign (albedofile, 'aflags.prn');
```

```
    assign (potemissions, 'ptemiss.prn');
    assign (puout, 'puemiss.prn');
    assign (amout, 'amemiss.prn');
    assign (info, 'resinfo.prn');

    reset (precipfile);
    reset (albedofile);
    reset (potemissions);

    rewrite (puout);
    rewrite (amout);
    rewrite (info);

    initialize;   (*Call procedure to initialize most global variables*)

    numdays := 366; (*1996 was a leap year*)
    numhours := 366 * 24;

    currenthour := 0;
    month := 0;
    precipflag := 0;
    albedoflag := 0;

(*Skip header lines in files*)

    readln (precipfile);
    readln (albedofile);
    readln (potemissions);

    totmassavail := 0.0;
    totmasspot := 0.0;
    totmassact := 0.0;
    totintrinsic := 0.0;
    totdep := 0.0;


    while (currenthour < numhours) do
        begin

(*This is the outer loop over all met data periods, by hour*)
(*Currenthour = 0 to start*)

            masshourlyemissions := 0.0;

            for source := 1 to 12 do
                    puhourlyemissions[source] := 0.0;

            for source := 1 to 10 do
                    amhourlyemissions[source] := 0.0;

            for quarterhour := 1 to 4 do
                begin

(*This is the inner loop for each hour, over four 15-minute periods*)

(*At first of hour, read next hourly albedo flag and update currenthour
  counter*)
```

```
                    if (quarterhour = 1)
                        then begin
                             readln (albedofile, month, day, hour, albedoflag);
                             currenthour := currenthour + 1;
                             end;

(*Next read in potential particulate matter emissions and precipitation flag
  for this 15-minute period*)

                    readln (potemissions, jday, period, potentialmass);
                    readln (precipfile, jday, period, precipflag);

(*Update running total potential particulate matter emissions for
  information file*)

                    totmasspot := totmasspot + potentialmass;

(*Check for snow cover or precipitation.  Under those conditions, no emissions
  are calculated but deposition and small-scale soil disturbances are assumed
  to continue*)

                    if ((albedoflag >= 1) or (precipflag >= 1))
                        then    (*no emissions*)
                            updatereservoir (month)
                        else
                            begin    (*emissions!*)

(*If no snow or precipitation, first update reservoirs for next time step's
  deposition and soil disturbance input, then calculate emissions*)

                                updatereservoir (month);

(*Figure out how much can be eroded*)

                                if (potentialmass <= massavailable)
                                    then actualmass := potentialmass
                                    else actualmass := massavailable;

(*Add to running total actual emissions for information file*)

                                totmassact := totmassact + actualmass;

(*Calculate activity emissions based on mass emissions and pCi/g in reservoir*)

(*First loop over Pu sources*)

                                for source := 1 to 12 do
                                    begin
                                        actualactivity := actualmass *
                                            puavailable[source]/massavailable;

(*Add to hourly emissions and decrement reservoir*)

                                        puhourlyemissions[source] :=
                                            puhourlyemissions[source] +
                                            actualactivity;
```

```
                                        puavailable[source] :=
                                            puavailable[source] -
                                            actualactivity;
                                    end;   (*for loop over Pu sources*)

(*Now loop over Am*)

                                for source := 1 to 10 do
                                     begin
                                        actualactivity := actualmass *
                                            amavailable[source]/massavailable;

(*Add to hourly emissions and decrement reservoir*)

                                        amhourlyemissions[source] :=
                                            amhourlyemissions[source] +
                                            actualactivity;

                                        amavailable[source] :=
                                            amavailable[source] -
                                            actualactivity;
                                    end;    (*for loop over Am sources*)

(*Add mass emissions and decrement reservoir*)

                                masshourlyemissions := masshourlyemissions +
                                    actualmass;
                                massavailable := massavailable - actualmass;

                            end;    (*else*)

(*Check for end of hour and output if necessary*)

                    if (quarterhour = 4)
                    then outputemissionsdata (month, day, hour);
                        (*month, day, hour were read from albedo file*)

                end;  (*for loop over quarter hours*)

        end;    (*outer while loop*)

(*Output to information file*)

        writeln (info, 'Total potential PM emissions: ', totmasspot:10:4);
        writeln (info, 'Total PM available: ', totmassavail:10:4);
        writeln (info, 'Total actual PM emissions: ', totmassact:10:4);
        writeln (info, 'Total PM intrinsic generation: ',totintrinsic:10:4);
        writeln (info, 'Total PM deposited: ',totdep:10:4);

(*Close files*)

    close (puout);
    close (amout);
    close (precipfile);
    close (albedofile);
    close (potemissions);
```

```
    close (info);

end.    (*main*)
```